STATE OF CALIFORNIA DEPARTMENT OF TRANSPORTATION

# TECHNICAL REPORT DOCUMENTATION PAGE

TR0003 (REV. 10/98)

| 1. REPORT NUMBER | 2. GOVERNMENT ASSOCIATION NUMBER | 3. RECIPIENT'S CATALOG NUMBER |
|---|---|---|
| CA20-3022 | | |

| 4. TITLE AND SUBTITLE | 5. REPORT DATE / 6. PERFORMING ORGANIZATION CODE |
|---|---|
| Seismic Response of Precast Columns with Non-Proprietary UHPC-Filled Ducts ABC Connections | 5. REPORT DATE: August 2020<br>6. PERFORMING ORGANIZATION CODE: UNR |
| 7. AUTHOR(S)<br>Mahmoud Aboukifa, Mohamed A. Moustafa, and Mehdi Saiid Saiidi | 8. PERFORMING ORGANIZATION REPORT NO.<br>UNR / CA20-3022 |
| 9. PERFORMING ORGANIZATION NAME AND ADDRESS<br>Department of Civil and Environmental Engineering<br>University of Nevada, Reno<br>1664 North Virginia Street<br>Reno, Nevada 89557-0152 | 10. WORK UNIT NUMBER<br><br>11. CONTRACT OR GRANT NUMBER<br>65A0607 |
| 12. SPONSORING AGENCY AND ADDRESS<br>California Department of Transportation<br>Engineering Service Center<br>1801 30th Street, MS 9-2/5i<br>Sacramento, California 95816<br><br>California Department of Transportation<br>Division of Research and Innovation, MS-83<br>1227 O Street<br>Sacramento CA 95814 | 13. TYPE OF REPORT AND PERIOD COVERED<br>Final Report<br>06/01/2017-07/31/2020<br>14. SPONSORING AGENCY CODE<br>913 |

15. SUPPLEMENTAL NOTES

Prepared in cooperation with the State of California Department of Transportation.

16. ABSTRACT

Accelerated bridge construction (ABC) has several advantages, such as reducing onsite construction time, reducing the traffic congestion around construction sites, and improving the quality of the prefabricated elements for both new bridges or rehabilitation or replacement of old bridges. ABC is considered a good and efficient candidate to replace the cast-in-place (CIP) conventional on-site construction techniques. ABC has been widely used in low seismic regions mostly in the superstructure elements. However, ABC is not widely implemented in the substructure elements such as column-base connections, especially in moderate and high seismic regions due to the uncertainty in the seismic performance of the substructure connections. Few ABC seismic connections were developed and have been demonstrated for potential use in high seismic regions. Among these is ultra-high performance concrete (UHPC) filled grouted-duct connection. The use of proprietary UHPC poses another challenge for wider implementation of this type of connection. The overall goal of this study was to develop non-proprietary, feasible alternative for the grouted-duct ABC seismic connection for precast bridge columns that can emulate the seismic performance of conventional CIP connections.

Reducing the costs and using non-proprietary materials was the focus of this study to establish a less expensive, less restrictive alternative for UHPC-filled grouted-duct connections and avoid sole-source specification. In the first phase of this project and a companion study (Subedi et al. 2019), several non-proprietary UHPC mixes were developed and two were selected at the University of Nevada, Reno. They were used in 22 large scale pullout specimens to determine the bond behavior of UHPC-filled duct systems. Given their observed satisfactory performance, one of the non-proprietary UHPC mixes was further used and incorporated into UHPC-filled duct connections of two 42%-scale column models to connect the precast columns to footings. Both column models were tested to failure under combined axial and cyclic lateral loading to investigate their seismic performance and evaluate their ability to emulate the seismic performance of the CIP system. Moreover, analytical investigation for each column model was conducted to simulate the global response of the column models. The analytical studies were conducted using finite element computer program OpenSEES. Specific modeling assumptions for these connections that include the bond-slip effects in bars and ducts and bar debonding effects were validated for future implementation and further use in the design of this connection in actual bridges. Overall, non-proprietary UHPC-filled duct connections were successfully demonstrated to have acceptable seismic performance and are, in turn, recommended as suitable precast column-to-footing or column-to-cap beam connections for moderate and high seismic regions. Using such connection with the proposed UHPC mix can assure the formation of full plastic moment in columns without any connection damage.

| 17. KEY WORDS | 18. DISTRIBUTION STATEMENT | |
|---|---|---|
| Non-Proprietary UHPC, Grouted Ducts, Large-scale Column Test, Seismic Response | No restrictions. This document is available to the public through the National Technical Information Service, Springfield, VA 22161 | |
| 19. SECURITY CLASSIFICATION (of this report) | 20. NUMBER OF PAGES | 21. PRICE |
| Unclassified | 89 | |

## DISCLAIMER STATEMENT

Report No. CCEER 20-08

# SEISMIC RESPONSE OF PRECAST COLUMNS WITH NON-PROPRIETARY UHPC-FILLED DUCTS ABC CONNECTIONS


Mahmoud Aboukifa

Mohamed A. Moustafa

and

M. Saiid Saiidi



California Department of Transportation, contract number 65A0607



**Center for Civil Engineering Earthquake Research**

University of Nevada, Reno

Department of Civil and Environmental Engineering, MS 258

1664 N. Virginia St.

Reno, NV 89557


October 2020

Final Report No. CA19-3022, CCEER 20-08

# SEISMIC RESPONSE OF PRECAST COLUMNS WITH NON-PROPRIETARY UHPC-FILLED DUCTS ABC CONNECTIONS

Mahmoud Aboukifa

Mohamed A. Moustafa

M. 'Saiid' Saiidi

Final Report Submitted to the California Department of Transportation (Caltrans)

under Contract No. 65A0607

---

**Center for Civil Engineering Earthquake Research**

University of Nevada, Reno

Department of Civil and Environmental Engineering, MS 258

1664 N. Virginia St.

Reno, NV 89557

October 2020

## ABSTRACT

Accelerated bridge construction (ABC) has several advantages, such as reducing onsite construction time, reducing the traffic congestion around construction sites, and improving the quality of the prefabricated elements for both new bridges or rehabilitation or replacement of old bridges. ABC is considered a good and efficient candidate to replace the cast-in-place (CIP) conventional on-site construction techniques. ABC has been widely used in low seismic regions mostly in the superstructure elements. However, ABC is not widely implemented in the substructure elements such as column-base connections, especially in moderate and high seismic regions due to the uncertainty in the seismic performance of the substructure connections. Few ABC seismic connections were developed and have been demonstrated for potential use in high seismic regions. Among these is ultra-high performance concrete (UHPC) filled grouted-duct connection. The use of proprietary UHPC poses another challenge for wider implementation of this type of connection. The overall goal of this study was to develop non-proprietary, feasible alternative for the grouted-duct ABC seismic connection for precast bridge columns that can emulate the seismic performance of conventional CIP connections.

Reducing the costs and using non-proprietary materials was the focus of this study to establish a less expensive, less restrictive alternative for UHPC-filled grouted-duct connections and avoid sole-source specification. In the first phase of this project and a companion study (Subedi et al. 2019), several non-proprietary UHPC mixes were developed and two were selected at the University of Nevada, Reno. They were used in 22 large scale pullout specimens to determine the bond behavior of UHPC-filled duct systems. Given their observed satisfactory performance, one of the non-proprietary UHPC mixes was further used and incorporated into UHPC-filled duct connections of two 42%-scale column models to connect the precast columns to footings. Both column models were tested to failure under combined axial and cyclic lateral loading to investigate their seismic performance and evaluate their ability to emulate the seismic performance of the CIP system. Moreover, analytical investigation for each column model was conducted to simulate the global response of the column models. The analytical studies were conducted using finite element computer program OpenSEES. Specific modeling assumptions for these connections that include the bond-slip effects in bars and ducts and bar debonding effects were validated for future implementation and further use in the design of this connection in actual bridges. Overall, non-

proprietary UHPC-filled duct connections were successfully demonstrated to have acceptable seismic performance and are, in turn, recommended as suitable precast column-to-footing or column-to-cap beam connections for moderate and high seismic regions. Using such connection with the proposed UHPC mix can assure the formation of full plastic moment in columns without any connection damage.

**ACKNOWLEDGEMENT**

This project was funded by California Department of Transportation (Caltrans) under award number 65A0607. The statements and findings presented as a result of this research represent the view of the authors and do not necessarily represent the views of Caltrans. The research team is indebted to Martin Marietta, Spanish Springs, NV and Perkins, Sacramento, CA for donating the aggregates required for this project. Also, thanks to Marv Christensen from C & K Johnson Industries, Inc. and Jake Meredith and Alese Glaus from Dayton Superior Corporation for generously donating materials for the project.

The vast experience and in-depth knowledge of Mr. Murugaiyah Piratheepan in the development and characterization of the mixes deserves great appreciation. His involvement and contribution was very crucial for this project. The experimental studies would not have been possible without the support of UNR Earthquake Engineering Laboratory staff members Dr. Patrick Laplace, Mark Lattin, Chad Lyttle and Todd Lyttle. The research team would like to thank everybody involved in the project.

## TABLE OF CONTENTS

**LIST OF TABLES**

## LIST OF FIGURES

# CHAPTER 1. INTRODUCTION

## 1.1. Overview

Accelerated bridge construction (ABC) techniques have advanced notably throughout the United States over the past few decades. A few departments of transportation across the US have focused on the seismic evaluation of such techniques and some have implemented these techniques in the construction of new bridges. ABC relies on the offsite prefabrication of structural components, shipping to the construction site and finally the assembly of these prefabricated elements on site. Numerous advantages could be achieved by implementing the ABC techniques in the construction of new bridges or the rehabilitation and replacement of old deteriorated bridges. Reducing onsite construction time, reducing the traffic congestion around the construction sites, and improving the quality of the prefabricated elements are the main advantages of ABC technology. Although ABC technology has been widely used in the bridge superstructure elements, it is not as widely implemented in substructure elements such as column-footing base connections.

The main challenge facing the adoption of the ABC technology in moderate and high seismic areas is the uncertainty in the adequacy of precast member connections to maintain the integrity of the structure under cyclic loads. It is important to develop ABC systems that can emulate conventional cast-in-place (CIP) construction systems because, if this can be achieved, typical analysis and design procedures can be used. The main difficulty with developing emulative systems is the detailing of connections because of their critical role in transferring forces and maintaining stability of the structure. Substructure connections, in particular, are critical in high seismic zones as they have to dissipate energy through significant cyclic nonlinear deformations while maintaining their load capacity and their integrity within the structural system.

There are several types of ABC substructure connections that have been developed in recent years such as, grouted-duct connections, pocket-type connections, and column-in-socket connections. The study presented in this report focuses on grouted-ducts connection, which is one of the most promising types. This connection can also be sometimes called non-coupled plunged connections or referred to as precast column with no couplers (PNC) detail for column-to-footing and column-to-cap connections. A PNC connection comprises a precast column with extended straight longitudinal reinforcing bars (rebars) that are anchored in grouted corrugated ducts installed in the connecting members (footing or cap beam). The column rebars are typically debonded at the connection interface to enhance energy dissipation during seismic events. A schematic representation of a PNC column-to-footing connection detail is shown in Figure 1.1. Past research by Tazarv and Saiidi (2015) has demonstrated the seismic performance of the PNC connection and proven its reliability. However, such development used a proprietary ultra-high performance concrete (UHPC) mix that is roughly 9 times as expensive as standard grout. The proprietary nature pose challenges for specification writers while high initial costs present an obstacle for the adoption of ABC by the bridge engineers.

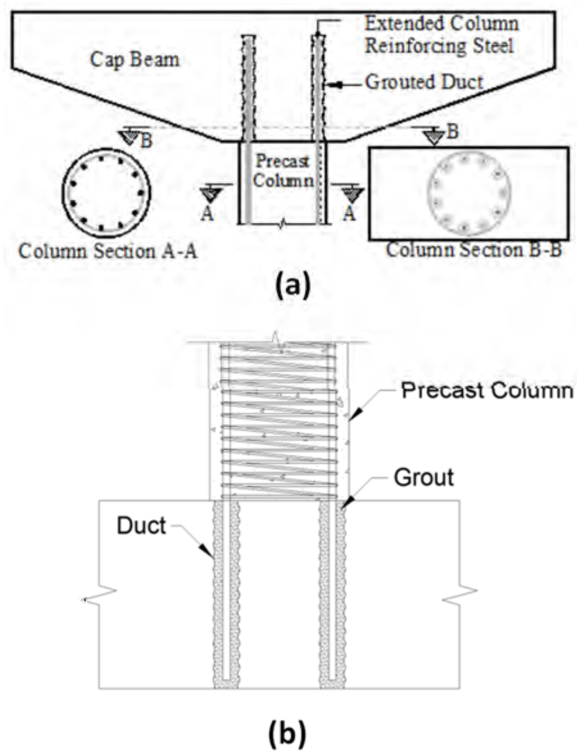


Figure 1.1 Schematic of Grouted Duct Connections: (a) Column to Cap Beam Connection, (b) Column to Footing Connection (adopted from Shrestha et al. 2018).

The goal of this research is to evaluate the seismic performance of grouted-duct connections using a non-proprietary UHPC mix that could replace proprietary UHPC without affecting the structural behavior of such connections. The non-proprietary UHPC mix was developed through the first phase of this project. The mix development and pullout tests conducted in the first phase of this project are discussed in Subedi et al. (2019). The large-scale column tests and demonstration for seismic performance of the ABC connections were carried out in the second phase of the project discussed in this report. It is noted that the non-proprietary UHPC mix developed in this study is less expensive and has lower compressive strength than the proprietary mixes. Furthermore, the UHPC mix was developed using locally available materials from California and Nevada. Details on the mix design can be found in Subedi et al. (2019). However, a comprehensive summary of the mix and a study on the effect of material variability are included in chapter 2 of this document for completeness.

## 1.2. Previous Studies

Many bridge substructure and superstructure members can be built offsite and then assembled on-site through using different types of precast connections. In high seismic zones, these connections are very critical and need to be well designed and constructed to be able to emulate the CIP connections. To produce emulative systems, ABC connections should maintain their load capacities while undergoing large cyclic deformations of adjoining members. This is even more challenging for bridge columns since these elements are required by most of the design specifications to undergo high plastic deformations during large seismic events. This study focuses on earthquake-resistant ABC connections for bridge columns using grouted ducts.

Marsh et al. (2011) investigated the seismic performance of seven types of precast column connections in moderate and high seismic regions: (1) bar couplers, (2) grouted ducts, (3) pocket connections, (4) member socket connections, (5) hybrid connections, (6) integral connections, and (7) emerging technologies. The authors showed that the precast concrete bridge pier systems have developed an emulative seismic behavior to the monolithic systems and they undergo similar damage to the monolithic systems due to the formation of plastic hinges in columns. A comprehensive literature review on the description of these seven types of connections beside their available experimental studies was conducted and presented by Tazarv and Saiidi (2014). For the purpose of the study presented herein, an updated literature search is conducted on the grouted-duct connections to include recent efforts done towards the implementation of this type of connection. The previous studies could be categorized into two main groups, the first group include the studies done to estimate the required development length for the rebars inside the ducts to ensure the bar fracture outside the duct zone through the pullout tests. The second group includes the experimental testing of large-scale columns incorporating the grouted-duct connection in their column-footing connections.

### *1.2.1. Pullout tests*

An extensive literature review on this type of pullout test is conducted and presented in Tazarv and Saiidi (2014), Shrestha et al. (2018), and Subedi et al. (2019). For completeness, a brief summary is adopted from the literature review provided in those studies and presented first. Matsumoto et al. (2001) carried out eight pullout tests. The tested parameters were the embedment length ($8.5d_b$, $12.8d_b$ and $17d_b$, where $d_b$ is the bar diameter), gout brand and bar anchorage (straight and headed bars). The authors concluded that the normalized bond strength of grout-filled duct system is 2.5 times stronger than conventional connections. Raynor et al. (2002) investigated the bond behavior of reinforcing bars anchored in grouted ducts and subjected to cyclic loading through 13 pullout tests. The tested parameters were the bar sizes. The test results showed that the normalized bond strength provided by grouted ducts was higher than that of conventional concrete. It was found that slippage of the bar from the grout was due to compressive failure of concrete against the bar ribs, which is in contrast with the radial bond cracks observed in pullout test of bars in concrete with no ducts.

Brenes et al. (2006) conducted 32 pullout tests to investigate the effect of varying the embedment length, duct material, number of ducts, bar coating, and bar eccentricity in the ducts. Test results showed that the galvanized steel ducts showed greater initial stiffness of bond-slip curves than the plastic ducts and that the embedment length has a minor effect on the initial stiffness of the system. The multiple duct tests showed less bond strength than that of a single duct test with minor difference in the initial stiffness. The test results of all the galvanized steel ducts showed that almost all the pullout tests, the grout fractured because of the lack of sufficient tensile strength of grout. Steuck et al. (2008) carried out a total of 17 pullout tests of large-diameter bars embedded in the grout-filled pipes/ducts. The tested parameters were the bar size, embedment length, grout type, and specimen scaling. The results showed that the bar size, adding fibers to grout and the specimen scale have minor effect on the bond behavior and the bond strength. It is also proved that embedment length of 6 bar diameters is sufficient to yield the rebars and 14 bar diameters is sufficient to fully anchor the bar to fracture.

Tazarv and Saiidi (2014) conducted 14 pullout tests to determine the bond strength of proprietary UHPC filled duct connections. the tested variables were the embedment length, bar size, duct diameter, number of ducts and bar bundling. The bar bundling, bar size and the presence of multiple ducts were proved to have insignificant effects on the bond strength unlike the duct size. The pullout tests showed that the bond strength of UHPC was eight times stronger than that in conventional grout and the required development length of the bars in the UHPC filled ducts can be reduced by 50% of the grouted-ducts. Based on the test data, equations for estimating the development length of bars in UHPC-filled ducts are proposed. Galvis et al. (2015) tested 18 pullout specimens of two or three bundled #8 bars and inserted in a 4 in. diameter galvanized steel ducts filled with grout. The test variable was the embedment length. It was shown that an anchorage length of $16.8d_b$ is enough for bundled bars to develop bars fracture without any bar or duct pullout, where $d_b$ is the sum of the bars diameter in the same bundle. Shrestha et al. (2018) tested 12 pullout specimens of #10 bars inserted in grout filled steel ducts. The tested parameters were embedment length, duct size, duct thickness, bar-eccentricity, and bar bundling. The measured response was found to be sensitive to the embedment length, bar bundling and eccentricity. The authors developed equations for the anchorage length based on their test results and another data from 31 other previous pullout tests.

Through the first phase of this research project, Subedi et al. (2019) provided the development of two non-proprietary UHPC mixes using local California and Nevada materials among other domestically produced ingredients such as steel fibers. The developed mixes were first used to carry out an extensive experimental study on the pullout behavior of bars inserted in non-proprietary UHPC filled ducts. The experimental study consisted of 22 pullout tests of #10 bars inserted in the UHPC filled ducts. The test variables were the embedment depth, single versus bundled bars, duct sizes, the non-proprietary UHPC mix and the material of the ducts. Moreover, the tests also compared the anchorage behavior of the developed mixes with the commercially available UHPC and standard grouts; the other alternatives in such connections. All rebars were eccentrically placed into the ducts to emulate more practical field and worst-case conditions. Based on the tests results, development length equations of rebars eccentrically placed in galvanized steel corrugated ducts filled with UHPC have been revised and presented for the developed non-proprietary UHPC. It is noted that the non-proprietary UHPC mix developed at the University of Nevada, Reno is approximately one-half the price of the proprietary UHPC, and the mix was demonstrated to provide the same anchorage behavior as the proprietary one, even though its compressive strength was approximately 30% lower than that of proprietary UHPC.

### *1.2.2. Columns with grouted-duct connection tests*

Matsumoto et al. (2001) tested a full-scale precast cap beam connected to a column using the grouted-duct system. The column was reinforced longitudinally with 4 epoxy-coated bars of #9 diameter and transversely with #3 spirals spaced at 4 in. resulting in reinforcement ratios of 0.57% for the former and 0.46% for the latter. The column clear height was 24 in while the diameter was 30 in. The embedment length of the bars in the ducts was 15 in. The specimen was tested using two vertical and one horizontal loading rams to obtain the load-deflection of the connection at the service and failure levels under different moment demands. The test results showed that the grouted-duct connection exhibited the same load-deflection response as the cast-in-place column model with the same expected strength, ductility, and bar anchorage.

Pang et al. (2008) did a comparative experimental study between 40% scale models of CIP and grouted-duct connection with the same scale and reinforcement ratios. The column diameter and height were 20 in and 60 in, respectively. The columns were tested under 8% axial load ratio and cyclic lateral loading till failure. The test results showed that the behavior of the grouted-duct connection was the same as the CIP connection. Both columns exhibited the same failure mode of bars buckling then bars rupture. The only observed difference between both columns is that the CIP column model had better crack distribution along the column than the precast connection which was observed to have a concentrated one large crack at the column-beam interface. Restrepo et al. (2011) tested a series of 42% scale column-cap beam connection incorporating different ABC techniques suitable for seismic zones. One of these connections was utilizing the grouted-ducts (GD). The column height was 45 in. while the column diameter was 20 in. The specimen was tested under cyclic lateral loading. Test results showed that the GD column model exhibited an emulative behavior to the CIP column model with stable hysteretic behavior. the GD column model showed an acceptable ductile behavior with a displacement ductility of 8 which was approximately 80% of that of the CIP column model.

Belleri and Riva (2012) tested a column model utilizing the grouted-duct connection but the ducts were buried in the column and the rebars were protruding out of the footing. The column height was 126 in. and the column diameter was 15.75 in. The embedment length into the footing was 45.25 in. The test results showed that the grouted steel ducts are suitable to be used in seismic regions and can develop high ductile behavior. The authors also claimed that the post-seismic repair of these connection may be simpler than CIP or pocket foundation connections. The authors suggested to use an unbonded length of projecting bars at the column-footing interface to increase ductility and reduce damage. Popa et al. (2015) tested two sets of columns under two different axial load level under cyclic lateral loading till 5% drift ratio. Each set consisted of two precast columns utilizing the grouted-duct connection and one CIP column. The grouted ducts were buried into the precast columns while the bars were protruding out of the footing. The test results showed that a similar hysteretic response was for both, the precast and the CIP, specimens for each level of applied axial force. Furthermore, all the precast columns were observed to show less severe final damage state than that obtained for the CIP specimens

Tazarv and Saiidi (2015) investigated the seismic performance of a precast column utilizing the grouted-duct connection using UHPC instead of high strength grout as a filler. A half scale bridge column was tested under axial load and cyclic lateral loading and then its seismic behavior is compared to a similar CIP column. The authors concluded that the UHPC-filled duct connections are emulative of the conventional CIP column-footing connection as the plastic moment capacity of the column is developed and a high drift capacity is achieved without connection failures such as bar pullout, duct pullout or concrete breakout failure. The test results also showed that the mode of failure, base-shear capacity, and strength and stiffness degradation of this connection were nearly the same as those of CIP.

### 1.3. Objectives

The overall goal of the present study, as part of the larger project presented in Subedi et al. (2019) and this report, was to develop an alternative non-proprietary UHPC, evaluate its pull-out performance, and evaluate columns that utilize it in grouted-duct connection. This was done with the understanding that the compressive strength of the new UHPC could be about 30% lower than that of standard UHPC. Reducing the costs and using non-proprietary materials was the focus of the study to establish a less expensive, less restrictive alternative for ABC column connections. To achieve this goal, research was conducted to develop the mix and demonstrate its validity for anchorage behavior using pullout tests (phase one), then conduct large-scale column tests for ultimate validation of the material and connection (phase two).

The objective of phase two of the study was to conduct two half-scale column tests at UNR Earthquake Engineering Laboratory under axial and cyclic lateral loading to investigate the seismic performance of the columns. The column models implemented the grouted-duct connection detail and incorporated the non-proprietary UHPC developed at UNR. Thus, the objective of the tests was to evaluate the ability of the ABC columns to emulate the seismic performance of the CIP system. The two column models used the same detail and non-proprietary UHPC mix but varied in the longitudinal reinforcement debonding in the vicinity of the column-footing interface. Another objective was to conduct analytical investigation for the two column models using finite element computer program OpenSEES to assess modeling assumptions for the connections including both bond-slip and bar debonding effects and to determine the ability of the analytical to reproduce the measured results.

### 1.4. Report Outline

This report consists of six chapters. The report starts with an introduction to ABC techniques and the grouted-duct connection. Furthermore, an overview of relevant literature is presented in Chapter 1. The non-proprietary UHPC material properties with regards to the mix design, compressive, tensile, and flexural behaviors are shown in Chapter 2. The Design procedure, structural detailing, and testing loading protocol for the two bridge column model tests are provided in Chapter 3. Column test results for each individual model are presented in Chapter 4. The evaluation of column models performance by comparing their seismic behavior with a reference CIP column model and a PNC with proprietary UHPC column model is also presented in Chapter 4. The analytical investigation for each column model using OpenSEES with focus on the modeling assumptions for the connections that include the bond-slip and bar debonding effects are shown in Chapter5. A summary of findings and conclusions is presented in Chapter 6.

# CHAPTER 2. NON-PROPRIETARY UHPC MATERIAL PROPERTIES

## 2.1. Introduction

In a companion report summarizing the efforts conducted in phase one of this project (Subedi et al. 2019), the authors developed a non-proprietary UHPC mix using locally available material in the West of the United States, mainly from California and Nevada, that reduced the UHPC cost and sole-source problem without compromising the essential properties required for the grouted-duct ABC seismic connections. The authors presented two different non-proprietary UHPC mixes with two different sources of aggregates. The first type of aggregate is a river sand that is uncrushed while the second aggregate type is a blended concrete sand that is 100% crushed. The mix developed using the uncrushed aggregates (sourced from California) was designated as UNR-UHPC-A while the mix developed using the crushed aggregates (sourced from Nevada) was designated as UNR-UHPC-B. Subedi et al. (2019) evaluated the behavior of 22 full-scale UHPC-filled ducts with embedded #10 rebars under pull out forces using the developed UHPC A and B mixes. The authors evaluated the effect of embedment depth, single versus bundled rebars, duct sizes, and duct material. Moreover, the tests also compared the anchorage behavior of the developed mixes with the commercially available UHPC and standard grouts.

The non-proprietary UHPC mix chosen to be used and applied to the UHPC-filled duct connections of the precast columns presented herein in the second phase of the study was UNR-UHPC-B mix. The second mix type was selected because crushed aggregates are easier to source and use, especially since the two mixes proposed in Subedi et al. (2019) did not show any significant difference in the pull-out strength or behavior of the UHPC. In this study, two batches of the referenced UHPC mix were sampled to characterize the material properties. The two batches were used to construct two precast columns with sleeve ducts connection as presented and discussed in Chapter 4. In this chapter, the material characteristics of the non-proprietary UHPC used in the experimental program is presented and discussed with regards to the material preparation and mix ratios, sampling, compressive behavior, tensile behavior and flexural behavior. A variability study is presented and discussed in this chapter to show the effect of mixing errors of the different mix constituents on the overall compressive strength of the mix.

## 2.2. Mix Design and Preparation

The materials used in the developed non-proprietary mix are cement, crushed aggregates, silica fumes, high range water reducer agents (HRWRA), steel fibers, and water. The mixing proportions used for the UHPC mix are shown in Table 2.1. Detailed information on the mix ingredients and mixing procedure is presented and discussed in Subedi et al. (2019).

Table 2.1 Non-Proprietary UHPC Mixing Proportions

| Material | Manufacturer | Description | specific gravity | batch mass (lb/ft3) | Batch mass (%) | Batch volume (%) |
|---|---|---|---|---|---|---|
| Cement | Nevada cement | Portland I/II | 3.15 | 58.18 | 37.8 | 29.6 |
| Fine aggregates | Martin Mariata (Spanish springs, NV) | Concrete Sand (passing #30 & retained #200) | 2.634 | 59.44 | 38.6 | 36.5 |
| Steel fibers | Nycon | 0.2mm D & 13mm L | 7.8 | 10.07 | 6.6 | 2.1 |
| Silica fume | BASF | MasterLife SF 100 | 2.2 | 11.26 | 7.3 | 8.2 |
| HRWRA | BASF | MasterGlenium 7920 | 1.076 | 1.63 | 0.9 | 2.1 |
| Water | UNR | Potable water | 1 | 13.44 | 8.7 | 21.5 |

## 2.3. Compressive Behavior

For compressive strength and behavior evaluation, two different sizes of compression test specimens were considered in this study: 3×6 in and 4×8 in cylinders. The material specimens were taken from each of the two batches and were tested according to ASTM C39 at the age of 14 days, 28 days, and at the columns' test days. The 28-day test cylinders were instrumented during the compression test to obtain the full stress-strain relationship according to ASTM C469: "Standard Test Method for Static Modulus of Elasticity and Poisson's Ratio of Concrete in Compression". The surface of the UHPC cylinders was prepared by making a rough cut by a saw machine to remove the weak surface crust formed on the top of the cylinder then grinding the surface to get smooth flat surfaces at the two ends for accurate strength evaluation as illustrated in Figure 2.1. For compression testing, a force-controlled universal testing machine with capacity of 500 kips was used and the applied loading rate was adjusted to be in the range of 15 kip/min (35 psi/sec). The test setup for compression tests is shown in Figure 2.2(a) and a sample of the tested cylinders, where the damage can be illustrated, is shown in Figure 2.2(b). The stress strain curves for the six 3×6 in and three 4×8 in cylinders of the two batches are shown in Figure 2.3. It can be observed from the Figure 2.3 that UHPC exhibited reasonable strain capacity and ductility after reaching the ultimate strength. It is also noted that the progression of damage and crushing did not exhibit a sudden explosive mode as conventional concrete, but rather more controlled damage as reflected by the post-peak behavior shown in Figure 2.3. A summary of the cylinders strength values along with their corresponding strains is provided in Table 2.2.

Figure 2.1 UHPC Cylinders Preparation.


Figure 2.2 UHPC Cylinders Compressive Testing; (a) Test Setup and (b) Cylinders Compression Damage.

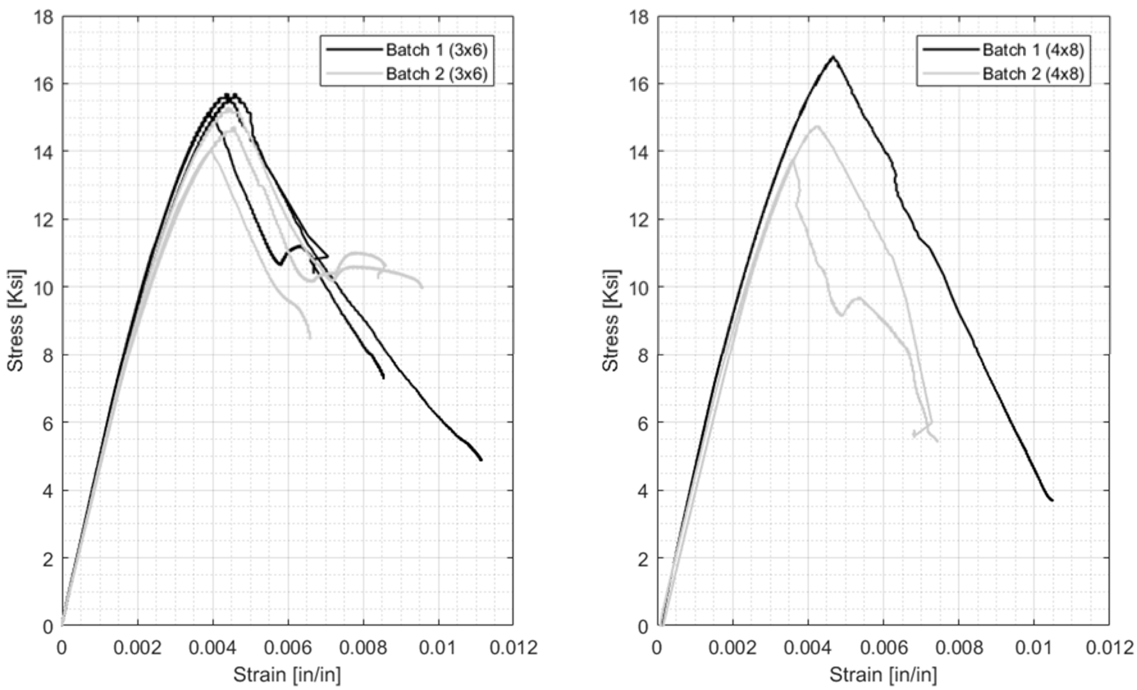


Figure 2.3 Compressive Stress-Strain Relationship; (Left) 3X6 in. cylinders and (Right) 4X8 in. cylinders.

Table 2.2 UHPC Cylinders Compressive Strength at 28 days

| Batch # | Sample Size | Sample # | Max Strength $f_{co}'$ (ksi) | Max Strain $\eth_{co}$ (%) | Ultimate Strength $f_{cu}'$ (ksi) | Ultimate Strain $\eth_{cu}$ (%) | Average $f_{co}'$ (ksi) | Average $f_{cu}'$ (ksi) |
|---|---|---|---|---|---|---|---|---|
| B 1 | 3X6 in. | S1 | 15.71 | 0.46 | 7.26 | 0.85 | 15.84 | 6.63 |
| | | S2 | 15.71 | 0.44 | 4.85 | 1.11 | | |
| | | S3 | 15.15 | 0.39 | 10.77 | 0.67 | | |
| | 4X8 in. | S4 | 16.8 | 0.47 | 3.66 | 1.05 | | |
| B2 | 3X6 in. | S5 | 14.03 | 0.39 | 8.45 | 0.66 | 14.51 | 8 |
| | | S6 | 14.72 | 0.46 | 10.23 | 0.84 | | |
| | | S7 | 15.29 | 0.45 | 9.95 | 0.96 | | |
| | 4X8 in. | S8 | 13.77 | 0.36 | 5.4 | 0.74 | | |
| | | S9 | 14.73 | 0.43 | 5.98 | 0.73 | | |

## 2.4. Flexural Behavior

The flexural strength test or also referred to as modulus of rupture test is considered an indirect way to express tensile strength. Thus, flexural tests were conducted here for the two UHPC batches and modulus of rupture was calculated in accordance with ASTM C78 “Standard Method of Test for Flexural Strength of Concrete (Using Simple Beam with Third-Point Loading)”. For each UHPC batch, four beams of 3×3×12 in beams were tested after 28 days with a bending span length of 9 in. A constant loading rate of 450 lb/min was applied until the rupture occurred. The typical flexural test setup and the UHPC flexural beams failure are shown in Figure 2.4. The modulus of rupture is the stress calculated in the tensile face of the beam specimen at maximum bending moment assuming linear-elastic behavior. The results of these tests are provided in Table 2.3.


Figure 2.4 Flexural Strength Test Setup (Left) and Typical UHPC beam Failure (Right).

Table 2.3 UHPC Cylinders Modulus of Rupture at 28 days

| Batch # | B1 | | | | B2 | | | |
|---|---|---|---|---|---|---|---|---|
| Specimen # | S1 | S2 | S3 | S4 | S1 | S2 | S3 | S4 |
| Flexural Strength (ksi) | 1.86 | 1.66 | 1.69 | 1.79 | 2.37 | 2.85 | 1.79 | 1.84 |
| Average Strength (ksi) | 1.75 | | | | 2.21 | | | |
| Coefficient of Variation | 5.26% | | | | 22.6% | | | |

From the table above, it is shown that the average flexural strength of both batches was almost 2 ksi after 28 days. The conducted flexural tests used built-in instrumentation in the testing machine to obtain the full flexural stress-strain relationships for all beams from the two batches at 28 days, which are shown in Figure 2.5. Note that the displacements used to calculate the strain were measured at the testing machine head and thus, the initial slope was not straight until all the test machine parts and fixtures get in full contact.

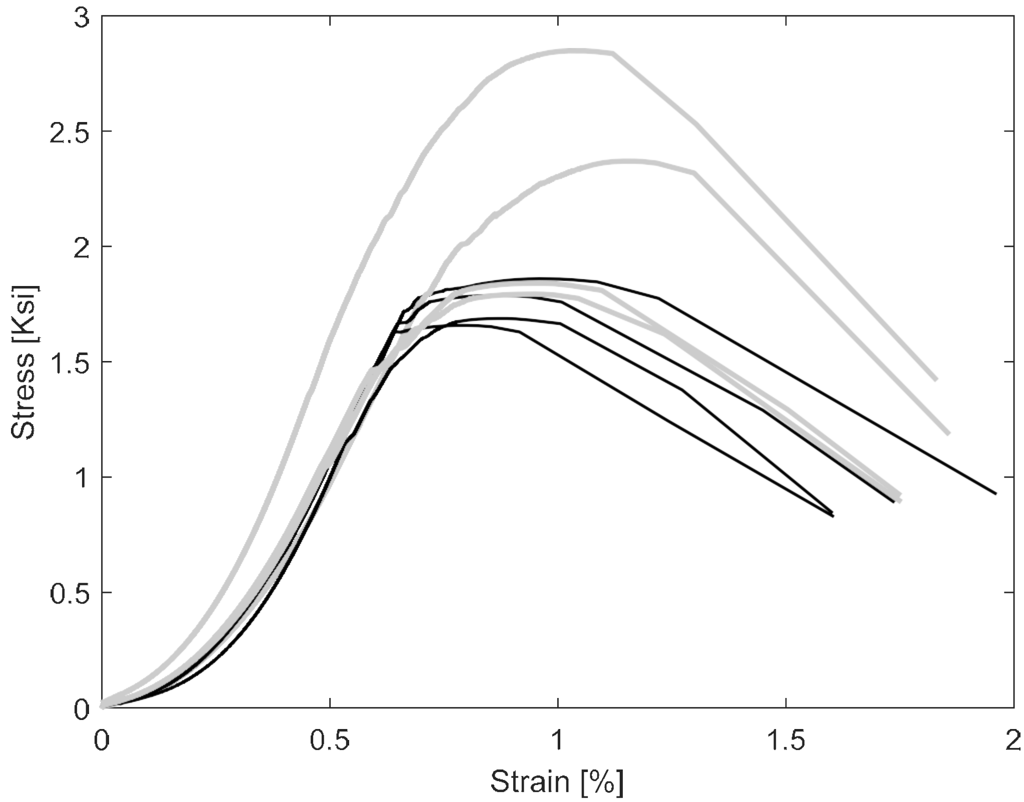


Figure 2.5 Flexural Stress-Strain Relationship for UHPC beams.

## 2.5. Tensile Behavior

To study the tensile behavior and obtain the direct tensile strength of the two UHPC batches, 12 dog bone specimens were tested under direct axial tensile stress until failure as shown in Figure 2.6. The dimensions of the 12 specimens and their distribution among the batches were as follows: four specimens of 1×1 in cross-section for the first batch; four specimens of ½ ×1 cross-section in for the first batch; and four specimens of 1×1 in for the second batch. Two cross-section sizes are used for the first batch in order to compare damage propagation in the two sizes and to measure the consistency of tensile strength results.

The specimens were anchored at two ends and were pulled under a constant displacement rate of 0.006 in/min until failure. To obtain the axial strain of the dog bone specimens, laser extensometer with a precision of 0.0001 in was used to measure the distance between two silver shiny stickers mounted on the middle quarter of the specimen height as shown in Figure 2.7. The dog bone specimens after the tensile failure are also shown in Figure 2.7. Almost all of the 1×1 in cross-section specimens showed multiple cracks before failure which stretched the portion of strain hardening further. However, the ½ ×1 in cross-section specimens had localized failure at only one section. This can be attributed to the fact the 1×1 in cross-section has more fibers engaged at the failure section than the ½ ×1 in, which helped transferring the crack localization from one section to another at different levels and improved the tensile ductility.

Figure 2.6 Direct Tension Test Setup.


Figure 2.7 The dog bone specimens after tensile failure.

The full stress-strain relationship for the UHPC dog bone specimens from the direct tension tests were obtained and plotted in Figure 2.8 for the 1×1 in cross-section specimens and ½ ×1 in cross-section specimens. The calculated 28-day direct tension strength values for both batches are tabulated in Table 2.4. Comparing the results of the ½ ×1 in specimens to the 1×1 in specimens of batch 1, it can be observed that although both cross-sections showed almost the same average strength, the 1×1 in. test specimens showed better consistency in the measured strength.

Table 2.4 UHPC Dog-bone Direct Tensile Strength at 28 days

| Batch # | B1 | | | | | | | | B2 | | | |
|---|---|---|---|---|---|---|---|---|---|---|---|---|
| Specimen # | S1 | S2 | S3 | S4 | S5 | S6 | S7 | S8 | S1 | S2 | S3 | S4 |
| Cross-section Dimensions (in.) | ½ × 1 in. | | | | 1 × 1 in. | | | | 1 × 1 in. | | | |
| Tensile Strength (ksi) | 0.46 | 0.62 | 0.79 | 0.92 | 0.70 | 0.66 | 0.83 | 0.74 | 0.82 | 0.65 | 0.82 | 0.68 |
| Average Strength (ksi) | 0.697 | | | | 0.732 | | | | 0.742 | | | |
| COV | 49.8% | | | | 17.2% | | | | 21.1% | | | |

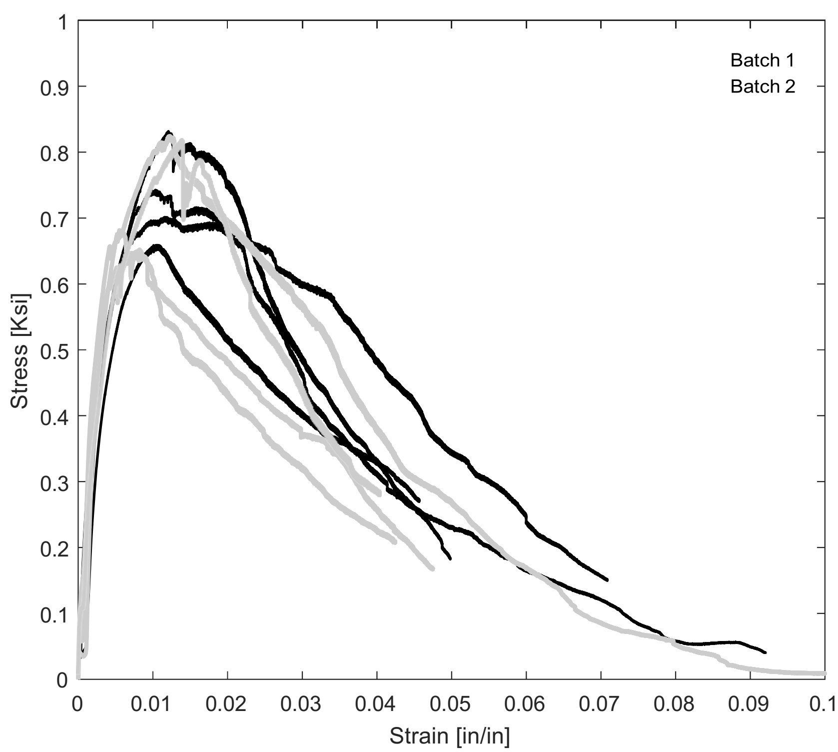


Figure 2.8 Direct Tension Stress-Strain Relationship of the 1x1 in Cross-section Specimens.

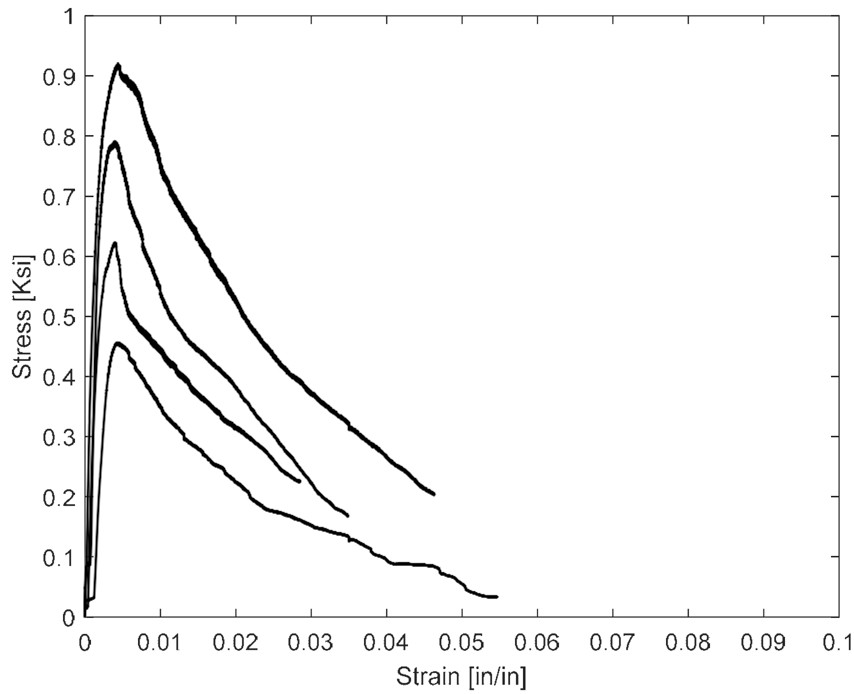


Figure 2.9 Direct Tension Stress-Strain Relationship of the ½ ×1 in Cross-section Specimens of Batch 1.

## 2.6. Variability Study

A variability study was conducted to show the effect of mixing errors of the different mix constituents on the overall compressive strength of the mix at the early strength (7-days) and standard 28-days strength. The mis-mixing or mixing errors are assumed to be resulted from unintentional errors or intentional mix modifications during mixing of the constituents. The errors percent was conservatively chosen to be 20% off the correct constituent portion based on a worst-case scenario. The assumed unintentional errors are decreasing the cement content by 20% or decreasing the fiber content by 20%, while the intentional mix modification is increasing the water content by 20% to increase the mix flowability as an option to increase the mix flowability in highly reinforced structural members. To avoid increasing the water content, which usually decreases the compressive strength, an increase in the HRWRA content was also considered where it was observed that 30% increase in HRWRA is equivalent to 20% increase in the water content for having the same flow as determined by the static flow test according to ASTM C 230.

The variability study was conducted by pouring five batches (see Figure 2.10 for typical batch illustration). The first batch was the original mix without any errors while the other 4 batches represented the different errors mentioned earlier and shown in Table 2.5 below. It is worth noting that all of the batches were mixed by using a high-shear hand mixer and sampled in 3×6 in cylinders where all the cylinders were subjected to the same environmental conditions until their test dates. The mixing proportions of the five batches are shown in Table 2.5 along with their corresponding static and dynamic flow test results according to ASTM C 230. Table 2.6 shows the results of the compressive strength of the 3×6 in cylinders at 7 days and 28 days. The compressive strength values represents the average of three cylinders tested at the same age.

Figure 2.10 Variability Study Mixing, Flow Testing and Sampling.

Table 2.5 UHPC Mixing Proportions for the Variability Study.

| Batch # | | 1 | 2 | 3 | 4 | 5 |
|---|---|---|---|---|---|---|
| Description | | Original mix | Cement decrease by 20% | Fibers decrease by 20% | Water increase by 20% | HRWRA increase by 30% |
| Constituents mass* (lb) | Cement | 58.18 | 46.54 | 58.18 | 58.18 | 58.18 |
| | Fine Agg. | 59.44 | 59.44 | 59.44 | 59.44 | 59.44 |
| | Steel fibers | 10.07 | 10.07 | 8.056 | 10.07 | 10.07 |
| | Silica fumes | 11.26 | 11.26 | 11.26 | 11.26 | 11.26 |
| | HRWRA | 1.63 | 1.63 | 1.63 | 1.63 | 2.12 |
| | Water | 13.44 | 13.44 | 13.44 | 16.13 | 13.44 |
| Flow test (in) | Static | 7.75 | 8.25 | 7.75 | 9.75 | 9.50 |
| | Dynamic | 8.5 | 9.25 | 8.75 | N/A | N/A |

* The constituents' mass is based on a 1 $ft^3$ batch size.

Table 2.6 Compressive Strength Results of the Variability Study.

| Batch # | Description | 7-day strength (ksi) | % difference from Batch 1 | 28-day strength (ksi) | % difference from Batch 1 |
|---|---|---|---|---|---|
| 1 | Original mix | 13.12 | 0 | 16.29 | 0 |
| 2 | Cement decrease by 20% | 9.90 | -24.58 | 11.62 | -28.66 |
| 3 | Fibers decrease by 20% | 14.79 | +12.70 | 16.37 | +0.45 |
| 4 | Water increase by 20% | 11.65 | -11.20 | 13.94 | -14.41 |
| 5 | HRWRA increase by 30% | 13.24 | +0.86 | 15.32 | -5.98 |

From the compressive strength results shown in Table 2.6, the following can be observed: (1) decreasing the cement content by 20% has resulted in strength loss by approximately 25% and 29% for the 7-day and 28-days strength, respectively; (2) decreasing the fibers content by 20% has resulted in a strength gain of approximately 13% at 7 days and almost the same strength as the control batch at 28 days, but it is important to mention that decreasing the fibers content commonly result in decreasing of the tensile strength and tensile ductility; (3) increasing the water content by 20% has resulted in a strength loss of approximately 11% and 14% for the 7-days and 28-days strength, respectively; (4) increasing the HRWRA content by 30% has resulted in almost the same flow as increasing the water content by 20% with almost no strength loss at 7-days and only 6% strength loss at 28-days. Thus, from the variability study conducted in this section, it is concluded that: (1) decreasing the cement content is the most influential parameter with most adverse effect on the compressive strength; (2) decreasing the fibers content will not affect the compressive strength significantly but it will decrease the tensile strength and tensile ductility of the mix; (3) increasing the HRWRA content could be a better way to increase the mix flowability without affecting the compressive strength in highly reinforced members instead of increasing the water content.

# CHAPTER 3. EXPERIMENTAL PROGRAM DEVELOPMENT

## 3.1. Introduction

In the current seismic design philosophy, bridge columns are allowed to undergo inelastic deformations under earthquake loads while maintaining the integrity of the full bridge. In other words, the columns are the key elements of the bridge in terms of dictating the structural performance during extreme events, such as earthquakes, and the safety and serviceability after the event. When adopting ABC techniques, connections of the columns to adjacent members are challenging since connections should be able to transfer forces while undergoing large inelastic cyclic deformations.

Two almost half-scale bridge column models with UHPC filled duct connection to the footing, as shown in Figure 3.1, were designed and tested under axial and cyclic lateral loading at the University of Nevada, Reno (UNR). The objective of the tests was to investigate the seismic performance of duct filled ABC column-to-footing connections using no-proprietary UHPC. The varied parameter in the experimental program was investigating the effect of debonding the longitudinal rebars at the column-footing interface which is commonly known to have a better strain distribution at the plastic hinge region and improved ductile behavior than the fully bonded reinforcement. The two column models are labeled "S1-Bond" and "S2-Debond" for the fully bonded and debonded columns reinforcement, respectively.

Two more column models from the literature that were also tested at UNR were considered to serve as benchmark models as adopted from Haber et al. (2014) and Tazarv and Saiidi (2015). Since these models were half scale column models, they were slightly larger than the models in the study. All test models, previous and current, have the same longitudinal and transverse reinforcement ratios. The first column model presented by Haber et al. (2014) was a standard CIP column, while the second column presented by Tazarv and Saiidi (2015) and labeled as "PNC" was a precast column with a proprietary UHPC filled duct connection to the footing. The design of the column models of the present experimental study and the previous two benchmark columns are shown in Table 3.1. The design, construction, Instrumentation, test setup, loading protocol and the material properties of the two column models, i.e. S1-Bond and S2-Debond, are presented in this chapter. A short review of the benchmark CIP and PNC column models is also presented.

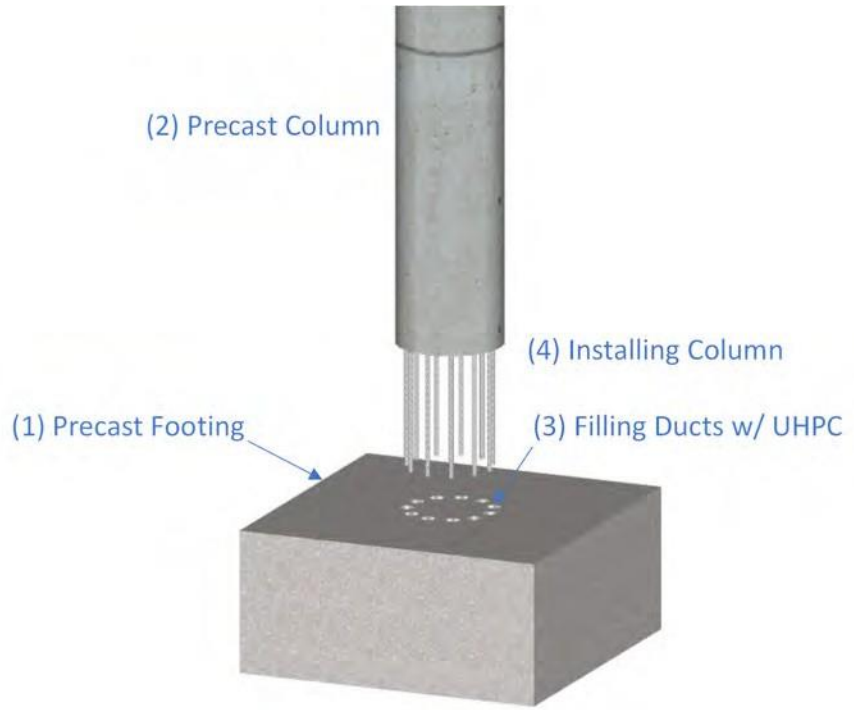


Figure 3.1 PNC Column w/ UHPC-Filled Duct Connection at Base (Adopted from Tazarv and Saiidi 2014).

Table 3.1 Summary of Column Models Design.

| Test | | Previous Research at UNR | | Present study | |
|---|---|---|---|---|---|
| Column model | | CIP | PNC | S1-bond | S2-debond |
| Study | | Haber et al. (2014) | Tazarv and Saiidi (2015) | This study | |
| Column-footing connection | | Monolithic connection | Proprietary UHPC filled ducts | Non-Proprietary UHPC filled ducts | |
| Debonding | | Do not exist | Exist | Do not exist | Exist |
| Column Dimensions | Diameter [in] | 24 | 24 | 20 | 20 |
| | Height [in] | 108 | 108 | 87 | 87 |
| | Aspect ratio | 4.5 | 4.5 | 4.35 | 4.35 |
| | Clear Cover [in] | 1.75 | 1.5 | 1 | 1 |
| | Anchorage [in] | N/A | 28 | 28 | 28 |
| Reinforcement | Longitudinal | 11-#8 | 11-#8 | 8-#8 | 8-#8 |
| | Ratio $\rho_l$ (%) | 1.92 | 1.92 | 2.01 | 2.01 |
| | Transverse | #3 @2in. | #3 @2in. | #3 @2.5in. | #3 @2.5in. |
| | Ratio $\rho_v$ (%) | 1.03 | 1.03 | 0.998 | 0.998 |
| Design Axial Load | Load (kips) | 226 | 200 | 157 | 157 |
| | Ratio | 10 | 10 | 10 | 10 |

## 3.2. Specimens Design and Construction

The cross section of the CIP and PNC column models was circular with a diameter of 24 in and their height were 108 in, while the cross section of the S1-Bond and S2-Debond column models was 20 in and their height were 87 in. It is noted that the height of the column is measured from the column-footing interface to the axis of the hydraulic actuator used to apply lateral loads. More details about each column is presented next.

### *3.2.1. CIP Column Model*

The CIP column presented by Haber et al. (2014) was a half-scale conventional cast-in-place column model and was designed based on Caltrans Seismic Design Criteria (SDC) version 1.4 (2006) with an aspect ratio of 4.5. The CIP column was constructed to represent a standard bridge column but with a thicker clear cover of 1.75 in. to account for the size of couplers to be used in other columns of the same study, as this column served as the reference column against which the precast columns were compared. The column was reinforced longitudinally with 11-#8 bars and transversely with #3 spirals at a 2 in pitch resulting in longitudinal and transverse steel ratios of 1.92% and 1.03%, respectively. The axial load index, which is the ratio of axial load to the product of column gross section area and the compressive strength of column concrete, was 10%. The specified compressive strength of concrete and yield strength of reinforcements were 5 ksi and 68 ksi, respectively. The column was initially designed for a minimum displacement ductility capacity of 5 but with the final detailing shown in Figure 3.2, the calculated displacement ductility capacity of the column was 7.

### *3.2.2. PNC Column Model*

A half-scale precast column model labeled “PNC” was constructed incorporating the UHPC-filled duct connection. The precast model had a similar geometry, bar size, and bar arrangement to CIP thus its performance was assumed to be emulative of the conventional construction. There was no additional design limitation for PNC with respect to CIP. The PNC column model is shown in Figure 3.3 and the base connection in detail is shown in Figure 3.4. The clear cover in the column was 1.5 in. Corrugated galvanized steel ducts with a nominal 3-inch diameter were used in the footing to be filled with UHPC. The confinement of the duct cage was similar to the column and was provided by #3 spiral spaced at a 2-inch pitch. The column longitudinal bars were extended 28 in at the base for insertion into the ducts. However, the required embedment length was only

19 in based on the design equations recommended for the proprietary UHPC bond length, assuming the concrete compressive strength is 5 ksi, the UHPC compressive strength is 20 ksi, and #8 bars had an ultimate strength of 110 ksi. The duct length was 1 in longer than the extended bar as a construction tolerance. To help spread bar yielding, 4 in of the column longitudinal bars were debonded above and below the column-footing interface as shown in Figure 3.4. Therefore, the effective bar embedment length in the UHPC-filled duct connection of PNC was 24 in, only 5 in. longer than the required development length. To minimize the precast column weight for transportation, hollow core circular section with a 6-inch wall thickness was used at initial stage of construction. After installing the column, the column core was filled with self-consolidating concrete (SCC).

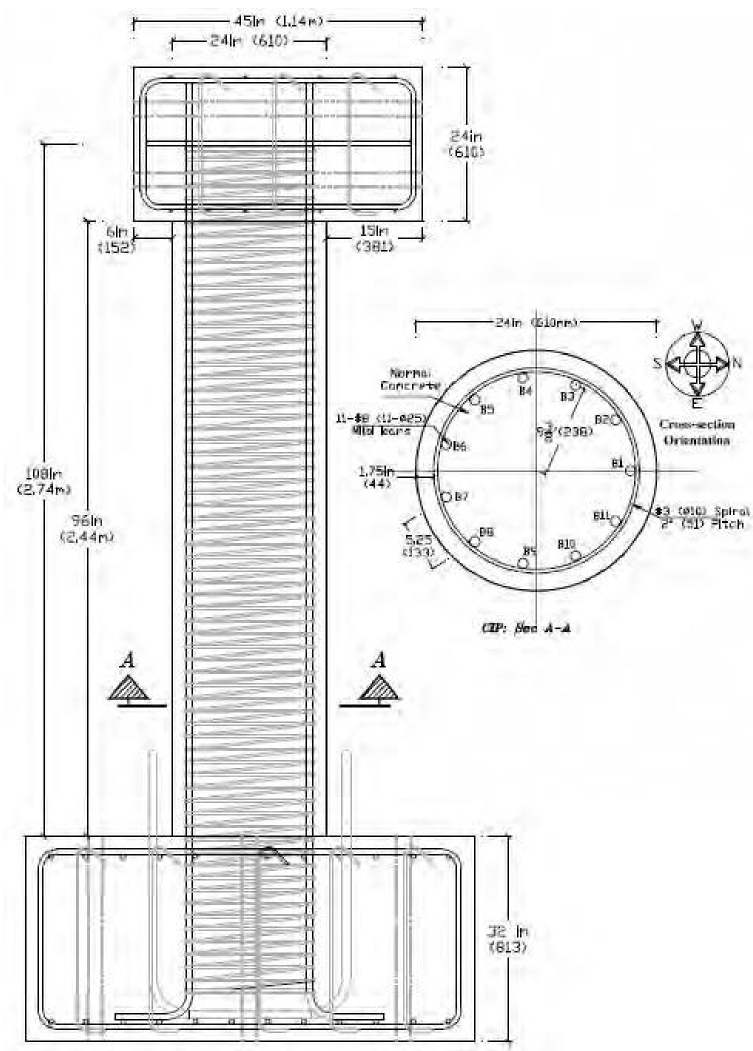


Figure 3.2 CIP Column Model by Haber et al. (2014) [Units: in (mm)] as presented in the study by Tazarv and Saiidi (2014).

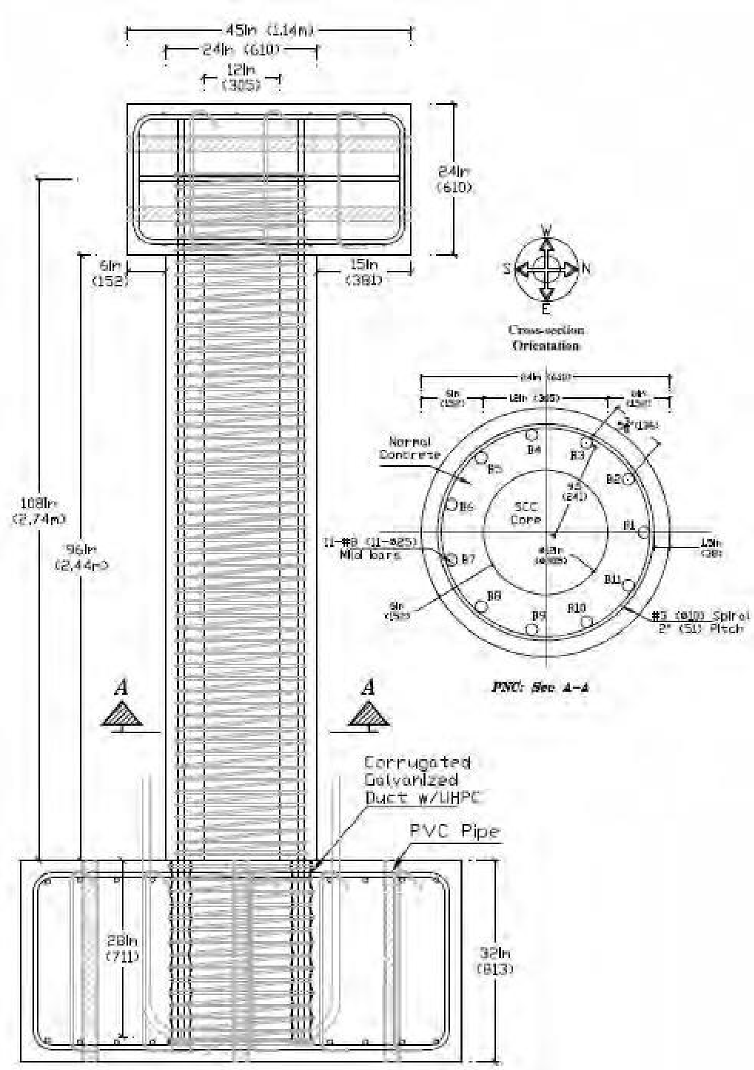


Figure 3.3 PNC Column Model [Units: in (mm)] as adopted from Tazarv and Saiidi (2014).

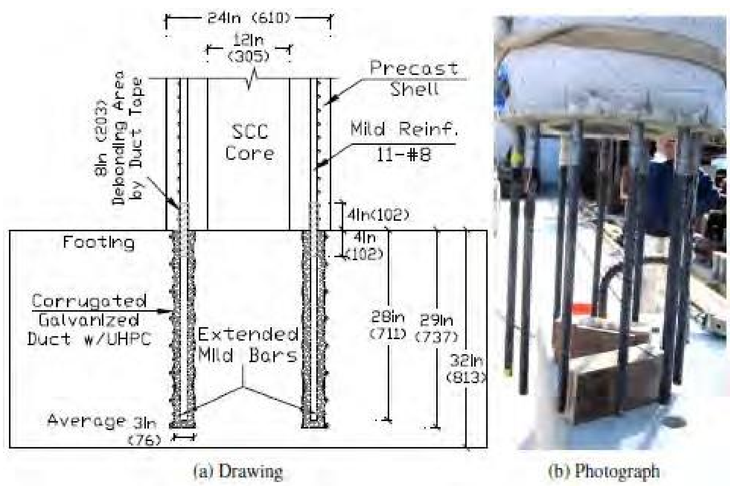


Figure 3.4 PNC Column Base Connection Detail (Adopted from Tazarv and Saiidi 2014).

### *3.2.3. S1-Bond and S2-Debond Column Models*

Two precast column models of exactly 5/12 scale (almost half scale) were constructed incorporating the UHPC-filled duct connection. The column dimensions shown in Figure 3.5 which are used for both test models, were chosen to have an aspect ratio almost equal to the CIP and PNC column models. The columns height was 87 in, measured from the column footing interface to the to the axis of the hydraulic actuator used to apply lateral loads, while the columns diameter was 20 in and the columns clear cover was 1 in. The precast columns were reinforced longitudinally with 8-#8 bars and transversely with #3 spiral at a 2.5-inch pitch resulting in longitudinal and transverse steel ratios of 2.01% and 0.99%, respectively, to represent similar ratios to the reference column models (CIP and PNC). The variation within the two columns was the debonding made to the longitudinal bars at the column footing interface region. For the S2-Debond column model, 4 in of the column longitudinal bars were debonded above and below the column-footing interface. The debonding was made to the longitudinal bars by wrapping a duct tape two times around the bar at the required location. The plan dimensions of the footing were 5×5 ft$^2$ and the depth was 32 in.

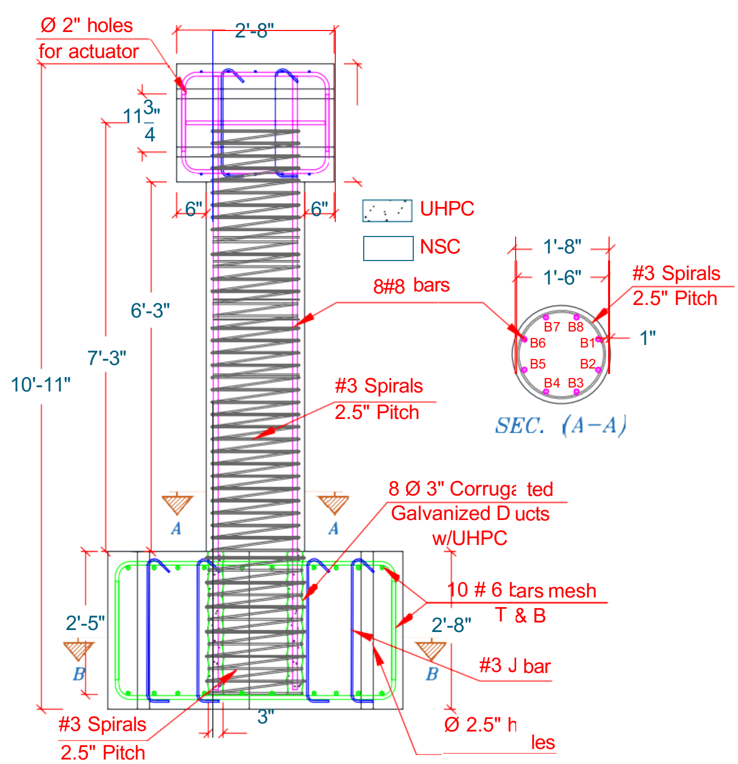


Figure 3.5 S1-Bond and S2-Debond Column Models.

Corrugated galvanized steel ducts with a nominal 3-inch diameter were used in the footing to be filled with the non-proprietary UHPC. The confinement of the duct cage was similar to the column and was provided by #3 spiral spaced at a 2.5-inch pitch. The embedment length of the column longitudinal reinforcement into the footing was the same as the PNC column model and was equal to 28 in. The ducts were kept in place during pouring process by using a wooden formwork pattern as shown in Figure 3.6.

Figure 3.6 Wooden Formwork Pattern to Keep the Ducts in Place While Pouring.

The construction stages of the column models are illustrated in Figures 3.7 through 3.10 and they are as follows:

(1) Casting the footing with ducts (Figure 3.7).
(2) Casting the precast column with extended longitudinal bars at the column base (Figure 3.8).
(3) Filling the ducts with UHPC using a tremie tube method (Figure 3.9).
(4) Installing the precast column in the footing through the ducts (Figure 3.10).

Although this was not adopted in this study, it is strongly recommended to use high strength grout or the UHPC overflow at the column-footing interface surface area when installing the column into the footing. This is to help keep the column leveled and eliminate any imperfections at the footing surface.

Figure 3.7 Precast Footings with Embedded Ducts.

Figure 3.8 Precast Columns with Extended Longitudinal Bars.

Figure 3.9 Casting UHPC into the Ducts using Tremie Tube Method.

Figure 3.10 Erecting and Installing the Columns in the Footings through Ducts.

## 3.3. Instrumentation Plan

Global and local responses of the tested column models were measured by 16 displacement transducers and string potentiometers. Strains of the reinforcements were measured by strain gages installed at different levels. Photographs of sample strain gages installed on bars and ducts are shown in Figure 3.11. Each specimen was instrumented with 48 reinforcement strain gages distributed along six levels in the column plastic hinge region and inside the footing to capture the longitudinal bars, transverse bars, and the embedded ducts strains as shown in Figure 3.12. The strain gages were labelled according to their position and their height levels. The notations of "N", "S", "E" and "W" stand for North, South, East and West directions, respectively, while the numbers following those notations denote the 6 levels of the strain gages, starting from level "1" at 6-inch below the column footing interface and ending with level "6" at 21-inch above the footing surface.


Figure 3.11 Installing Strain Gages on Bars and Ducts.

Rotations and curvatures of the columns at plastic hinges were measured by 12 vertical displacement transducers distributed onto six levels and placed at opposite faces of the columns in the loading plane as shown in Figure 3.13. The columns lateral displacements were measured by four displacement transducers (string potentiometers) installed on the column head. The applied lateral forces were measured by the actuator load cell.

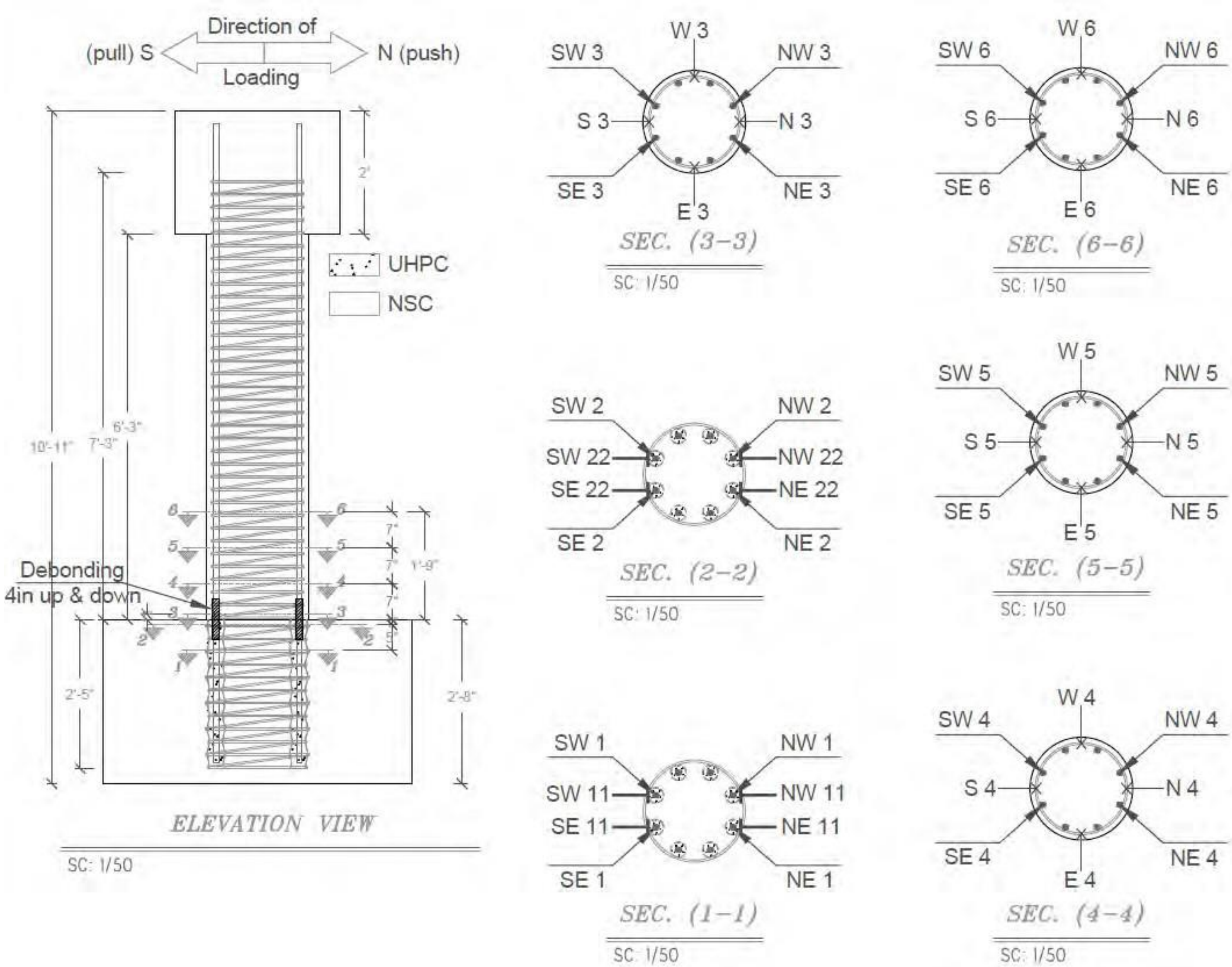


Figure 3.12 Locations of Strain Gages in S1 and S2 Column Models.

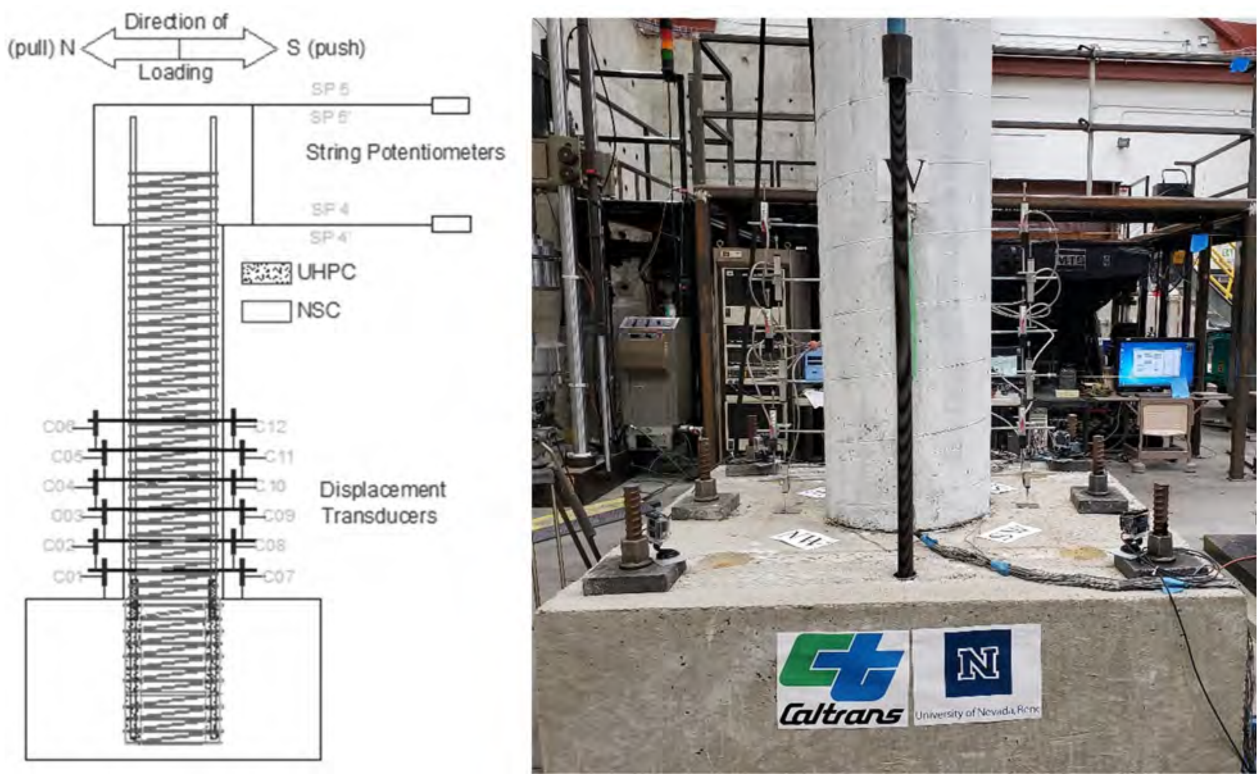


Figure 3.13 Displacement Measurement at Opposite Face of Columns in Plastic Hinge.

### 3.4. Test Setup and Loading Protocol

The columns were tested in a cantilever configuration setup as shown in Figure 3.14. Support for the actuator was provided by mounting it on the laboratory strong wall, while the specimen was fixed to the ground through prestressed bars attached to the laboratory strong floor. A 220-kip servo-hydraulic actuator was used to apply cyclic loads to the column models with displacement-controlled loading. Axial load was applied to the columns using two 200-kip hollow core jacks installed on a spreader beam perpendicular to the loading direction.

The column models were subjected to a 157-kip axial load and was kept constant during test. The axial load was equivalent to an axial load index of 10% based on the design column concrete compressive strength of 5 ksi at 28 days. The axial load index is the ratio of the axial load to the product of the column gross section area and the specified compressive strength of the concrete column. The cyclic loading protocol was adopted and matched from the previously tested CIP and PNC column models and is shown in Figure 3.15. Two full cycles were completed at each of the following drift ratio levels: 0.25%, 0.5%, 0.75%, 1%, 2%, 3%, 4%, 5%, 6%, 8%, 10%, and 12%. The drift ratio is the ratio of the lateral displacement to the height of the column measured from the top of the footing to the center line of the horizontal actuator. Two displacement rates of 1 in/min and 5 in/min were used in the test. The former was used for drifts below 3.0% and was chosen to be slow enough to allow online checking of strain values for the purpose of capturing the rebars yield. The latter rate was to measure the post-yield strength of the column models from 3% drift to failure. The rates were based on ASTM limits for strain rates of bar tests.

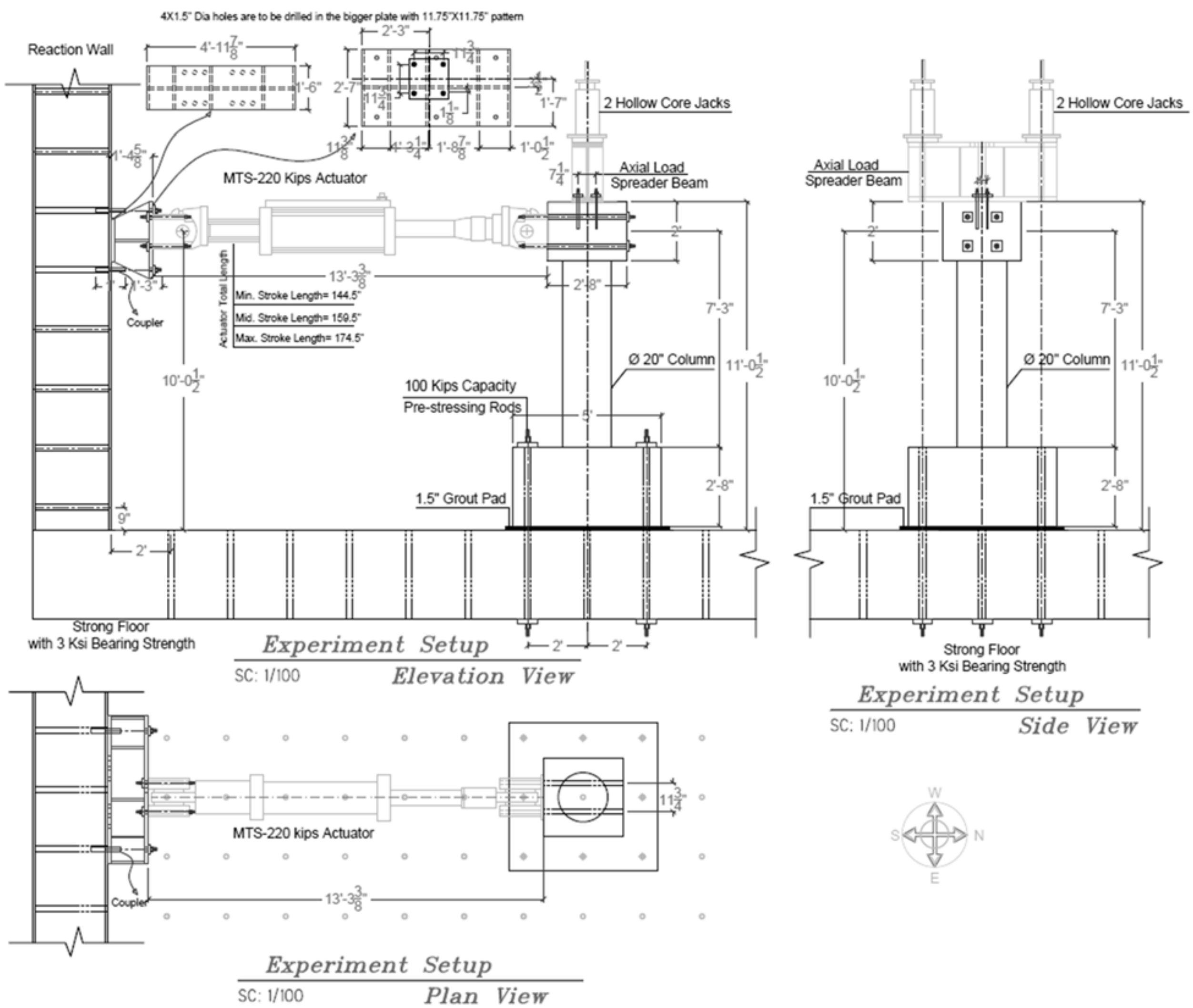


Figure 3.14 Column Test Setup under Combined Axial and Bending at UNR.

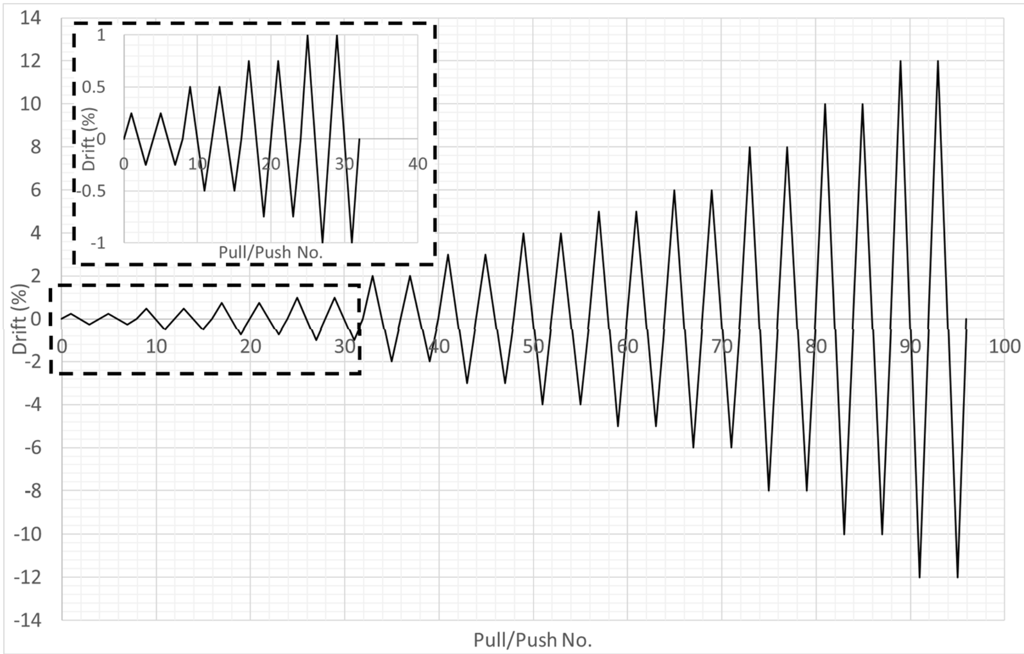


Figure 3.15 Cyclic Loading Protocol for Lateral Loading of the Column Models.

## 3.5. Measured Material Properties

In this section, the material characteristics of the conventional concrete, the non-proprietary UHPC, and the reinforcing bars are presented and discussed with regards to the material preparation, sampling, and mechanical strength (compression for concrete materials, and tension for steel).

### *3.5.1. Conventional Concrete*

Conventional normal strength concrete was used in the footings, the columns, and the columns hummer heads of both S1 and S2 column models. Two concrete batches were cast for the two column models: one for the footings of both models, and the other for the columns of both models. For each casting, nine cylinders of 6×12 in were sampled and tested at the following ages: 7 days, 28 days, and the column test day. Column S1was tested after 128 days from the column concrete pour, while Column S2 was tested after 131 days from the pouring day. Thus, both columns were considered to almost have the same concrete compressive strength and their test day strengths were measured at the test day of column S2. Table 3.2 presents the measured compressive strength for the conventional concrete of the different batches at the different ages. The concrete cylinders were tested according to ASTM C39/C39M-12 and only the average of at least three tested cylinders at each date is reported.

Table 3.2 Measured Compressive Strength of Conventional Concrete.

| Tested Batch | Age at Testing | Average Strength (ksi) |
|---|---|---|
| Footings | 7 days | 3.75 |
| | 28 days | 4.86 |
| | Test day | 7.02 |
| Columns | 7 days | 3.83 |
| | 28 days | 4.75 |
| | Test day | 6.18 |

### ***3.5.2. UHPC***

As previously discussed, the UHPC mix used in the column models was a non-proprietary UHPC developed at UNR through the first phase of this project (Subedi et al. 2019). As mentioned in Chapter 2 above, 3×6 in cylinders were used for the UHPC compressive test sampling molds. The UHPC cylinders were prepared and tested as previously discussed in chapter 2. At least three samples were used for the UHPC compressive testing at each testing date and for each batch but only the average of the test data is presented in Table 3.3. Two separate UHPC batches were used for the column models, and the batches compressive strength was comparable with an approximate difference of 6% at the test day.

Table 3.3 Measured Compressive Strength of non-proprietary UHPC.

| Tested Batch | Age at Testing | Average Strength (ksi) |
|---|---|---|
| S1-Bond | 7 days | 12.67 |
| | 28 days | 14.7 |
| | Test day | 17.14 |
| S1-Debond | 7 days | 14.47 |
| | 28 days | 15.5 |
| | Test day | 18.21 |

### *3.5.3. Reinforcing Bars*

Two types of reinforcing steel bars conforming to ASTM A615 and ASTM A706 were used in the models for the columns transverse and longitudinal reinforcing bars, respectively. The tensile test procedure used to determine the mechanical properties of reinforcing steel was done according to ASTM E8. Figure 3.16 shows a typical measured stress-strain curve for a #8 coupon from the columns longitudinal steel, and the summary of the average results from all #8 coupons are tabulated in Table 3.4.

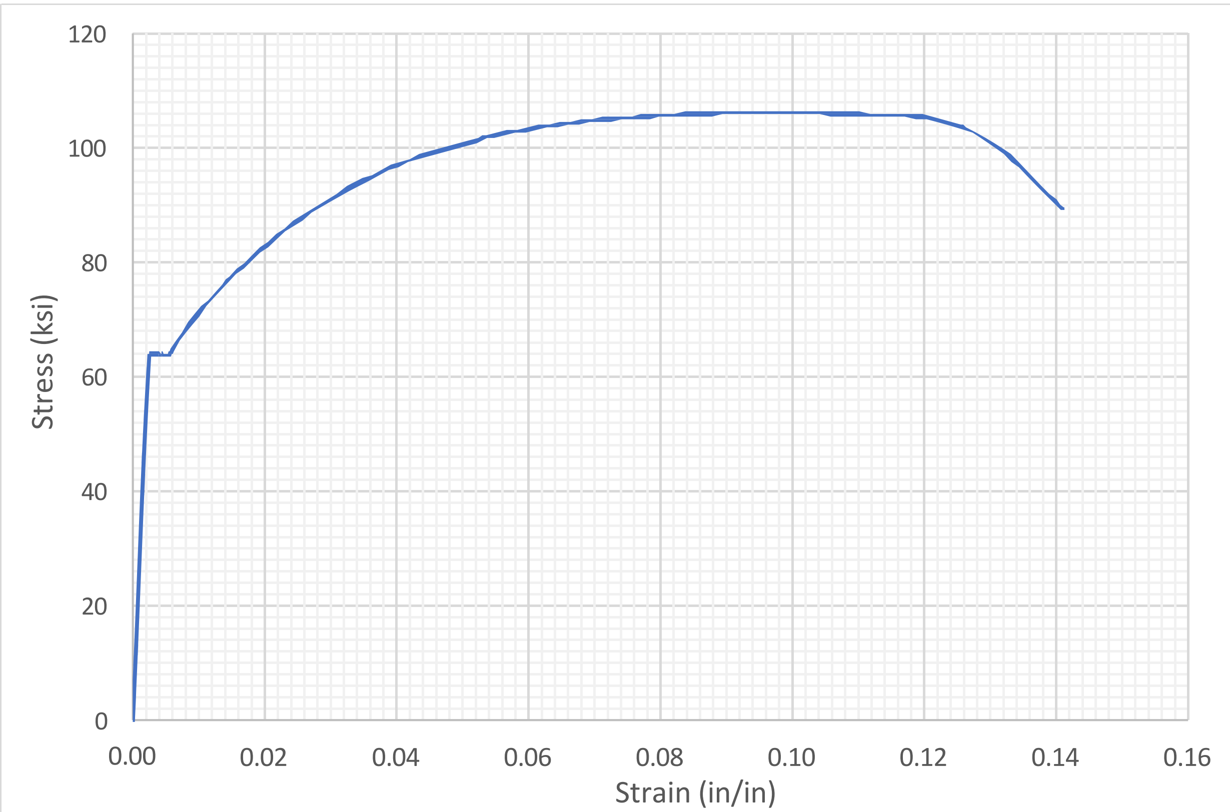


Figure 3.16 Stress-Strain Tensile Relationship of #8 Bars.

Table 3.4 Measured Tensile Properties of #8 Reinforcing Bars.

| #8 Bars | $f_y$ (ksi) | $ð_{Y}$ (ðð/ðð) | $ð_{sh}$ (ðð/ðð) | $f_u$ (ksi) | $ð_{U}$ (ðð/ðð) |
|---|---|---|---|---|---|
| | 64.05 | 0.0025 | 0.0055 | 106.41 | 0.141 |

# CHAPTER 4. TEST RESULTS AND DISCUSSION

## 4.1. Introduction

This chapter presents the experimental test results of specimens S1-Bond and S2-Debond with respect to their global and the local behavior perspectives. The chapter also provides a normalized comparison with the two previous columns tested at UNR as found in the literature, i.e. CIP and PNC columns. The test results include observed plastic hinge damage, force-displacement relationships, energy dissipation, residual drifts, strain profiles, curvature profiles, and moment-rotation relationships.

## 4.2. Columns Global Behavior

### *4.2.1. Plastic Hinge Damage and Mode of Failure*

The columns cross-section orientation and their longitudinal bars labeling were previously shown in Figure 3.5. The columns were loaded in the North-South direction. The push load was defined as the loading of the column from North to South while the pull load was designated to the loading from the South to North (Figure 3.14). The observed mode of failure for both columns started with complete concrete cover spalling, followed by longitudinal bar buckling then spirals fracture and finally longitudinal bars fracture above the column-footing interface during the 10% and 12% drift cycles. No damage of the UHPC-filled duct connection such as bar pullout, duct pullout, or concrete breakout failure of the footing was observed.

For specimen S1-Bond, flexural cracks were observed during the 0.5% drift cycles and minor shear cracks were observed during the 1% drift cycles. The column experienced its first bar yielding at bar B1 at 0.84% drift ratio during the 1% drift cycle at 28.57 kips lateral load. Concrete cover spalling was observed to start on the North and South sides of the column during the 3% drift cycle while complete cover spalling and rebars exposure were observed during the 8% drift cycles. The longitudinal bar B1 started to buckle in the first cycle of 10% drift cycle. The first bar fracture was observed on the South side of the column during the second cycle of 10% drift in bar B1 then the spirals fractured on the same side of the column. Afterwards, bars B5 and B6 on the North side of the column ruptured during the second cycle of 10% drift. Finally, bar B2 ruptured during the first cycle of 12% drift. The test was stopped after the rupture of the four bars, i.e. B1, B2, B5 and B6, before the rupture of the rest longitudinal bars for the test setup stability purposes and especially that the capacity of the column was already dropped below 80% of the maximum lateral load capacity. Figures 4.1 through 4.10 show the progression of damage at the plastic hinge region of the column at selected different drift ratios for specimen S1-Bond.


(a) North-East Side


(b) North-West Side


(c) South-East Side


(d) South-West Side

Figure 4.1 S1-Bond Plastic Hinge Damage, 0.5% Drift Cycle.


(a) North-East Side


(b) North-West Side


(c) South-East Side

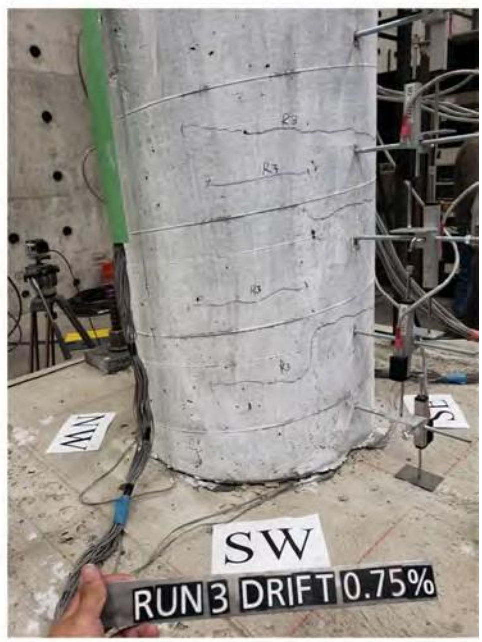


(d) South-West Side

Figure 4.2 S1-Bond Plastic Hinge Damage, 0.75% Drift Cycle.


(a) North-East Side


(b) North-West Side

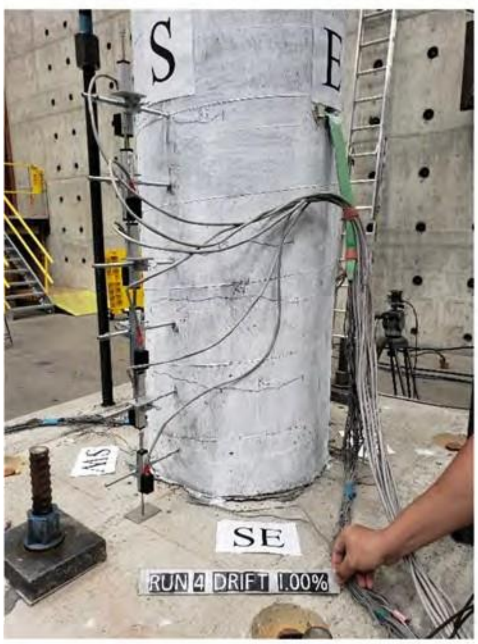


(c) South-East Side

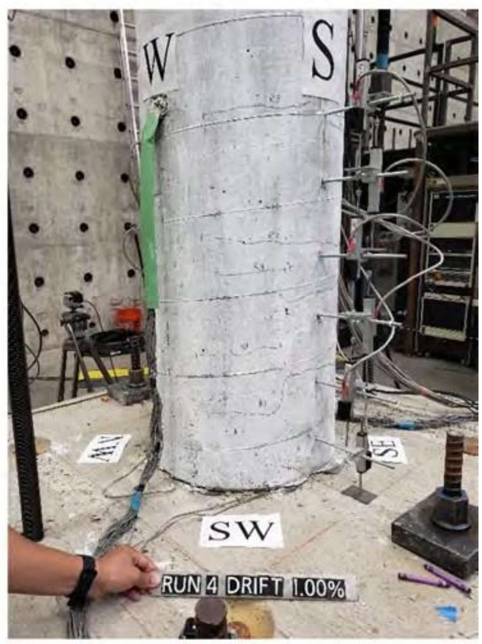


(d) South-West Side

Figure 4.3 S1-Bond Plastic Hinge Damage, 1% Drift Cycle.

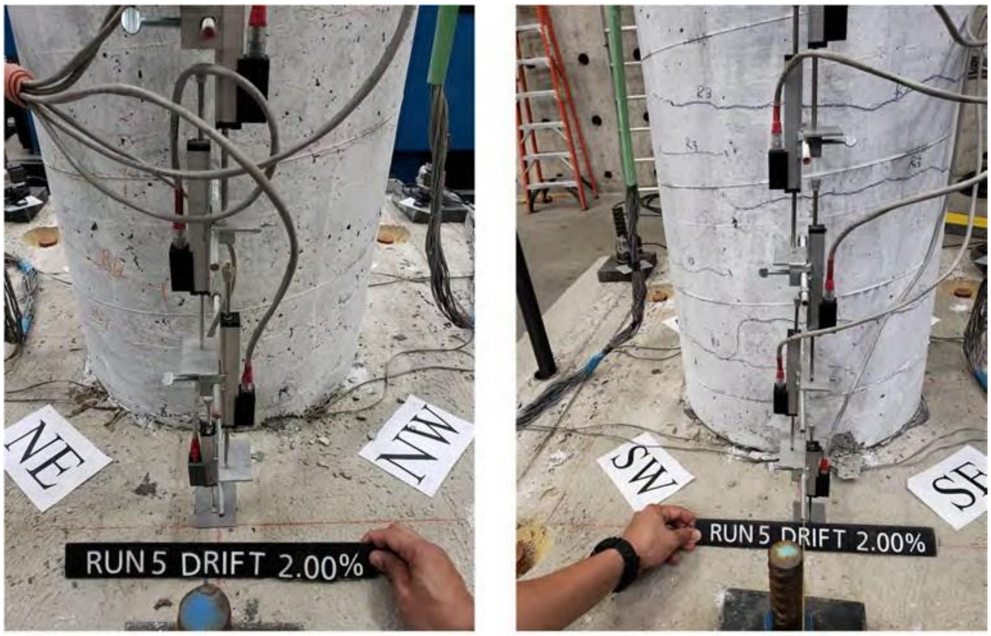


(a) North Side (b) South Side

Figure 4.4 S1-Bond Plastic Hinge Damage, 2% Drift Cycle.

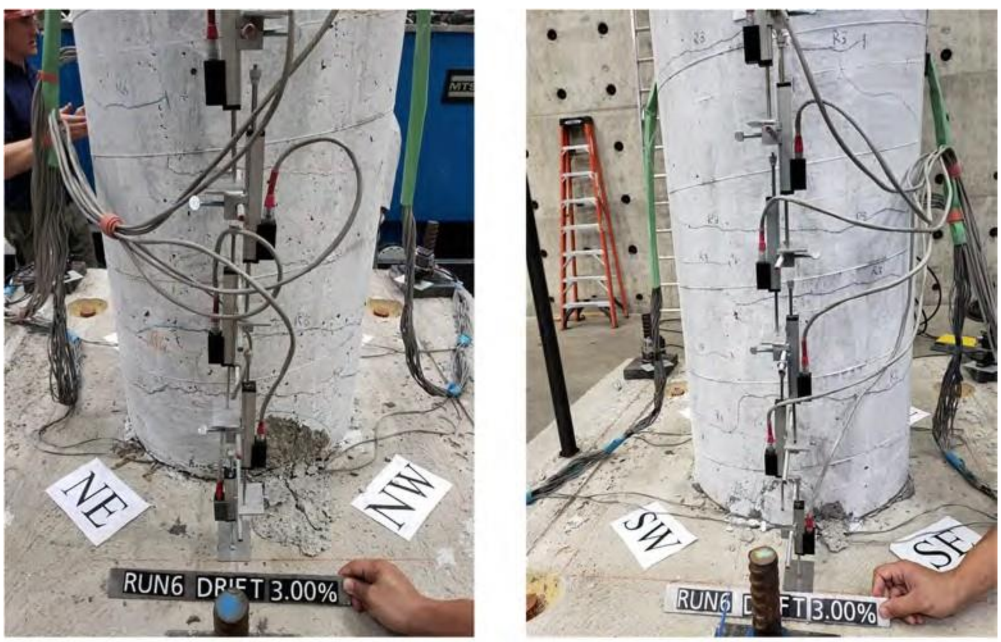


(a) North Side (b) South Side

Figure 4.5 S1-Bond Plastic Hinge Damage, 3% Drift Cycle.

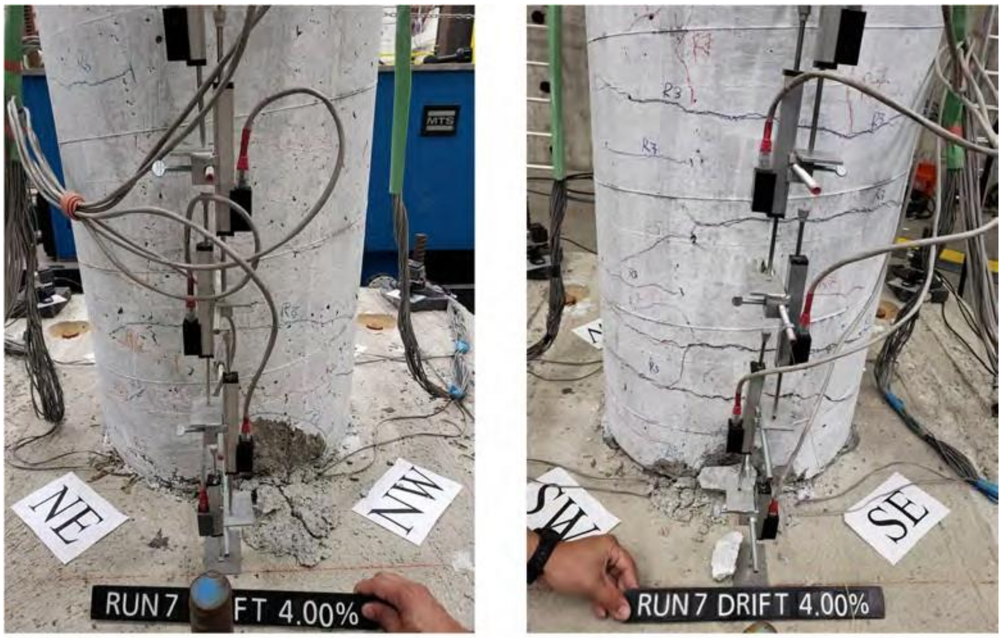


(a) North Side (b) South Side

Figure 4.6 S1-Bond Plastic Hinge Damage, 4% Drift Cycle.

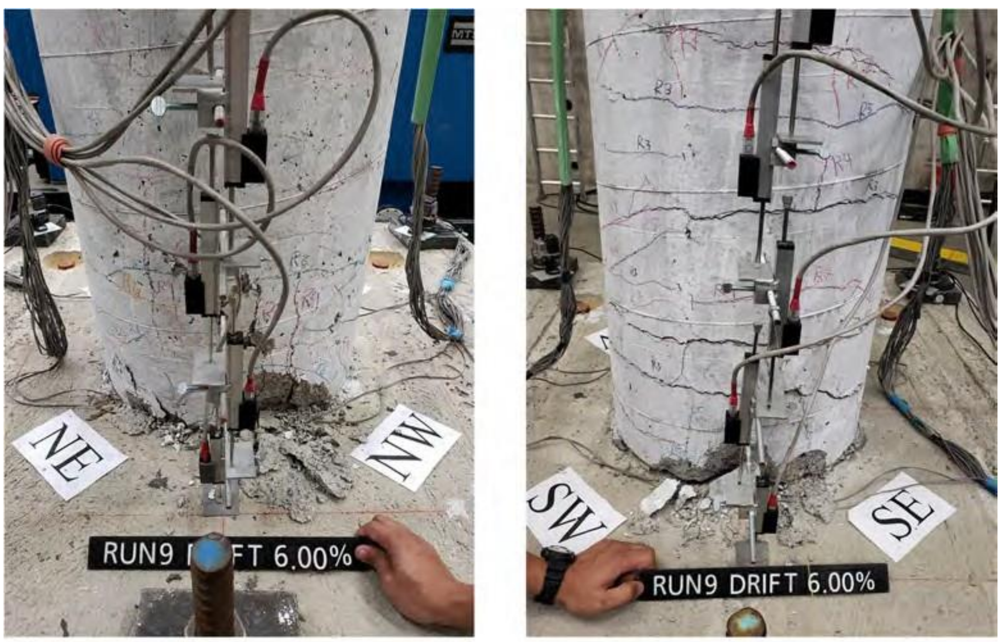


(a) North Side (b) South Side

Figure 4.7 S1-Bond Plastic Hinge Damage, 6% Drift Cycle.

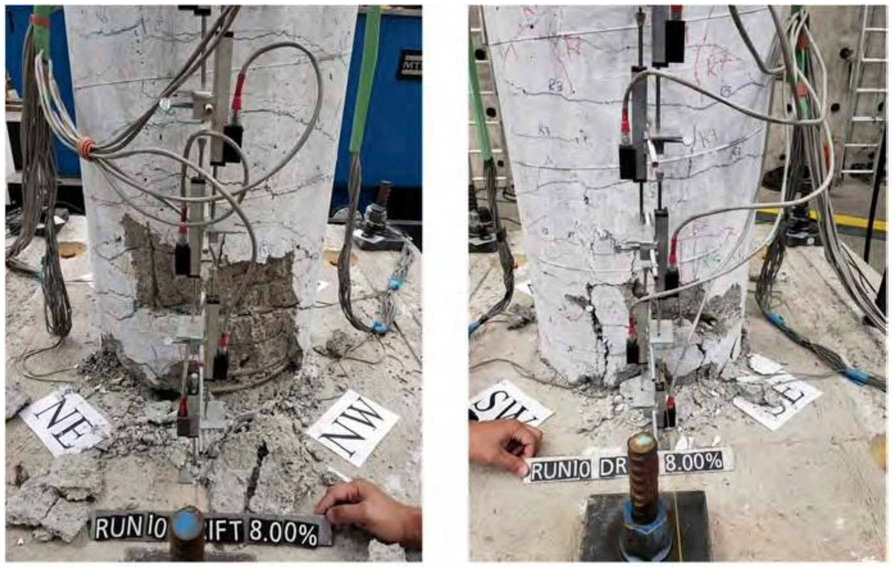


(a) North Side (b) South Side

Figure 4.8 S1-Bond Plastic Hinge Damage, 8% Drift Cycle.

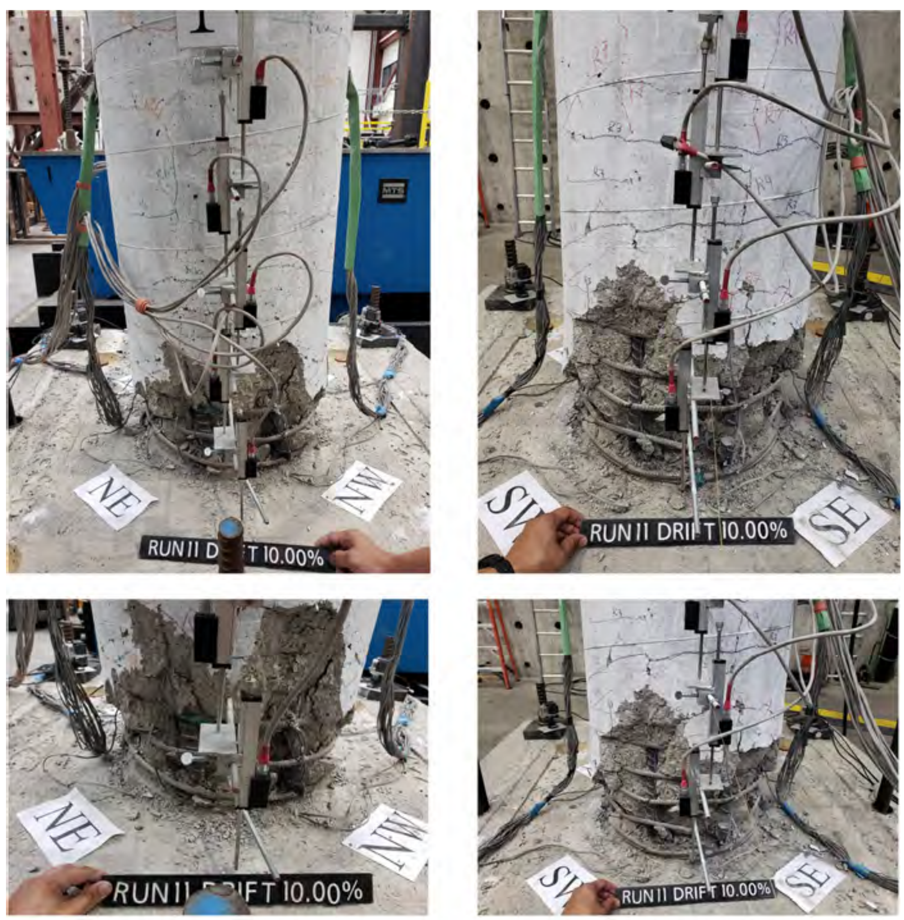


(a) North Side (b) South Side

Figure 4.9 S1-Bond Plastic Hinge Damage, 10% Drift Cycle.


(a) North-West Side (b) South-West Side

Figure 4.10 S1-Bond Plastic Hinge Damage, 12% Drift Cycle.

For specimen S2-Debond, flexural cracks were observed during the 0.5% drift cycles and again minor shear cracks were observed during the 1% drift cycles. The column experienced its first bar yielding at bar B2 at 0.79% drift ratio of 1% drift loading cycle at 21.63 kips lateral load. Concrete cover spalling was observed to start on the North-West side of the column during the 4% drift cycle while complete cover spalling and rebars exposure were observed during the 8% drift cycles. The longitudinal bar B1 started to buckle at the second cycle of 8% drift cycle. The first two bars fracture were observed on the South side of the column at the first cycle of 10% drift in bar B1 and B2, respectively. Afterwards, the spirals fractured on the same side of the column. Finally, bars B5 and B6 on the North side of the column ruptured at the first cycle of 12% drift. The test was stopped after the fracture of the four bars B1, B2, B5 and B6 as in case of S1-Bond. Figures 4.11 through 4.21 show the progression of damage at the plastic hinge region of the column at selected different drift ratios for specimen S2-Debond.

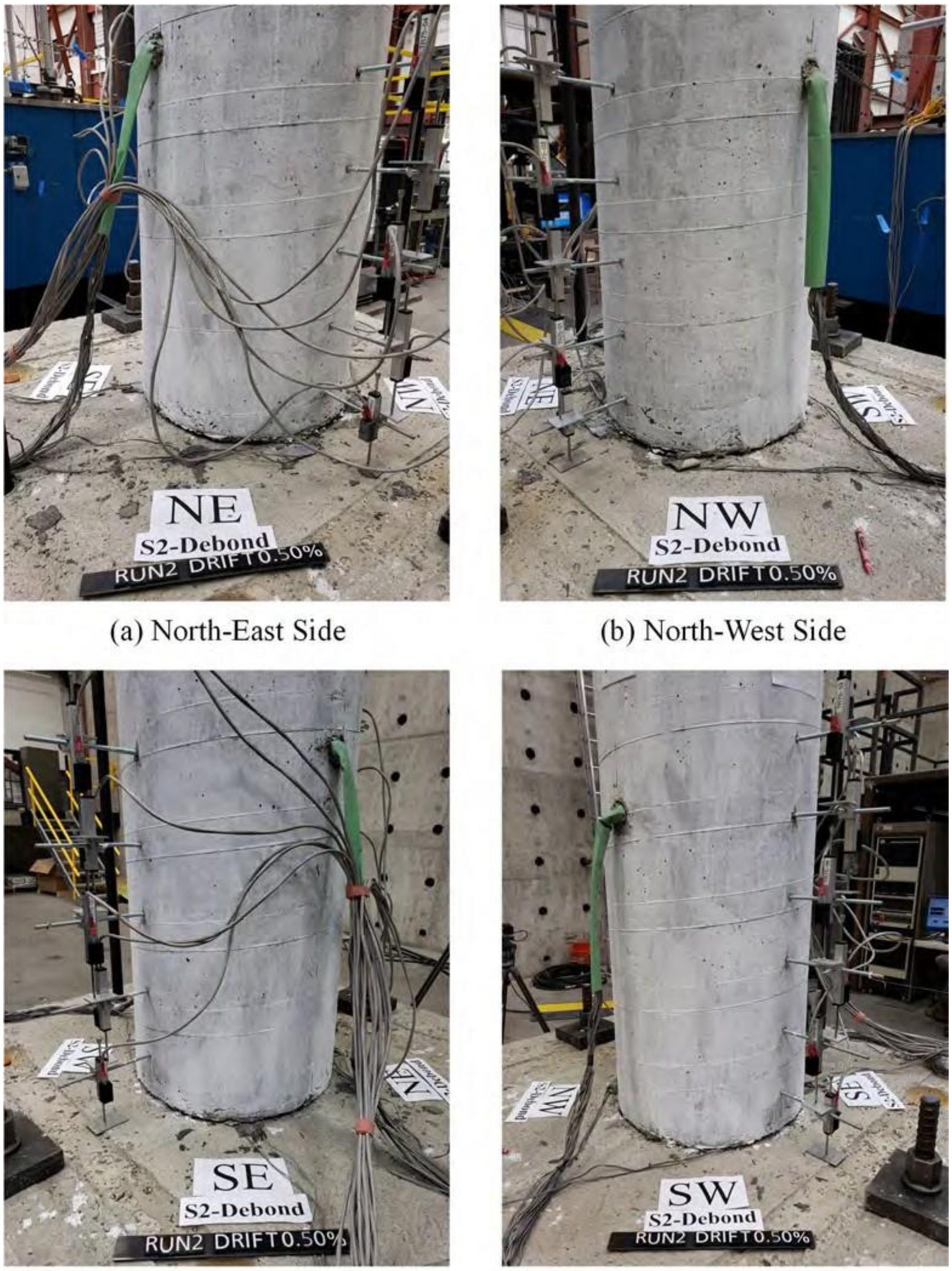


(a) North-East Side (b) North-West Side

(c) South-East Side (d) South-West Side

Figure 4.11 S2-Debond Plastic Hinge Damage, 0.5% Drift Cycle.


(a) North-East Side


(b) North-West Side


(c) South-East Side


(d) South-West Side

Figure 4.12 S2-Debond Plastic Hinge Damage, 0.75% Drift Cycle.


(a) North-East Side


(b) North-West Side


(c) South-East Side

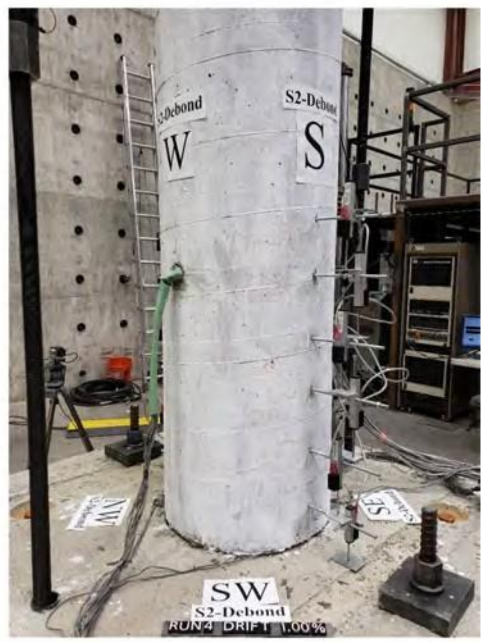


(d) South-West Side

Figure 4.13 S2-Debond Plastic Hinge Damage, 1% Drift Cycle.


(a) North-East Side


(b) North-West Side


(c) South-East Side


(d) South-West Side

Figure 4.14 S2-Debond Plastic Hinge Damage, 2% Drift Cycle.

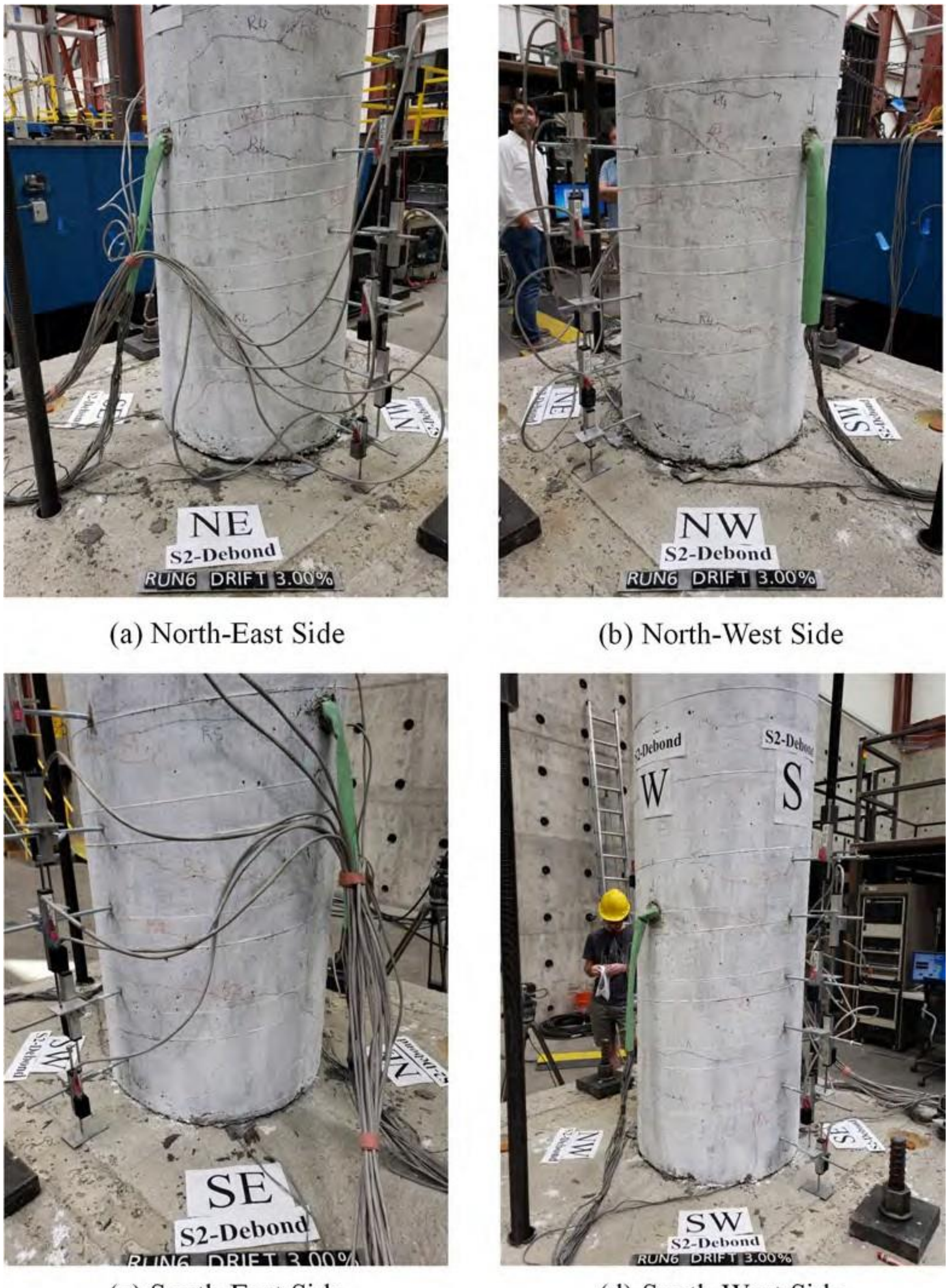


(a) North-East Side

(b) North-West Side

(c) South-East Side

(d) South-West Side

Figure 4.15 S2-Debond Plastic Hinge Damage, 3% Drift Cycle.

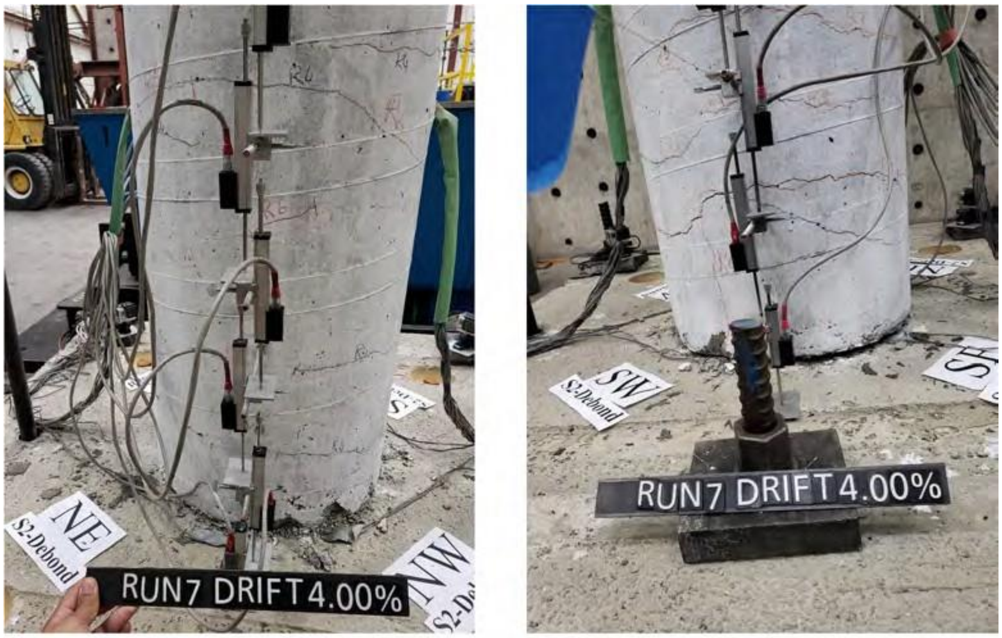


(a) North Side (b) South Side

Figure 4.16 S2-Debond Plastic Hinge Damage, 4% Drift Cycle.

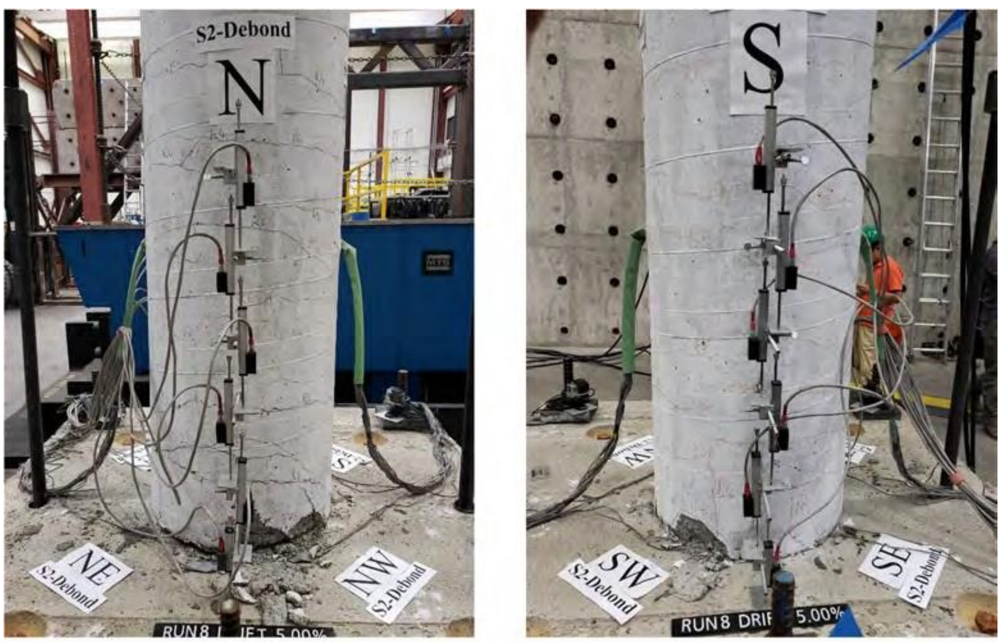


(a) North Side (b) South Side

Figure 4.17 S2-Debond Plastic Hinge Damage, 5% Drift Cycle.

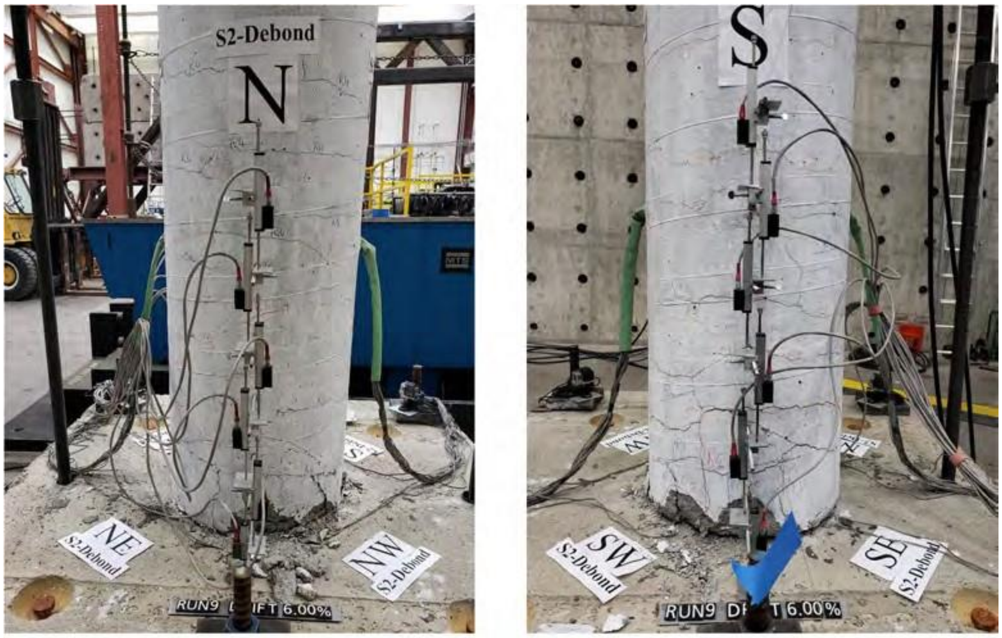


(a) North Side

(b) South Side

Figure 4.18 S2-Debond Plastic Hinge Damage, 6% Drift Cycle.

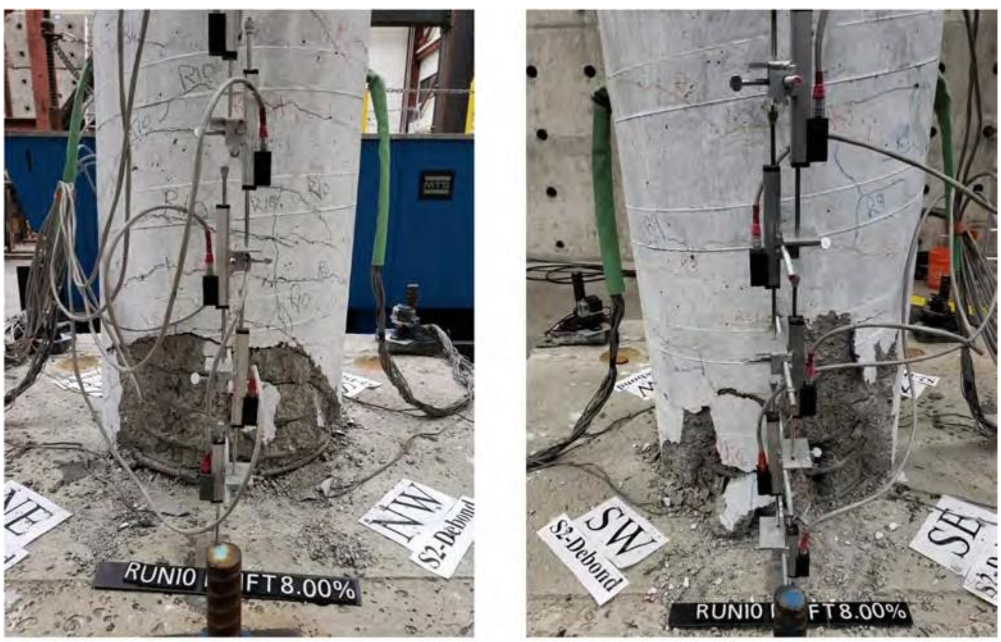


(a) North Side

(b) South Side

Figure 4.19 S2-Debond Plastic Hinge Damage, 8% Drift Cycle.


(a) North Side (b) South Side

Figure 4.20 S2-Debond Plastic Hinge Damage, 10% Drift Cycle.


(a) North Side (b) South Side

Figure 4.21 S2-Debond Plastic Hinge Damage, 12% Drift Cycle.

### *4.2.2. Force-Displacement relationship*

The measured lateral force-drift hysteretic relationship along with the envelope or backbone response of S1-Bond are shown in Figure 4.22. The sequence of bars rupture is also illustrated in Figure 4.22. The average of the push/pull envelope responses is shown in Figure 4.23. The envelopes are shown up to 80% of the push/pull base shear capacity. The S1-Bond column did not exhibit any strength degradation up to 8% drift ratio neither in the push nor in the pull direction. However, significant strength and stiffness loss was observed during the following cycles due to the successive bars and spirals ruptures. The column exhibited an almost symmetrical response for the push and pull directions with regards to the initial stiffness and ductility. However, the column exhibited a slightly higher load capacity in the pull direction than the push direction with measured lateral load capacities of 59 kips and 52.7 kips, respectively. The longitudinal bar yielded in the push direction at 0.84% drift ratio under a 27.6 kips force. The bar yielded in the pull direction at −0.82% drift ratio under a −29.2 kips force.

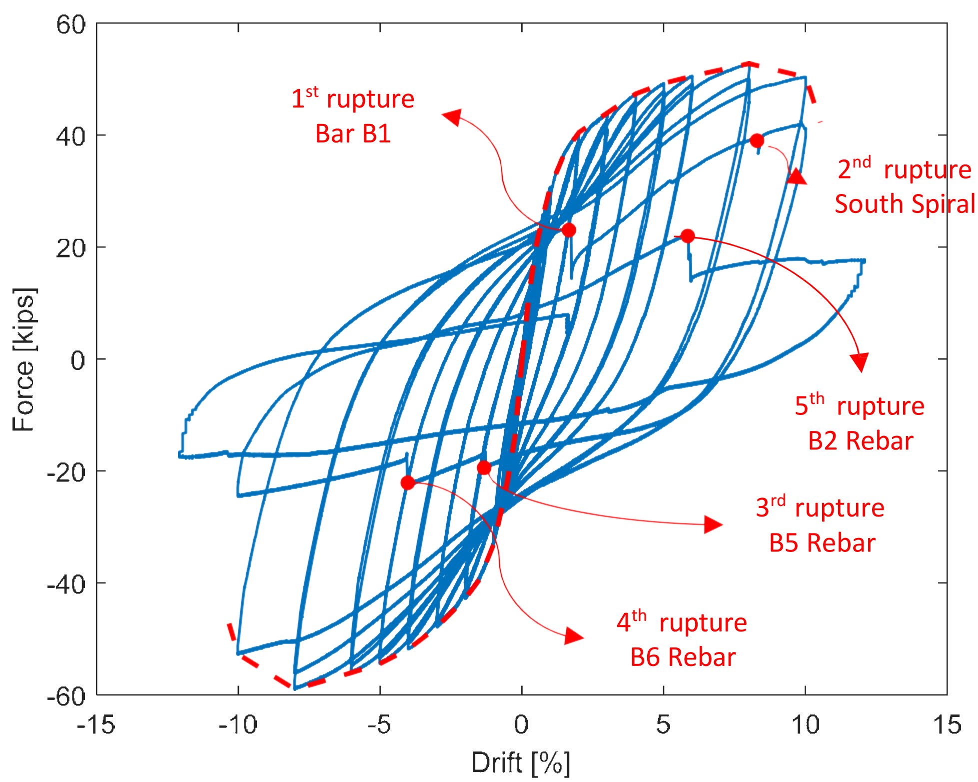


Figure 4.22 S1-Bond Column Force-Drift Hysteretic and Envelope Responses.

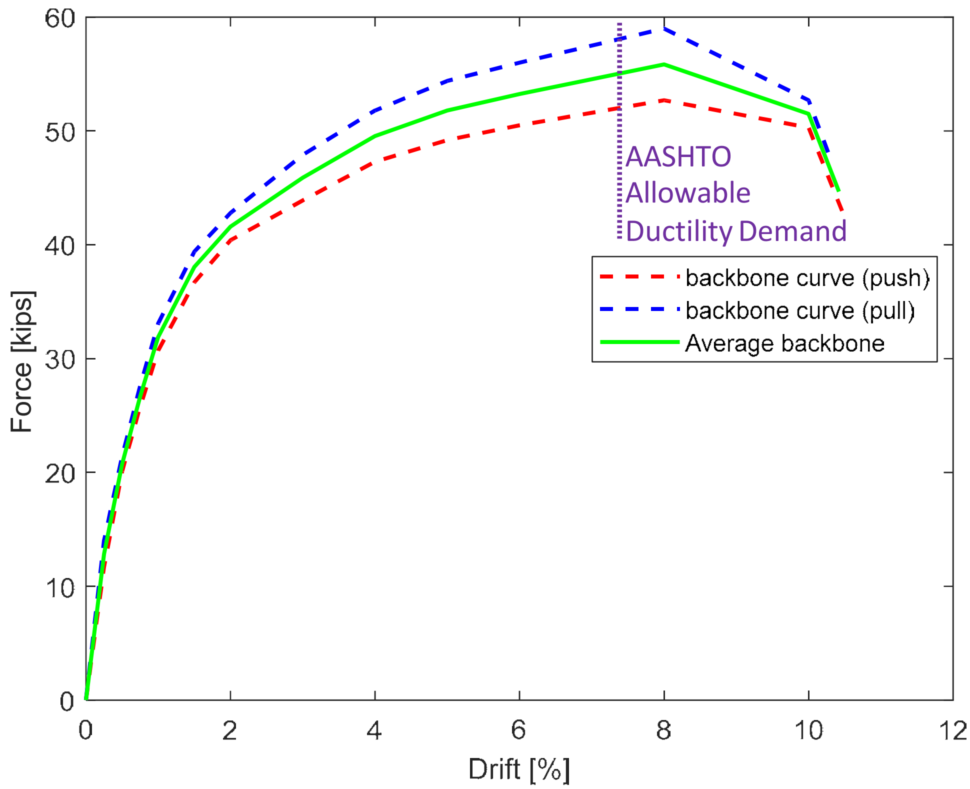


Figure 4.23 S1-Bond Column Average Push/Pull Force-Drift Envelope.

For the S2-Debond column, the measured lateral force-drift hysteretic relationship and envelope responses are shown in Figure 4.24. The sequence of bars rupture is also illustrated in Figure 4.24. The average of the push/pull envelope responses is shown in Figure 4.25. Similar to S1-Bond, the envelopes are shown only up to 80% of the push/pull base shear capacity. The S2-Debond column also did not exhibit any strength degradation up to 8% drift ratio neither in the push nor in the pull direction. However, significant strength and stiffness loss was observed during the following cycles due to the successive bars and spirals ruptures. The column exhibited an almost symmetrical response for the push and pull directions with regards to the initial stiffness. However, the column exhibited a slightly higher load capacity in the pull direction than the push direction with measured lateral load capacities of 54.9 kips and 50.3 kips, respectively. Also, the column exhibited a higher drift capacity in the push direction than the pull direction with corresponding drift capacities of 10.52% and 9%, respectively. The longitudinal bar yielded in the push direction at 0.79% drift ratio under a 21.05 kips force. The bar yielded in the pull direction at −0.84% drift ratio under a −24 kips force.

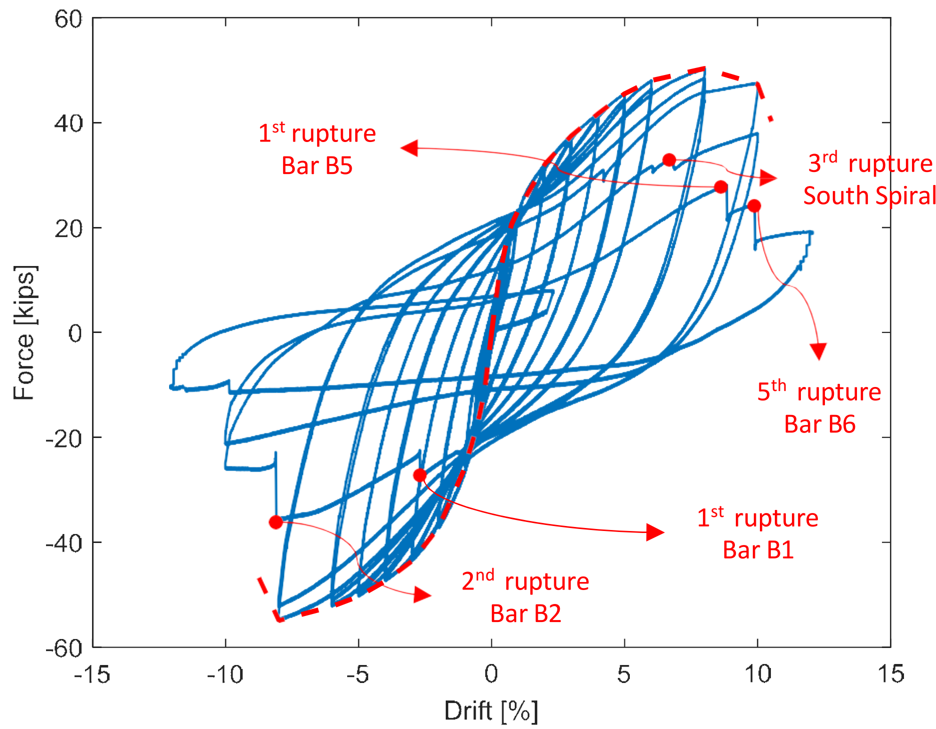


Figure 4.24 S2-Debond Column Force-Drift Hysteretic and Envelope Responses.

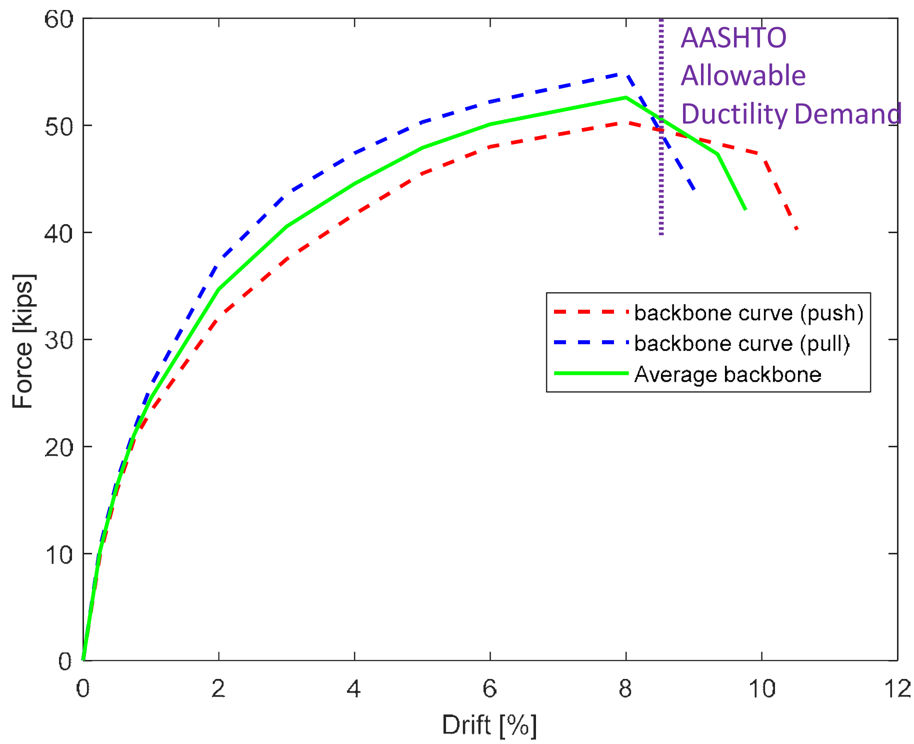


Figure 4.25 S2-Debond Column Average Push/Pull Force-Drift Envelope.

Displacement ductility is considered to be a good representation for the ability of a column member to undergo post-yield displacements. For this study, the displacement ductility was determined by idealizing the force-displacement average envelope with an elastoplastic bi-linear curve as illustrated in Figure 4.26. The slope of the elastic branch is adjusted such that the curve begins at the origin and passes through the measured first longitudinal bar yield point. The plastic branch is set to have equal areas enclosed above and below the bi-linear plastic branch and the actual force displacement curve. The effective yield displacement $\Delta_{y,Eff}$ is defined as the displacement corresponding to the point of intersection between the elastic and plastic curves. Also for this study, the failure of the bridge concrete column is considered when the column lateral load resistance drops to 80% of its peak strength due to either bar rupture or the column core concrete crushing. Hence, the ultimate displacement is determined at this point. The displacement ductility is defined as the ratio of the ultimate displacement to the effective yield displacement.

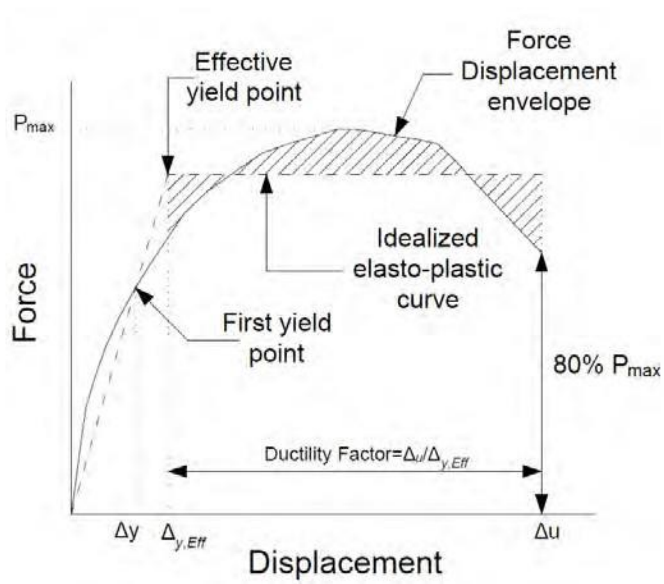


Figure 4.26 Illustration of displacement ductility calculation using elastoplastic response.

The measured average drift ratios corresponding to the first yield for the S1-Bond and S2-Debond columns were 0.84% and 0.79%, respectively. Meanwhile, the effective yield drift ratios were estimated based on the procedure in Figure 4.26 to be 1.48% and 1.70% for S-Bond and S2-Debond, respectively, and their estimated ultimate drift ratios were 10.42% and 9.77%, respectively. Accordingly, the measured displacement ductility for S1-Bond and S2-Debond columns were almost 7.02 and 5.74, respectively. It is noted that both columns have met and exceeded the AASHTO (2014) requirements for maximum displacement ductility demand of 5.0. The equivalent drift ratio at the corresponding ductility of 5 is indicated in Figures 4.23 and 4.25 for S1-Bond and S2-Debond, respectively, which confirms the acceptable seismic response of both columns. However, S1-Bond column is shown to have exhibited a more ductile behavior than the S2-Debond column, i.e. approximately 20% increase in the displacement ductility. This observation is not typical and was unexpected. The debonded longitudinal bars in S2 specimen were supposed to help reduce bars strains at the interface and help distribute the strains along the bars in the plastic hinge region. In turn, debonding is expected to affect the column in two ways: (1) the column will exhibit a softener behavior at the lower drift ratios because the debonding induce more bond slip to the longitudinal bars resulting in higher effective yield displacement, which was observed in the tests; and (2) the debonding will help in delaying the failure of the column to larger drift ratios, which was not fulfilled in the tests. To further investigate the reason behind the early failure of the S2-Debond, a detailed investigation was conducted on the columns and photographs were thoroughly inspected throughout all the stages starting from construction and until the test cycles up to failure. It was found that the reason for the early failure might be attributed to the fact that the longitudinal bars of S2-Debond within the plastic hinge region were somehow far from the spirals due to some construction error as shown in Figure 4.27. This adversely affected the restraining of the bars, i.e. aggravated the local buckling of the bars because of the increase of the bars unsupported length, which could explain the slightly earlier rupture of rebars in case of S2-Debond when compared to S1-Bond that did not have this construction error.

Figure 4.27 Spirals apart from the longitudinal bars.

In addition to the above observations, it can also be seen from Figures 4.23 and 4.25 that both S1-bond and S2-Debond columns had more than 40% and 15% reserve displacement capacity, respectively, when compared to AASHTO demand. This adequate displacement capacity allows both columns to be used in high seismic regions. The reserve displacement capacity was estimated as the percent increase of the column displacement capacity more than the column displacement demand corresponding to the displacement ductility demand of 5.

### *4.2.3. Energy Dissipation*

The cumulative dissipated energy of S1-Bond and S2-Debond are shown in Figure 4.28 at different drift levels. It can be seen that the energy dissipation was comparable in the two columns with slightly larger energy dissipation in S1-Bond. The lower energy dissipation in S2-Debond is more visible under larger drift ratios and it is attributed to the debonding of the longitudinal bars that induced more bond slip effects on the longitudinal bars resulting in lesser strength per each cycle and also because of the less restrained reinforcement as previously shown in Figure 4.27.

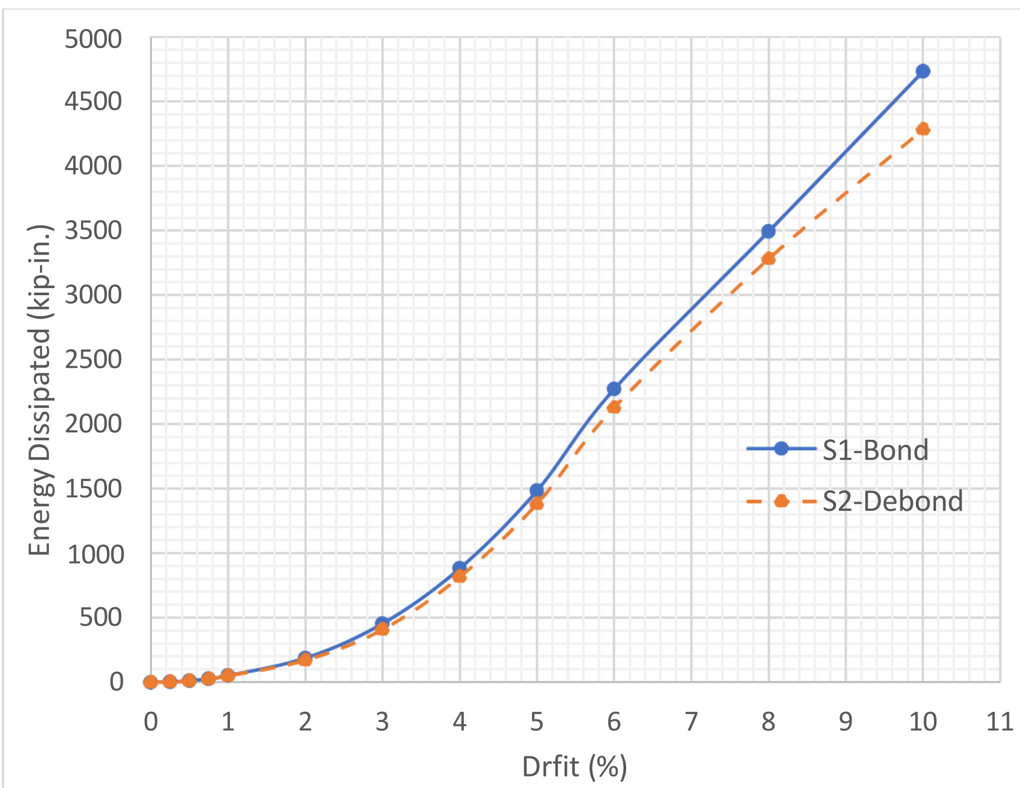


Figure 4.28 Cumulative Energy Dissipation for S1-Bond and S2-Debond Specimens.

## 4.3. Columns Local Behavior

### *4.3.1. Strain Profiles*

Both S1-Bond and S2-Debond column models were comprehensively instrumented with 48 reinforcement strain gages distributed into six levels in the column plastic hinge region and inside the footing to capture the longitudinal bars, transverse bars, and the embedded ducts strains (see Figure 3.12 above). Figures 4.30 and 4.31 show the maximum measured tensile strains at different drift ratios for bars B1, B2, B5 and B6 which are the North-East, North-West, South-East and South-West bars. It is worth noting that most of the strain gages near the column-footing interface were damaged and stopped working at higher drift ratios. It can be observed that the strains at level 2 and level 3 which were located at 1 in below and above the column-footing interface, respectively, have experienced the largest strain readings among other locations. This confirms the full development of the reinforcing bars in the plastic hinge into the footing where both column models showed a similar behavior as a typical CIP column.

Figures 4.32 to 4.35 show the maximum measured tensile strains of bars B1, B2, B5 and B6 versus the height of the column. The strain profiles were uniform along the column height prior to bar yielding. However, strains started to go higher in the plastic hinge of the column at and above 2% drift ratio at which strains exceeded the yield strain significantly. Debonding of the longitudinal bars was a successful technique to spread the strain in the footing and above the column-footing interface, which resulted in prevention of strain concentration in the UHPC. Comparing Figure 4.32 to Figure 4.33, it can be observed that the bars experienced a higher stress outside the debonded region in the footing. For example, comparing the strains at level 1 for the S1-Bond column (Figure 4.32) to the same strains at level 1 for the S2-Debond column (Figure 4.33), it is observed that the latter has higher strains on average. If both columns' strains are compared at level 2 and 3, which were at the column-footing interface, it is noticed that S2-Debond exhibited lower strain readings than S1-Bond. Based on the previous observations, debonding of the bars proved to be effective in preventing localized rebars strain concentration by well distributing the strains along the plastic hinge region.

The measured strains in the spirals in the North, South, East and West directions for S1-Bond and S2-Debond columns are shown in Figures 4.36 and 4.37, respectively. Almost all spirals remained elastic and had uniform distribution up to 5% drift ratio. Comparing the spirals strains at the North and South sides of the S1-Bond and S2-Debond, it is obvious that the latter had less strains, which proves the less utilization of confinement in the S2-Debond column because of the previously discussed construction error (Figure 4.27) that eventually affected the drift capacity of that column.

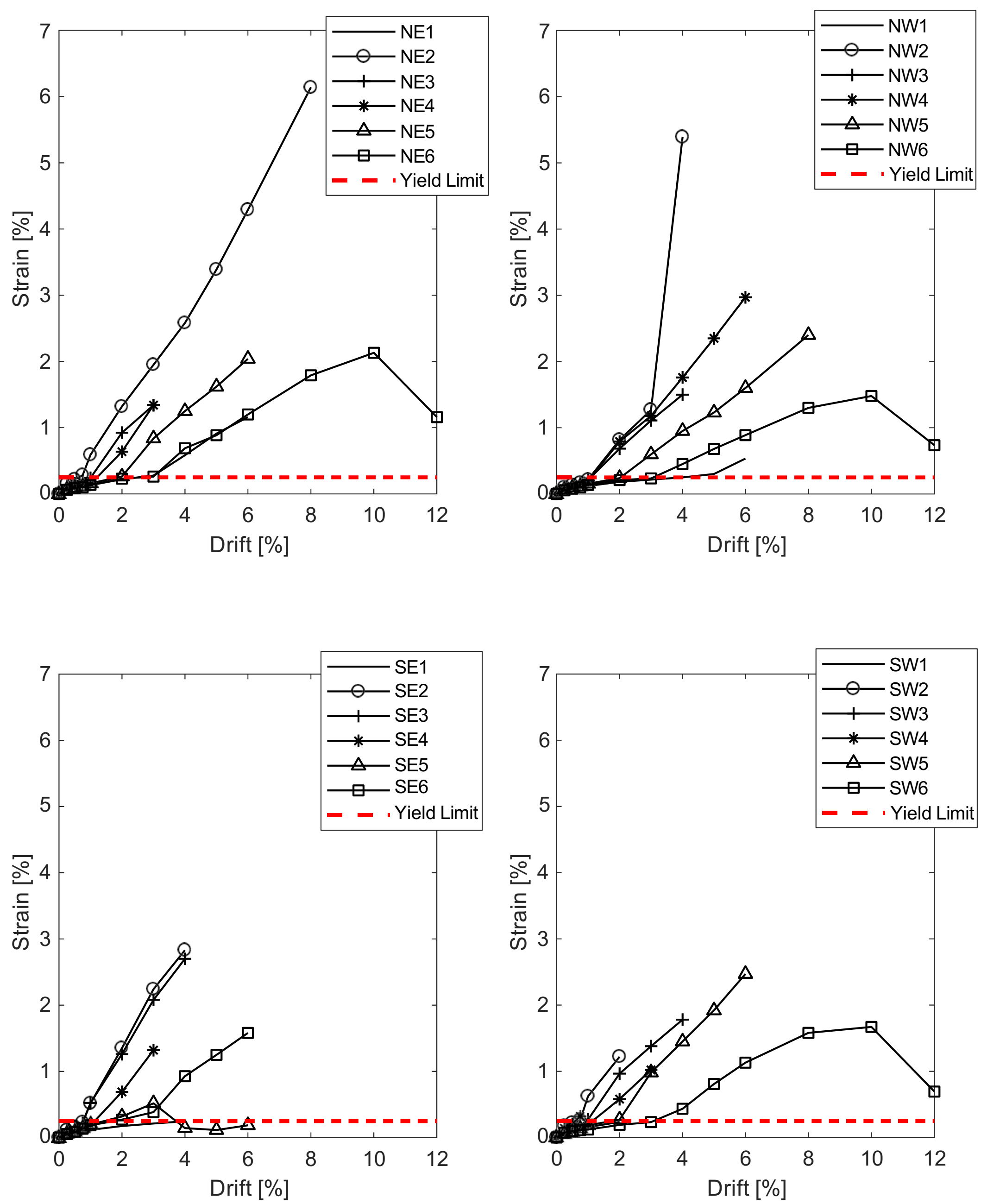


Figure 4.29 S1-Bond Column Strains versus Drift Ratio.

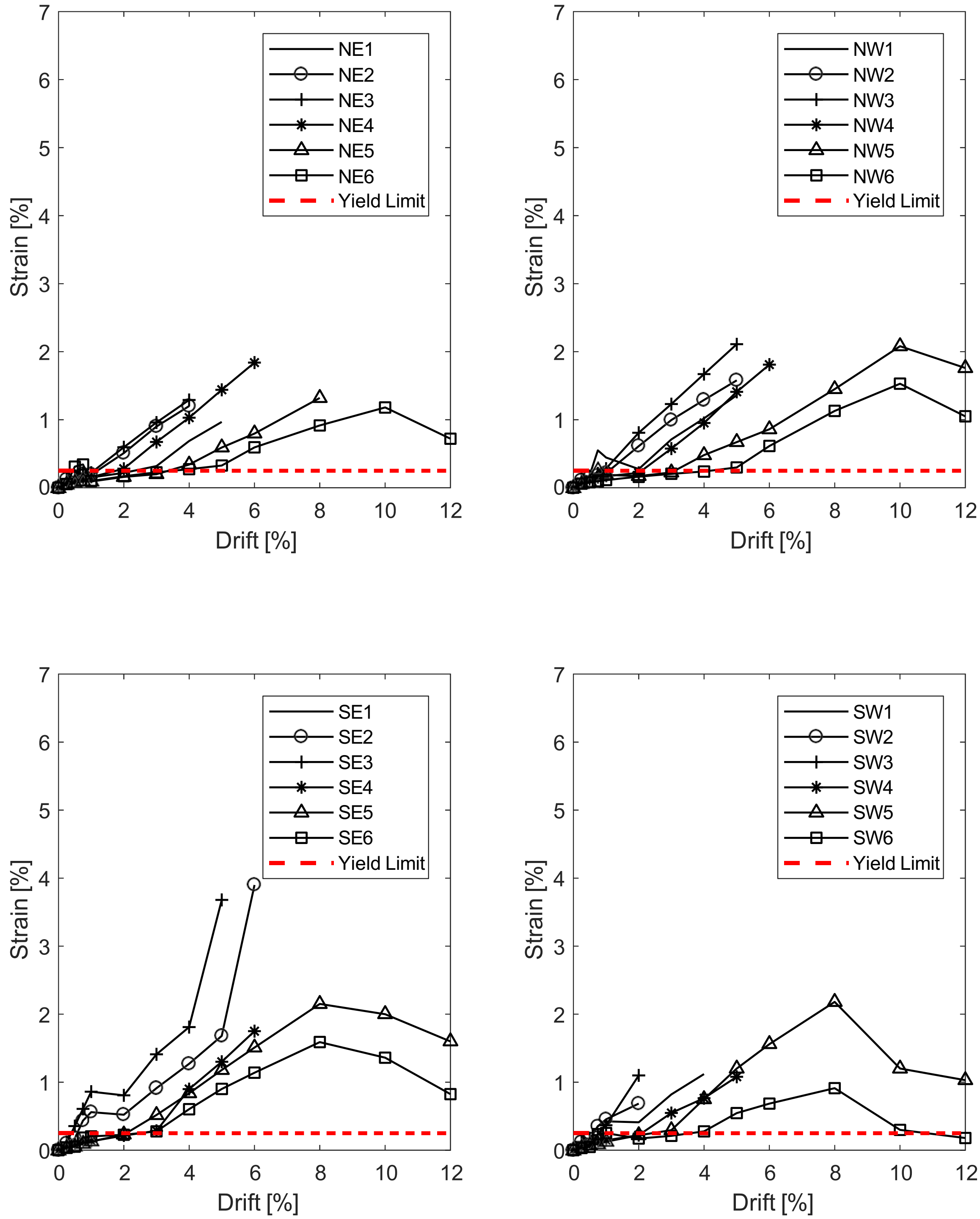


Figure 4.30 S2-Debond Column Strains versus Drift Ratio.

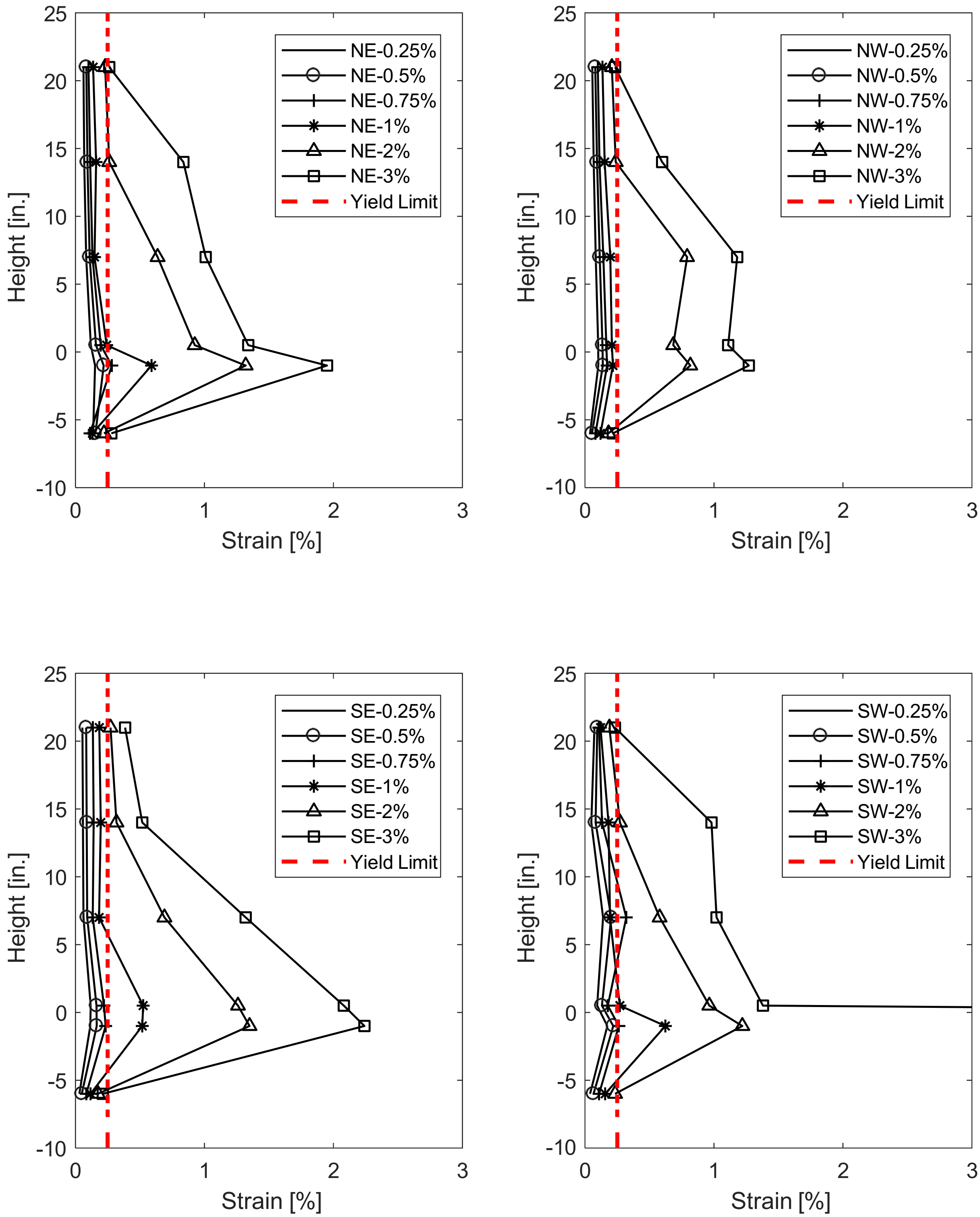


Figure 4.31 Strain Profile for Longitudinal bars of S1-Bond Column for Lower Drift Ratios.

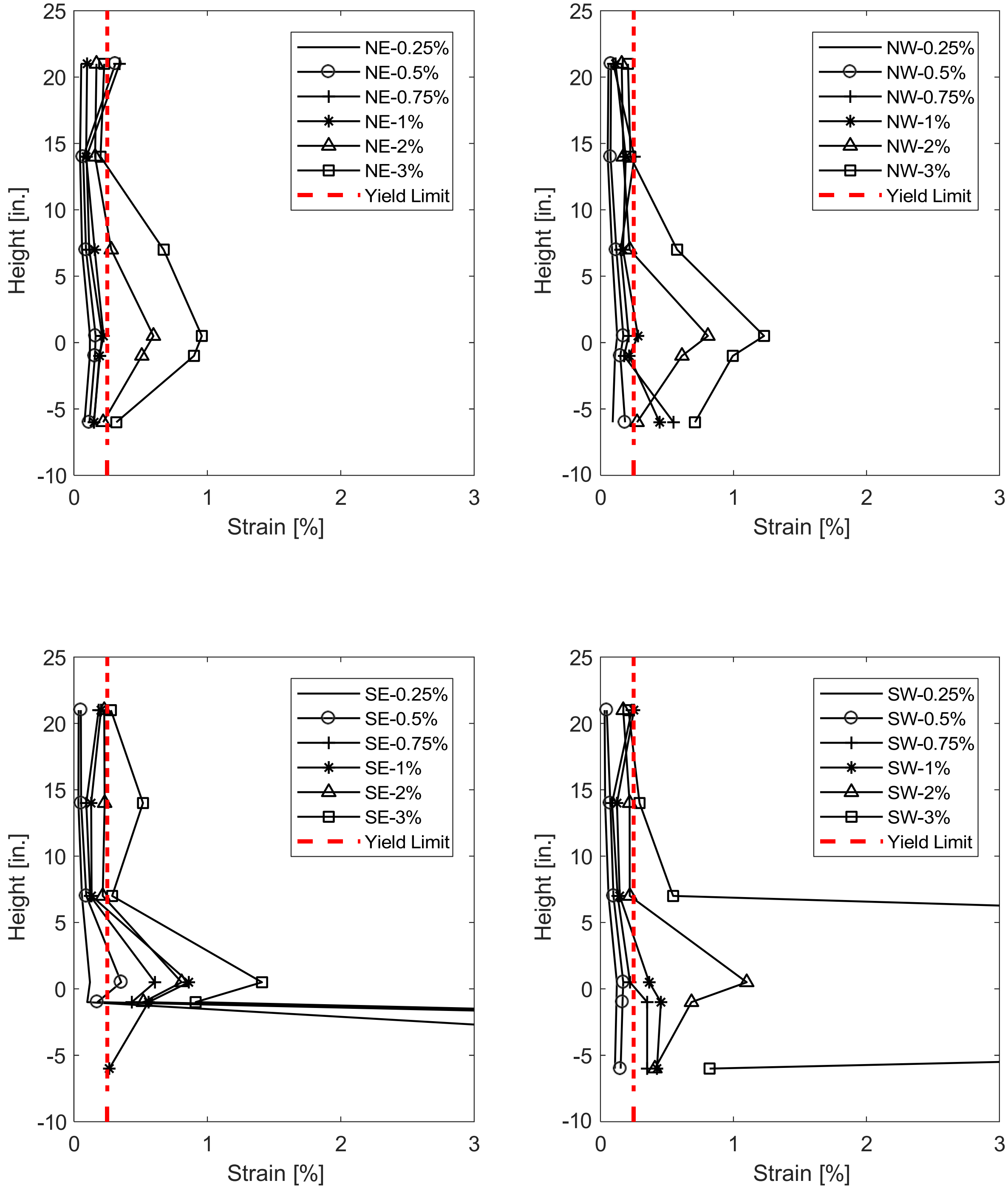


Figure 4.32 Strain Profile for Longitudinal bars of S2-Debond Column for Lower Drift Ratios.

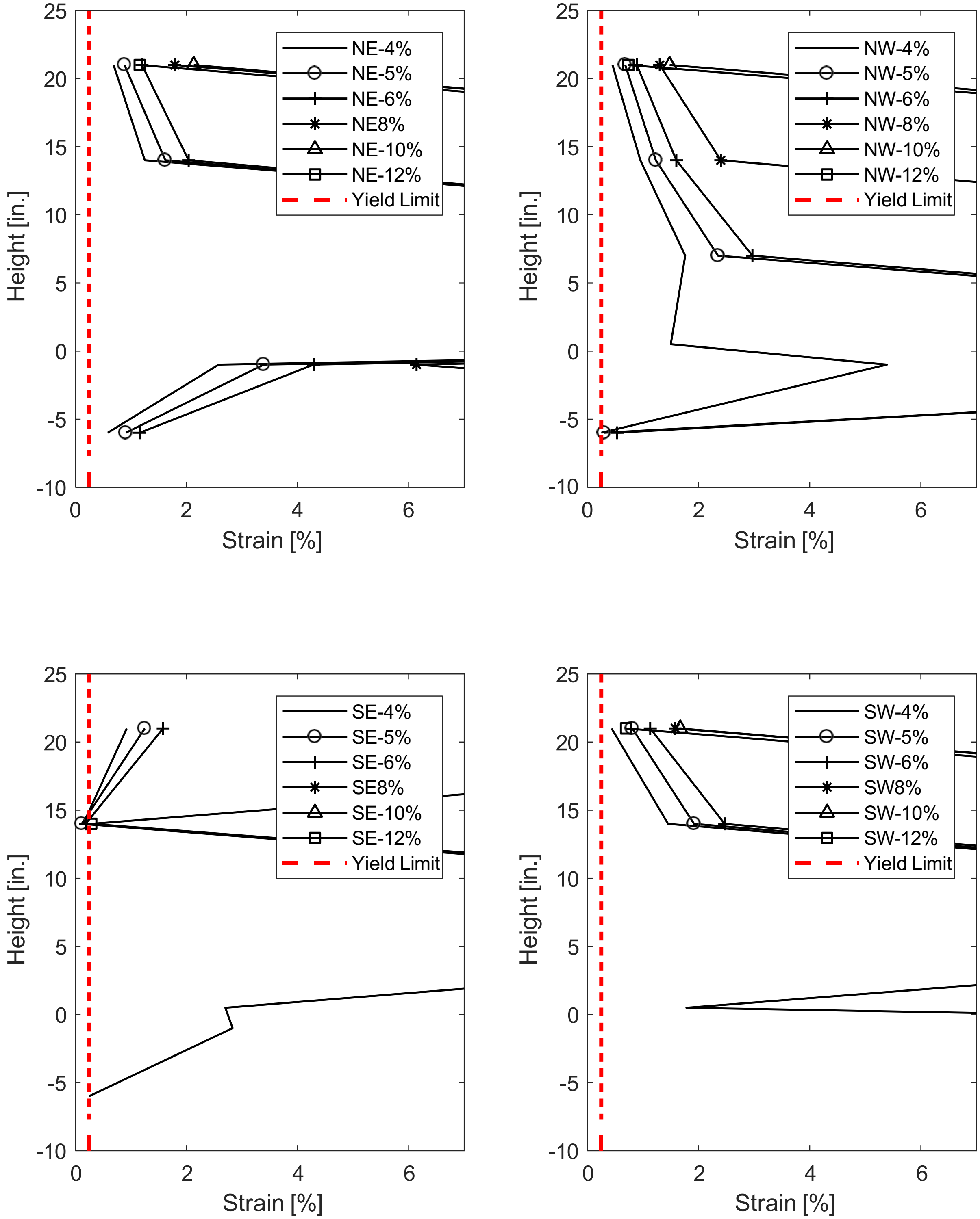


Figure 4.33 Strain Profile for Longitudinal bars of S1-Bond Column for Higher Drift Ratios.

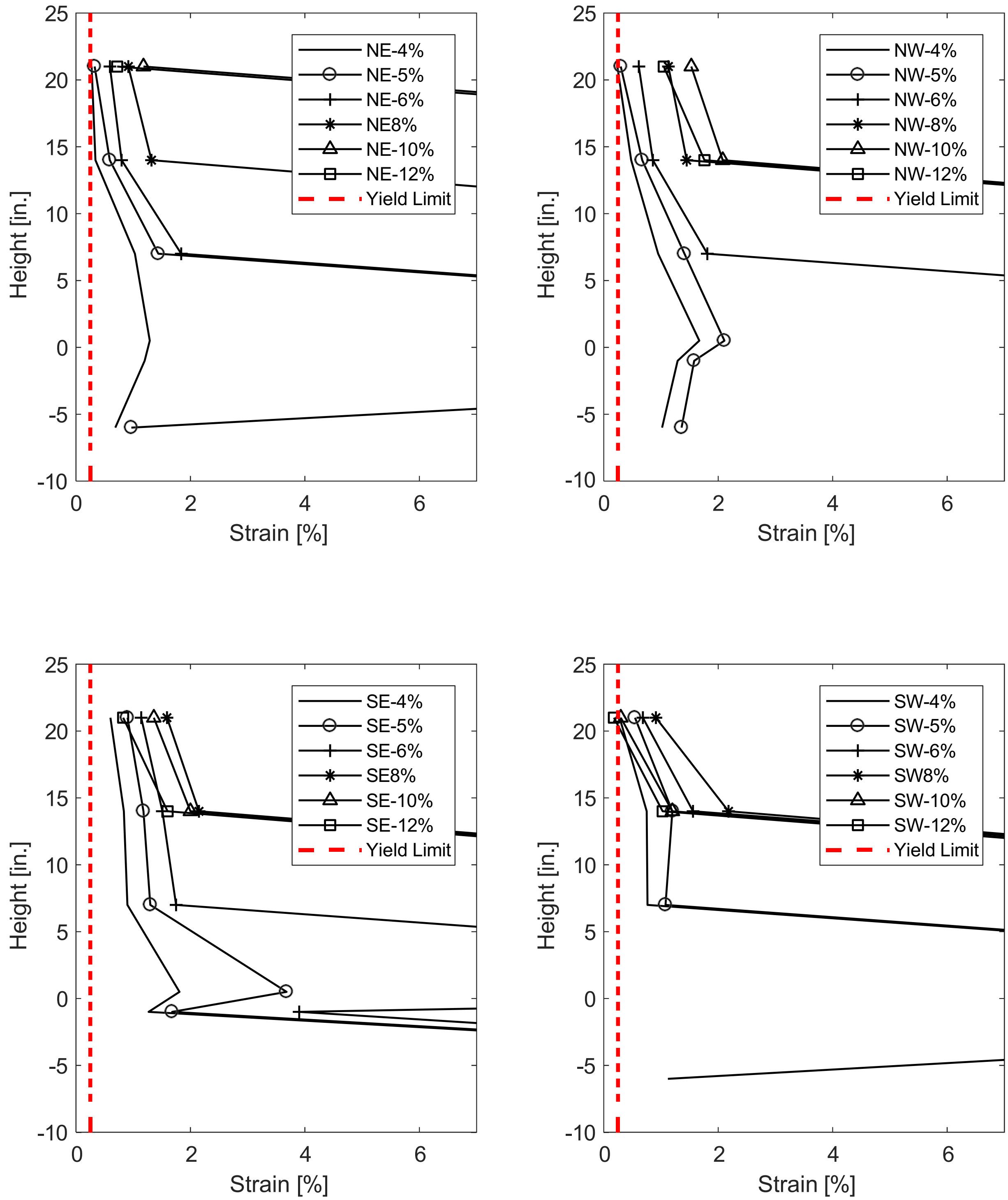


Figure 4.34 Strain Profile for Longitudinal bars of S2-Debond Column for Higher Drift Ratios.

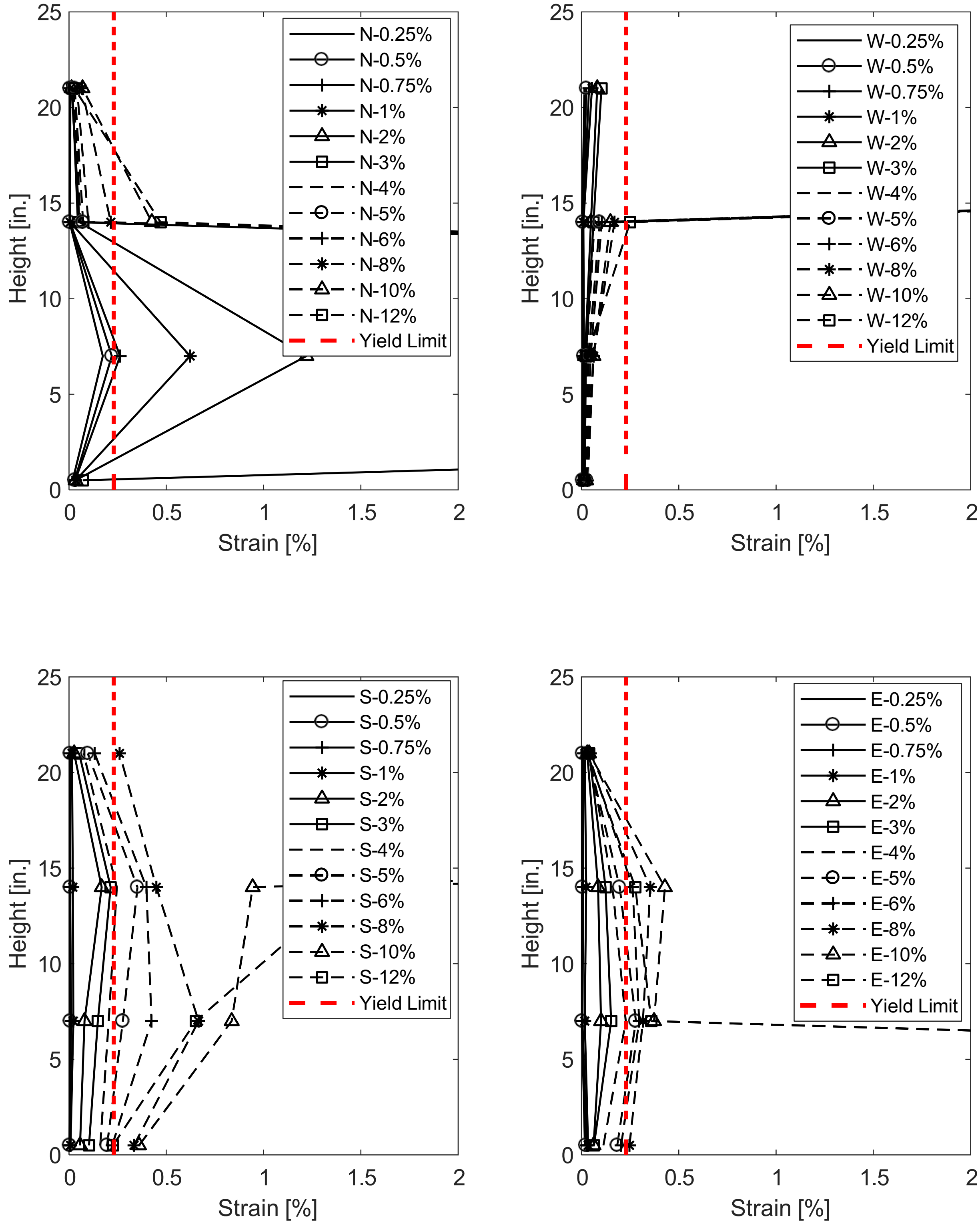


Figure 4.35 Strain Profile for Spirals of S1-Bond Column.

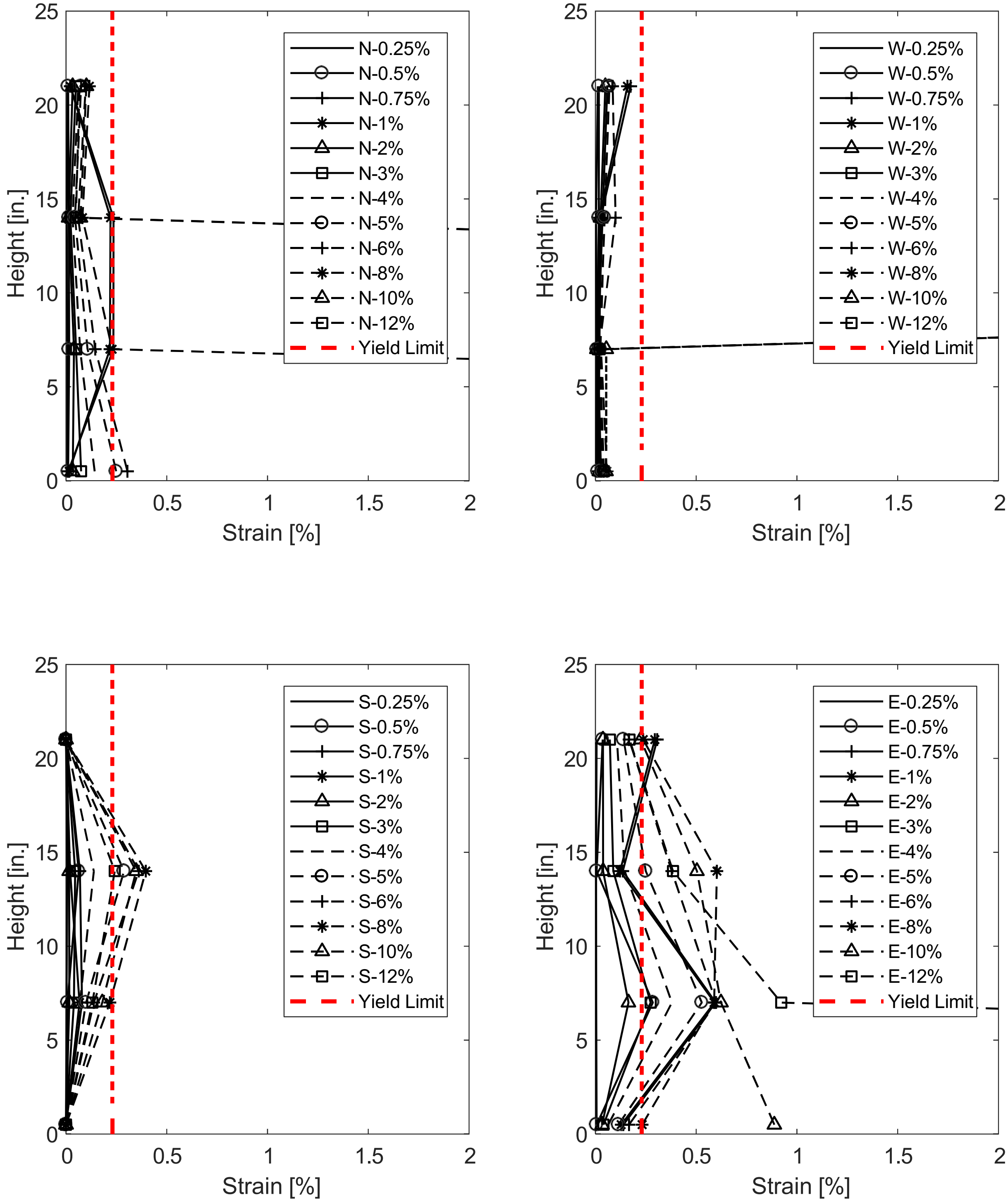


Figure 4.36 Strain Profile for Spirals of S2-Debond Column.

### 4.3.2. *Curvature Profiles*

The curvature profiles at the plastic hinge region reported at different drift levels are shown in Figures 4.38 and 4.39 for S1-Bond and S2-Debond, respectively. Curvatures were measured indirectly by using displacement transducers mounted on both loading sides of the columns as illustrated before in Figure 3.13. Curvatures at each level were computed as the ratio of the section rotations of that level to the vertical distance of the transducers. The rotations were, in turn, the ratio of the summation of the relative displacements to the horizontal distance between the transducers in the same level. The curvature was measured at six levels. The curvature of the column at the base, i.e. footing interface, was the highest mainly because of yield penetration at the column-footing interface. It is worth noting that the curvature displacement transducers at the column-footing interface were not effective at the higher drift ratios loading cycles beyond 8% when they reached their maximum stroke. On average, the curvature readings for S2-Debond column were higher than those in S1-Bond and this is attributed to the softener force-drift behavior in case of the S2-Debond column relative to S1-Bond.

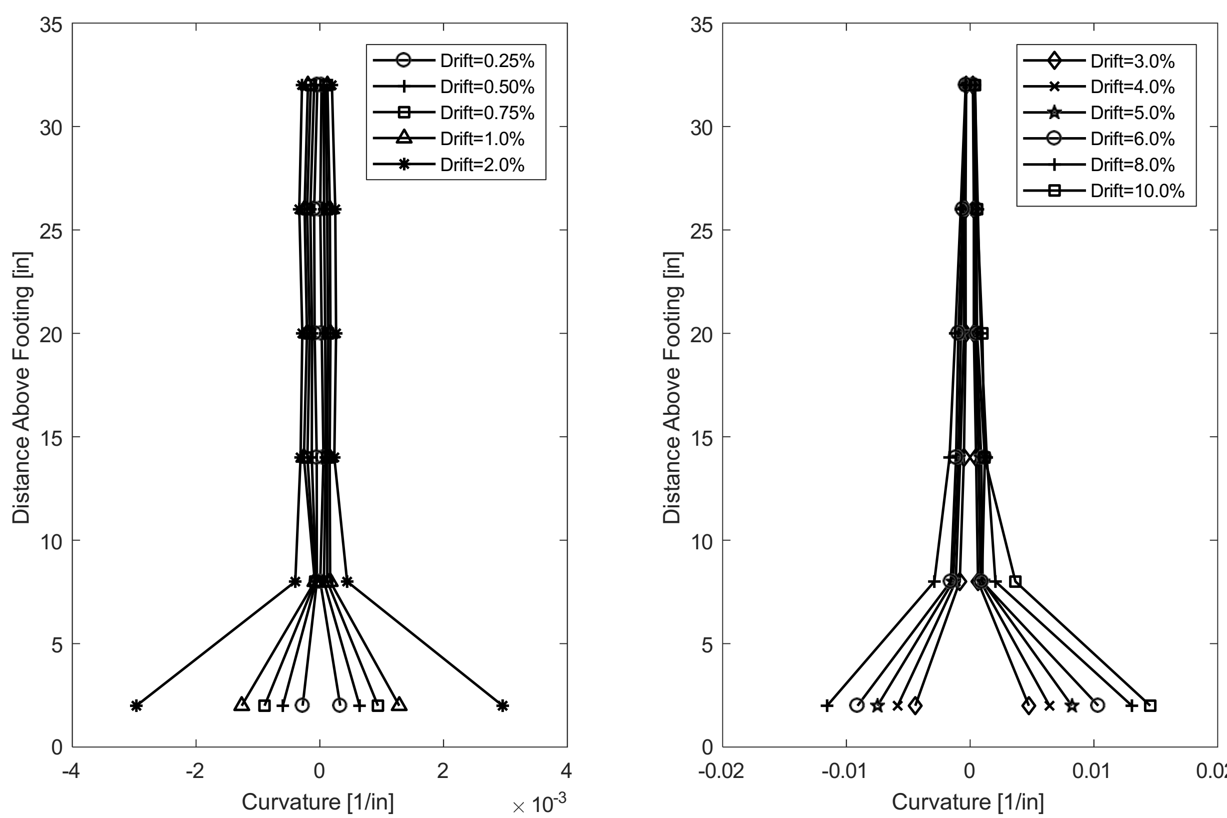


Figure 4.37 Curvature Profile of S1-Bond Column.

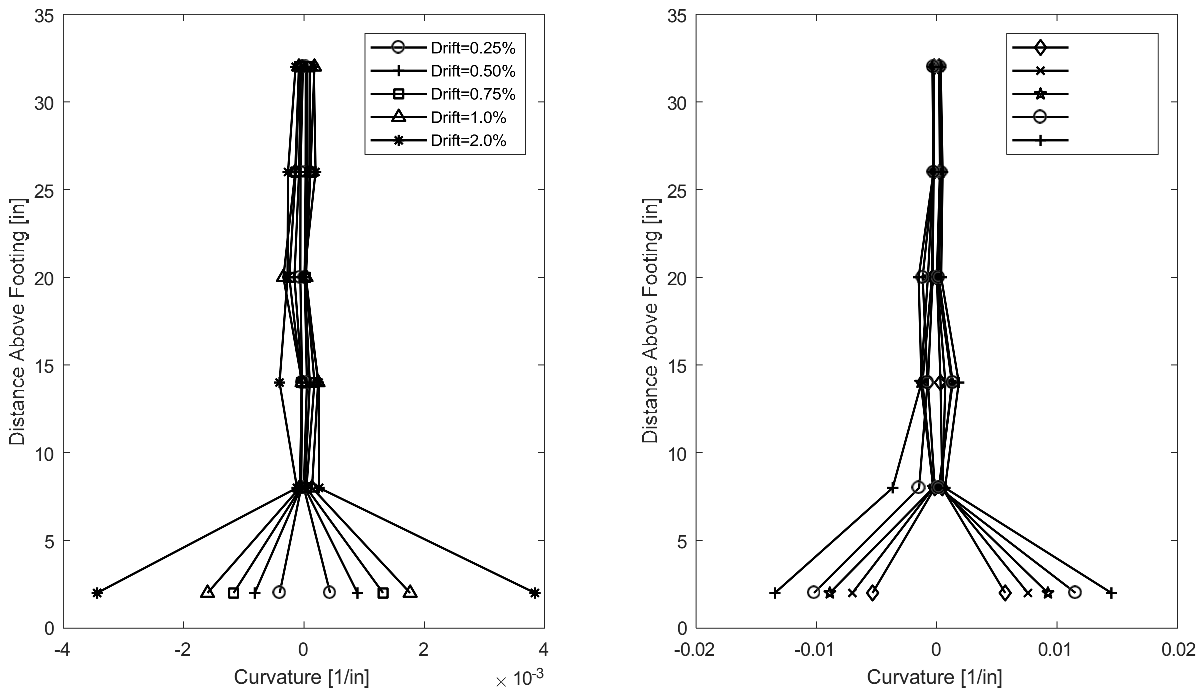


Figure 4.38 Curvature Profile of S2-Debond Column.

### *4.3.3. Moment-Curvature Behavior*

The measured base moment-rotation relationship (closest level to the footing) of S1-Bond and S2-Debond columns is shown in Figures 4.40 and 4.42, respectively. The corresponding base moment-drift relationships are also shown for S1-Bond and S2-Debond in Figure 4.41 and 4.43, respectively. The behavior implied through the figures is the same explained above using force-drift relationships. Nevertheless, the maximum moment capacities can be reported from the figures in this section in the push and pull loading sides for S1-Bond as 4,585 kip-in and 5,133 kip-in, respectively. Similarly, the push and pull moment capacities for S2-Debond were 4,376 kip-in and 4,776 kip-in, respectively, which is approximately 6% less than that of S1-Bond.

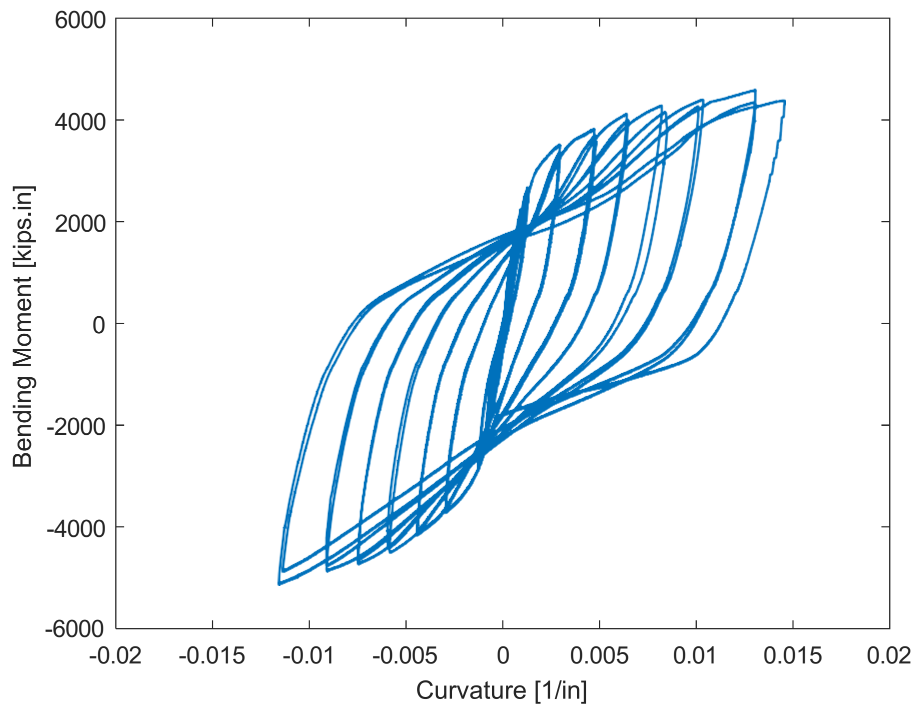


Figure 4.39 Moment-Curvature Hysteretic Behavior of S1-Bond Column at 2 in above column-footing interface.

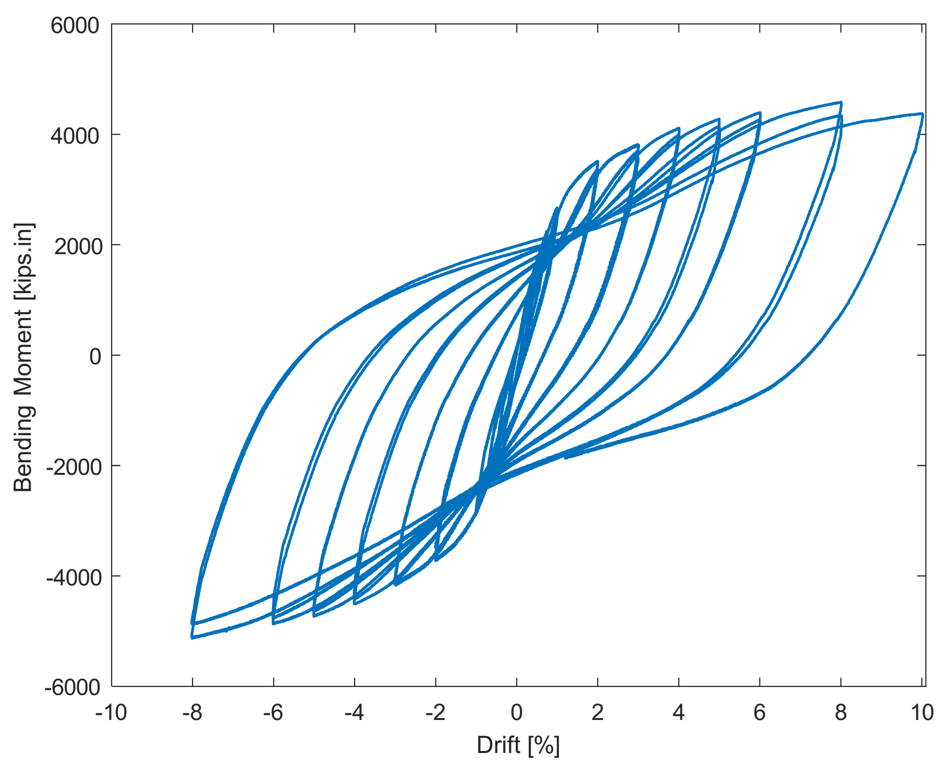


Figure 4.40 Moment-Drift Hysteretic Behavior of S1-Bond Column.

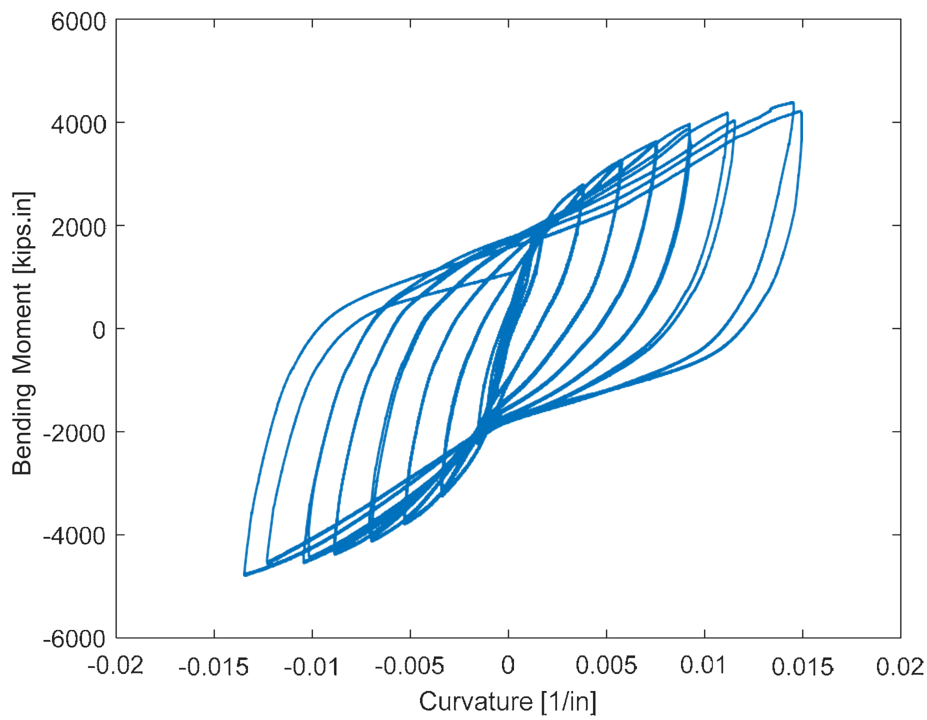


Figure 4.41 Moment-Curvature Hysteretic Behavior of S2-Debond Column at 2 in. above column-footing interface.

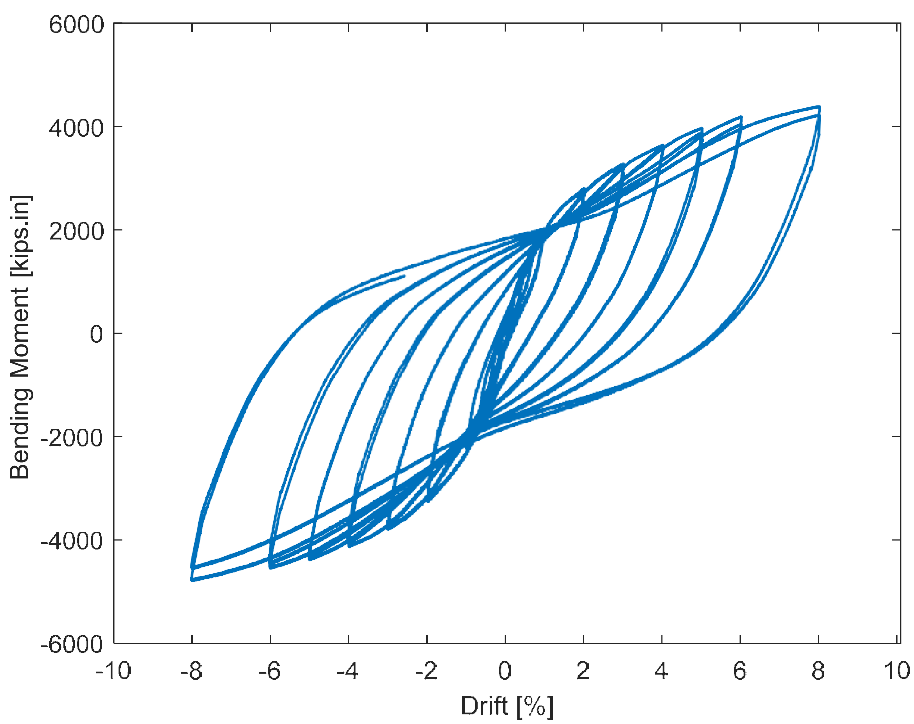


Figure 4.42 Moment-Drift Hysteretic Behavior of S2-Debond Column.

### 4.4. Column Models Evaluation with Respect to Previous Studies

The results of the two column models tested in this study, i.e. S1-Bond and S2-Debond, were independently presented in the previous sections and compared only amongst each other. In this section, the overall seismic performance of those columns is further assessed and compared with a reference CIP column tested by Haber et al. (2013) as well as another PNC column model with ducts filled with proprietary UHPC tested by Tazarv and Saiidi (2014). The summary of the different column models design was previously shown in Table 4.1. The so-called PNC model was a precast column model that had its longitudinal bars extended into a proprietary UHPC-filled duct placed in the footing. All the column models experienced the same mode of failure as it started with concrete cover spalling followed by longitudinal bar buckling and then finally bar fracture. No damage of the UHPC-filled duct connection such as bar pullout, duct pullout, or conical failure of the footing concrete was observed in all the UHPC-filled ducts column models. PNC and S2-Debond withstood two full cycles of 8% drift ratio without any strength degradation. Buckling of the bars was observed at this drift level. However, the longitudinal bars fractured during the following loading cycle of 10% drift. The CIP and S1-Bond withstood one cycle of 10% drift followed by bar fracture at the second cycle of the 10% drift ratio. The drift capacities for the CIP, PNC, S1-Bond and S2-Debond were 9.93%, 8.96%, 10.42% and 9.77%, respectively.

Table 4.1- Displacement Capacity for All Column Models.

| Column model | First yield point | | | Effective yield point | | | Ultimate Point | | | Disp. Ductility capacity |
|---|---|---|---|---|---|---|---|---|---|---|
| | Disp., (in) | Drift, (%) | Force, (kips) | Disp., (in) | Drift, (%) | Force, (kips) | Disp., (in) | Drift, (%) | Force, (kips) | |
| CIP | 0.86 | 0.79 | 38.8 | 1.46 | 1.35 | 66 | 10.7 | 9.93 | 68.5 | 7.36 |
| PNC | 0.96 | 0.89 | 40.3 | 1.54 | 1.42 | 63.7 | 9.67 | 8.96 | 56.24 | 6.3 |
| S1-Bond | 0.731 | 0.84 | 28.57 | 1.29 | 1.48 | 50.5 | 9.06 | 10.42 | 44.68 | 7.02 |
| S2-Debond | 0.689 | 0.79 | 21.63 | 1.48 | 1.7 | 46.5 | 8.5 | 9.77 | 42.08 | 5.74 |

The normalized average push and pull force-drift envelopes for all the column models is shown in Figure 4.43. It is observed that all the UHPC-filled ducts column models reached their lateral load capacities without any strength degradation at 8% drift while the CIP column reached its load capacity at 10% drift. Overall, the PNC and CIP column models showed almost the same normalized average envelope, while the S1-Bond and S2-Debond column models showed an overall softer behavior compared to the other two column models. This is attributed to the fact that the column-footing interface was not well prepared to ensure full contact between both members which affected the overall force-drift response by inducing higher end rotations at lower drift ratios resulting in lower lateral force readings. This specific observation is what support the recommendation previously mentioned in the construction discussion, i.e. high strength grout is better used for bedding when precast columns are installed into the footing.

Table 4.1 provides the displacement capacities for all the column models. The displacement ductility capacities for the CIP, PNC, S1-Bond and S2-Debond were 7.36, 6.30, 7.02 and 5.74, respectively. The S1-Bond and the CIP column models showed a very close ductility capacities while S2-Debond and PNC column models had a lower ductility capacity than the CIP with 22% and 14% difference, respectively. The lower ductility capacity of S2-Debond was because of the construction error of the poorly restrained reinforcement in the plastic hinge region due to the spirals distanced from the longitudinal bars with no contact. Meanwhile, the lower displacement ductility capacity of PNC could be attributed to lower concrete compressive strength of the shell compared to the CIP column concrete, which slightly reduced the confinement effectiveness and resistance against bar buckling.

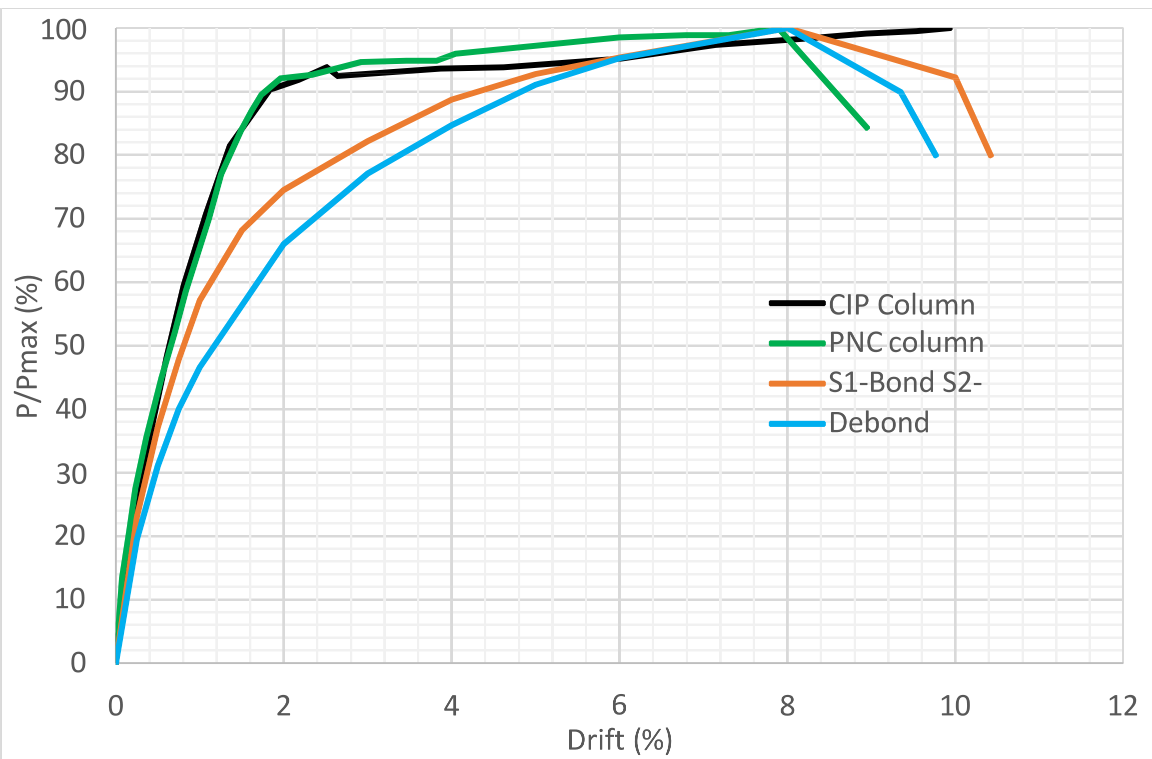


Figure 4.43 Normalized Average Push and Pull Force-drift Envelopes for all Column Models.

A comparison between the peak tensile strain values of the extreme bars measured in the plastic hinge region of all the column models are shown in Table 4.2 at 1%, 2%, 3%, 4% and 5% drift ratios. The strains for the higher drift ratios are not shown because most of the strain gages were damaged and their data were not reliable. It is observed that all the columns showed a close strain values at the lower drift ratios. A comparison between the peak plastic hinge rotations is shown in Table 4.3 and a graphical representation of the same results is also shown in Figure 4.45. It can be shown that the S1-Bond and S2-Debond columns exhibited higher column end rotations, specially at drift ratios higher than 2%. The higher end rotations is again resulting from the imperfect surface preparation of the interface between the column and the footing which resulted in a reduced column stiffness than the other two column models (CIP and PNC) as previously discussed and illustrated in Figure 4.43.

Table 4.2- Peak Tensile Strains for All Column Models.

| | Column model | Drift Ratio (%) | | | | |
|---|---|---|---|---|---|---|
| | | 1 | 2 | 3 | 4 | 5 |
| Peak Tensile Strains (%) | CIP | N/A | 1.35 | N/A | 2.5 | 3.1 |
| | PNC | 0.26 | 2.2 | 2.55 | 3.45 | 3.48 |
| | S1-Bond | 0.6 | 1.3 | 2.25 | 2.85 | 3.45 |
| | S2-Debond | 0.8 | 1.1 | 1.4 | 1.85 | 3.75 |

Table 4.3- Peak Plastic Hinge Rotations for All Column Models.

| | Column model | Drift Ratio (%) | | | | | | |
|---|---|---|---|---|---|---|---|---|
| | | 1 | 2 | 3 | 4 | 5 | 6 | 8 |
| Peak Column Curvature (1/in) | CIP | N/A | 0.0044 | N/A | N/A | 0.0094 | 0.0118 | 0.0179 |
| | PNC | N/A | 0.0073 | N/A | N/A | 0.0215 | 0.0308 | 0.0473 |
| | S1-Bond | 0.0051 | 0.0118 | 0.0184 | 0.0245 | 0.0314 | 0.0387 | 0.0493 |
| | S2-Debond | 0.0067 | 0.0146 | 0.0220 | 0.0291 | 0.0363 | 0.0435 | 0.0559 |

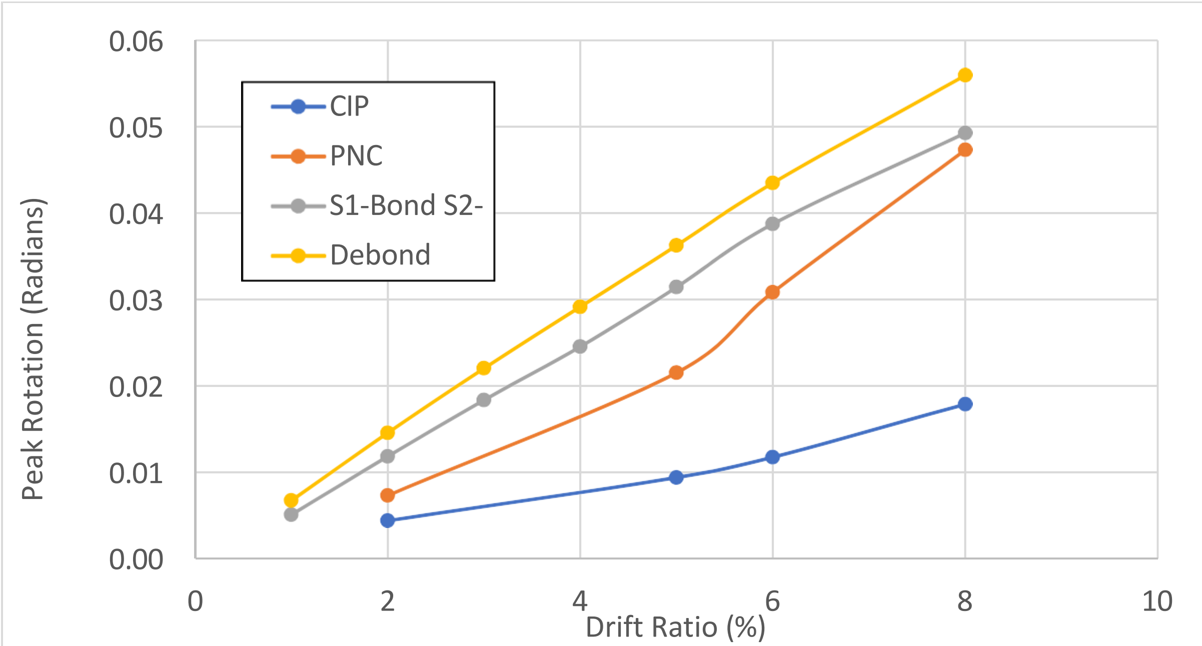


Figure 4.44 Peak Plastic Hinge Rotations for all Column Models.

# CHAPTER 5. ANALYTICAL MODELING

This chapter presents the analytical modeling and results for specimens S1-Bond and S2-Debond with focus on the global force-drift relationships. For all analytical studies, the finite element computer software OpenSEES (McKenna et al. 2000) was used.

## 5.1. Model Description

In this part of the study, OpenSEES (McKenna et al. 2000) was used to conduct nonlinear pushover and cyclic loading analysis for the tested column models under the same load protocol used in the experimental testing to predict the force-drift relationship. The numerical OpenSEES model, which is illustrated in Figure 5.1, was developed using similar modeling assumptions as in a previous OpenSEES model by Tazarv and Saiidi (2014). The model from the previous study was calibrated against an experimentally tested normal strength concrete column and another PNC column subjected to a combined axial and cyclic lateral loading. Such modeling assumptions were shown by Tazarv and Saiidi (2014) to exhibit a good agreement with the experimental results, especially the strength at each cycle, the residual drifts upon unloading, and the loading and unloading paths.

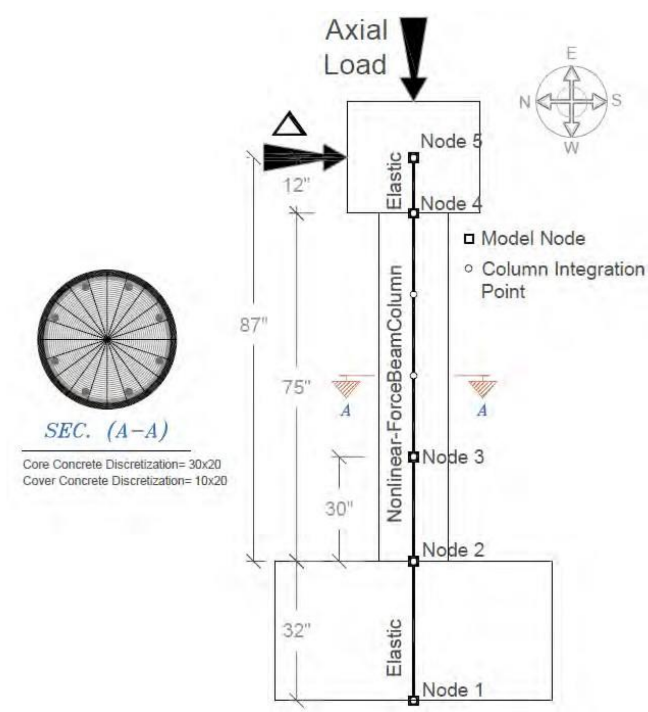


Figure 5.1 Schematic illustration of OpenSEES model components and modeling assumptions.

A three-dimensional five-nodes fiber-section model was developed for the S1-Bond and S2-Debond column models. The footing and the column head were modeled using elastic elements with a stiffness calculated based on their measured test-day concrete compressive strength. The column part was modeled using nonlinear force-based element, *forceBeamColumn*, with *PDelta* geometric stiffness matrix. Five integration points were used and distributed along the column element length. Gauss-Lobatto integration rule with the same sections at each integration point was used. It is noted that the first and the last integration points were located at the column element ends. The column cross-section was defined using a fiber section that was divided into two parts, the core part material modeled using confined concrete while the cover part modeled using unconfined concrete. The confined concrete properties were calculated using Mander's model (Mander et al. 1988). Both concrete parts were modeled using the *Concrete01* material model in which the concrete tensile strength is neglected while the reinforcement bars were modeled using *Steel02* and *ReinforcingSteel* material models as discussed later. The core section was meshed into 30 circumferential divisions and 20 radial divisions while the cover section was meshed into 20 radial divisions and 10 circumferential divisions.

The column part consisted of two elements that differed only in the steel material modeling. The first element extending from node 2 to node 3 used *ReinforcingSteel* with a modified stress-strain behavior accounting for bond-slip softening as discussed in Tazarv and Saiidi (2014). The second element extending from node 3 to node 4 used *Steel02* with no bond-slip effects included. The bond-slip softening effect were accounted for using a modified reduced modulus of elasticity for the longitudinal bars that was calculated based on Equation 1.

$$ð^{J}_{s} \quad ð_{Y} / ð^{J}_{Y} \tag{1}$$

where $ð_{Y}$ is the yield strength of the bar (ksi) and $ð^{J}_{Y}$ is the modified yield strain to account for the extra induced strains due to the slippage of the bars and the ducts at their yielding force $ð_{Y}$. The modified strain of the bar $ð^{J}_{Y}$ is calculated using Equations 2 through 5.

$$ð^{J}_{Y} \quad ð_{Y} \quad \frac{}{ð_{\circ}} \quad \frac{}{ð_{ð}} / ð_{ððð} \quad ð_{ð ð ð ð ð} \tag{2}$$

$$ð_{ð} \quad 2920 ð_{ð}. \quad \overline{\phantom{x}}_{UHPC} \tag{3}$$

$$ð_d \quad 11310 ð_d . \ldots \tag{4}$$

$$ð_{elong} \quad \frac{ð_Y}{2} \quad , ððð \; ð_s \quad ð_Y \tag{5}$$

where $ð_{elong}$ is the strain resulting from debonding the bars, $ð_b$ is the bar bond force-slip stiffness (lb/in), $ð_d$ is the duct bond force-slip stiffness (lb/in), $ð_b$ is the diameter of the bar (in), $ð_d$ is the inner diameter of the corrugated galvanized ducts (in), $ð_{emb}$ is the embedment length of the bar in the footing (in), $ð^J_C$ is the compressive strength of concrete (psi), $ð^J_{UHPC}$ is the compressive strength of UHPC (psi). When the previous equations were adopted, the resulting modified modulus of elasticity needed to account for bar and duct slip was estimated to be 8,473 ksi and 6,218 ksi for S1-Bond and S2-Debond column models, respectively. It should be noted that these formulations are valid if bar pullout from a UHPC-filled duct is prevented, which was the case in the two tests.

## 5.2. Analytical Simulation Results

Full hysteretic force-drift relationships as well as envelop/backbone curves were obtained from the nonlinear OpenSEES analyses. The calculated average push and pull force–drift envelopes of the S1-Bond and S2-Debond column models are shown first in Figures 5.2 and 5.3 and compared against corresponding measured response from the tests. The figures show that the analytical model was able to reproduce the column behavior with reasonable accuracy. However, the calculated force-drift response of S2-Debond was observed to be slightly stiffer than its measured response.

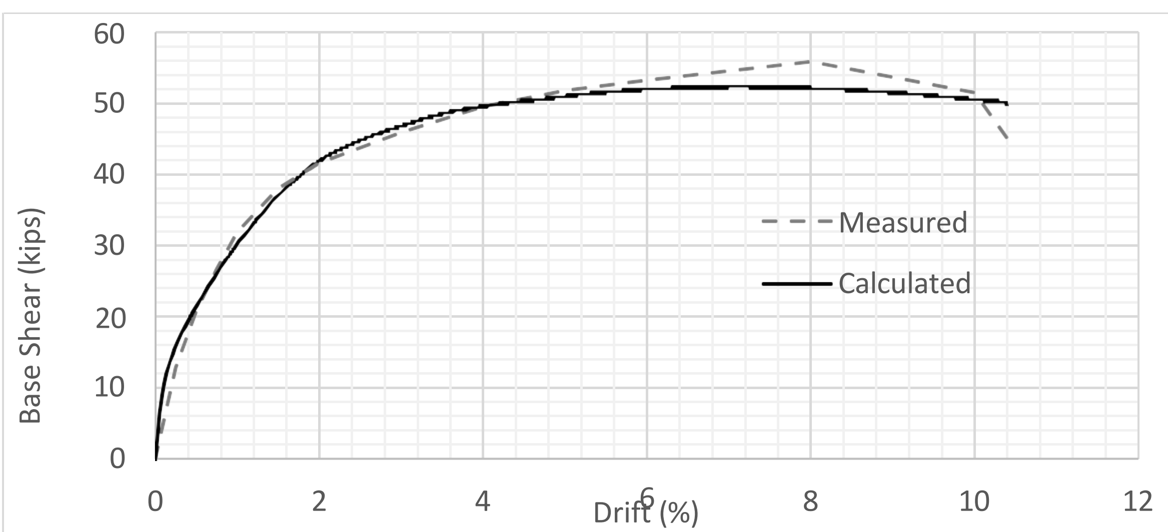


Figure 5.2 Measured and Calculated Average Force-Drift Envelopes of S1-Bond Column.

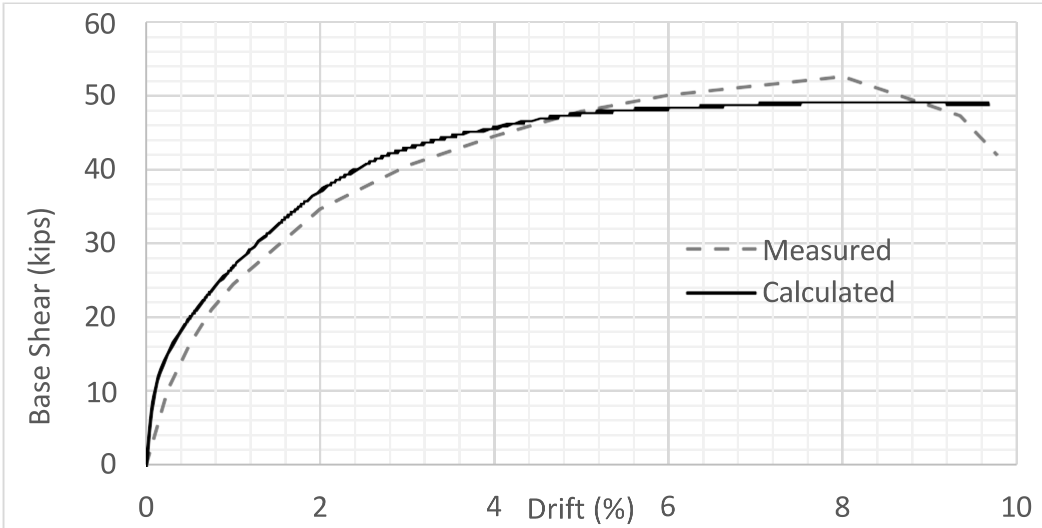


Figure 5.3 Measured and Calculated Average Force-Drift Envelopes of S2-Debond Column.

Moreover, the measured and calculated force–drift hysteretic curves of S1-Bond and S2-Debond are shown in Figures 5.4 and 5.5. It is evident that the calculated cyclic response correlated well with the test data. This was true with respect to the peak forces at different cycles, loading and unloading slopes, the pinching effect, and the width of the hysteretic curves. Overall, the analytical model was able to simulate the column global response with good accuracy. An analytical model with the type of elements used in this study appears to be representative of the behavior of precast columns utilizing UHPC-filled duct connections.

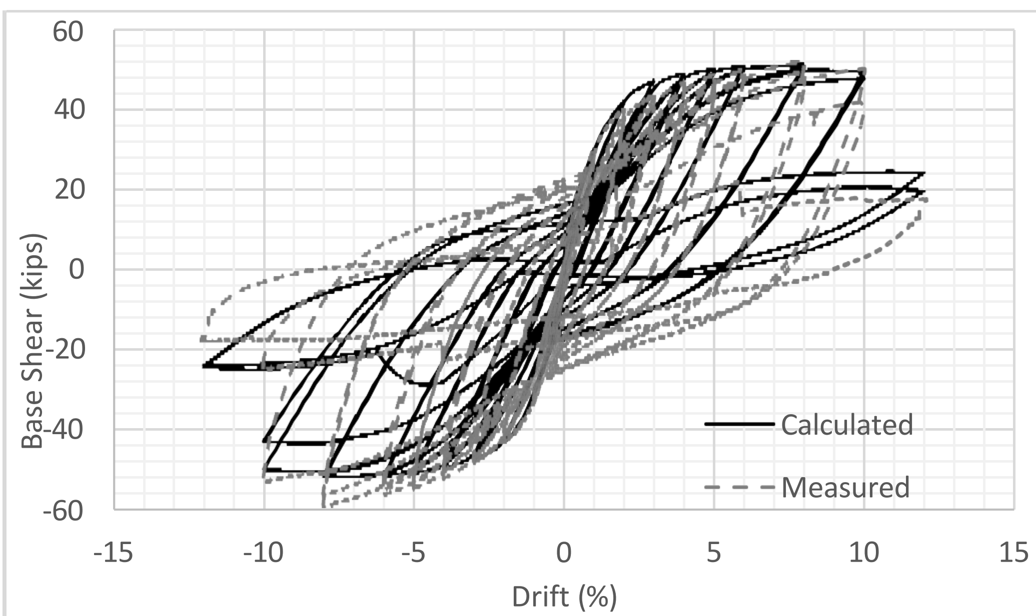


Figure 5.4 Measured and Calculated Force-Drift Hysteretic Responses of S1-Bond Column.

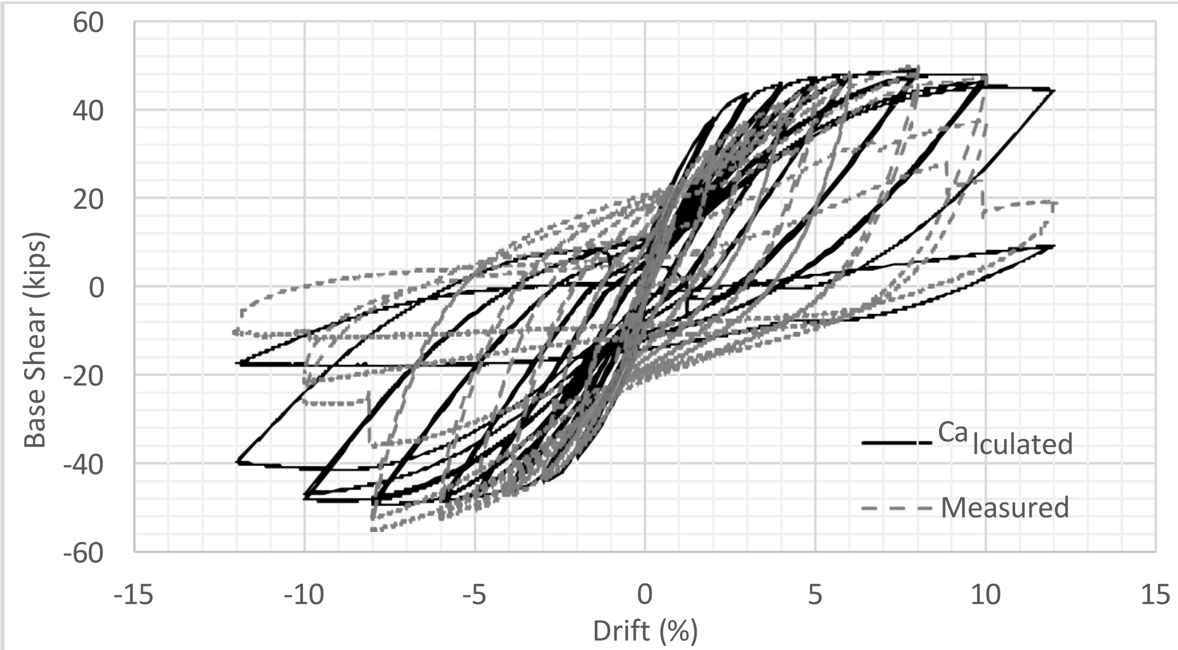


Figure 5.5 Measured and Calculated Force-Drift Hysteretic Responses of S2-Debond Column.

In order to investigate the effect of adding the bond slip effects to the numerical model on the force-drift relationship, a sensitivity analysis was conducted on each of the two columns. For S1-Bond, a pushover analysis was conducted twice: (1) with including the bar slip only, and (2) with including both bar slip and duct slip. The results of the two pushover curves are compared to the average backbone curve resulted from the experimental and are shown in Figure 5.6. It is observed that the numerical model that included both the bar and duct bond slips were able to adequately capture the force-drift response resulting from the experimental.

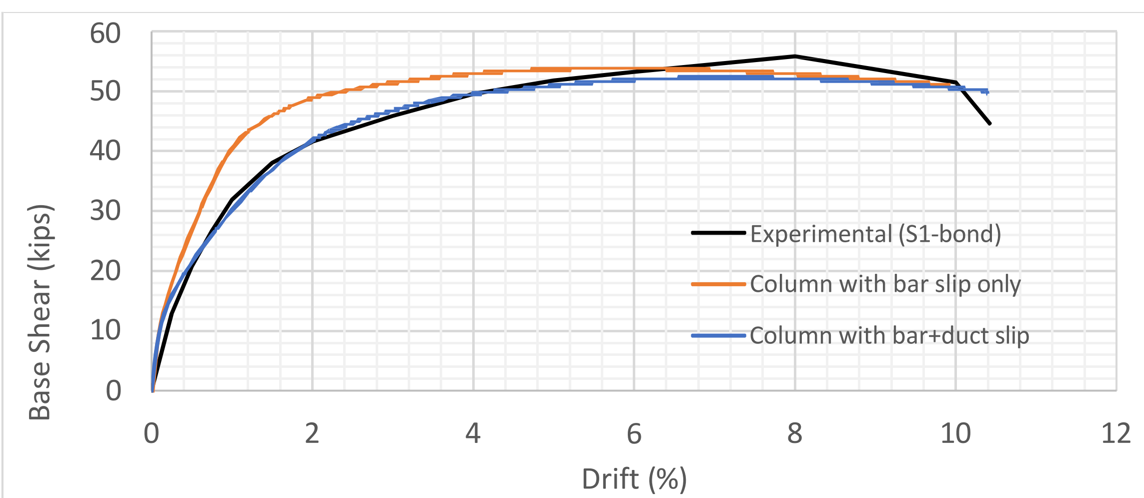


Figure 5.6 Sensitivity Analysis Study on The Pushover Force-Drift Response of S1-Bond.

For S2-Debond, a pushover analysis was conducted three times: (1) with including the bar slip only, (2) with including the bar slip and the duct slip, and (3) with including the bar, duct, and debonding slip effects. The results of the three pushover curves are compared to the average backbone curve resulted from the experimental and shown in Figure 5.7. It is observed that the numerical model that included the bar, duct and debonding bond slips were able to closely capture the force-drift response resulting from the experimental, however it was still somehow stiffer than the experimental response. This is again attributed to the fact that the experimented specimen had surface imperfection at the column-footing interface which resulted in a softer behavior and induced more plastic hinge rotations to the column.

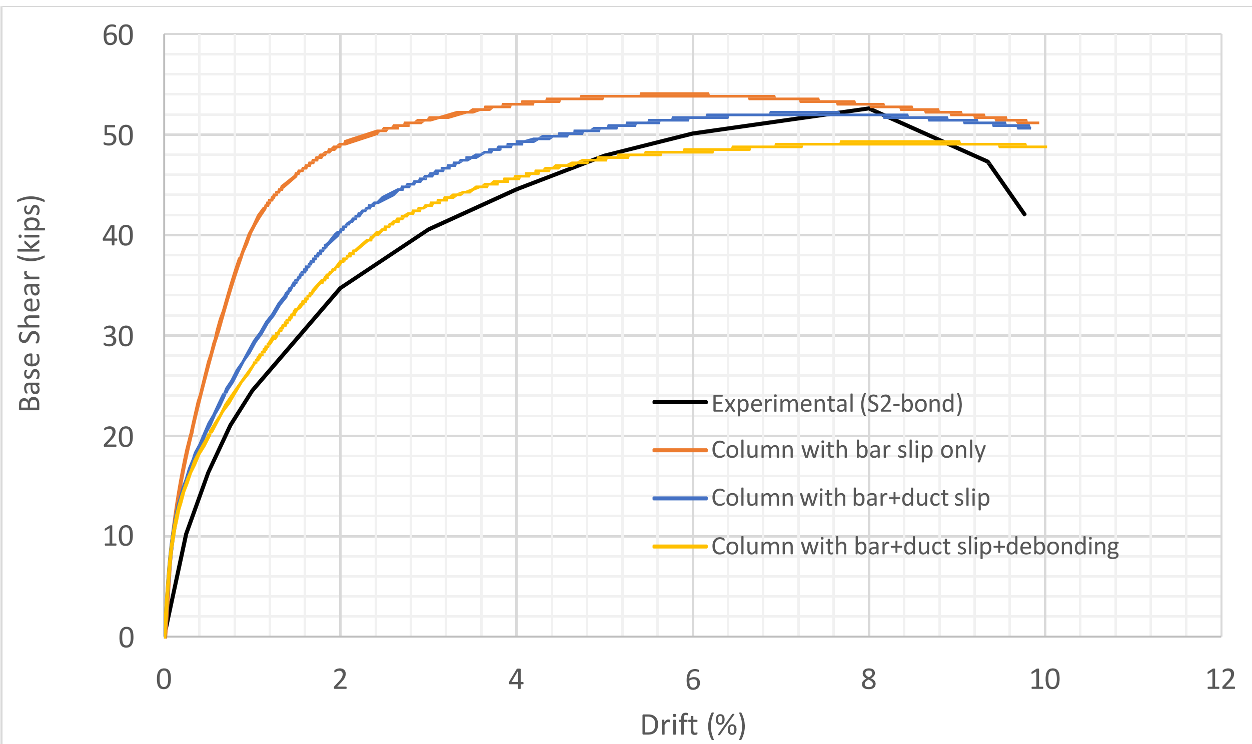


Figure 5.7 Sensitivity Analysis Study on The Pushover Force-Drift Response of S2-Debond.

# CHAPTER 6. SUMMARY AND CONCLUSIONS

## 6.1. Summary

Accelerated bridge construction (ABC) utilizes advanced planning, new construction techniques and innovative detailing to expedite construction. Numerous advantages could be achieved by implementing ABC for new bridges or the rehabilitation and replacement of old deteriorated bridges, such as: reducing onsite construction time, reducing the traffic congestion around the construction sites, and improving the quality of the prefabricated elements because they are typically built in better controlled plants. According to the Feral Highway Administration (FHWA), more than 150,000 bridges in USA need rehabilitation, repair, or total replacement. ABC is a good and efficient alternative to cast-in-place (CIP) conventional on-site construction as it helps decrease the economical, social, and construction costs or impact associated with long bridge construction duration.

ABC has been widely used in recent years in low seismic regions of the country and mostly implemented in the superstructure elements. However, ABC is not utilized extensively in substructure elements such as column-base connections, especially in moderate and high seismic regions due to the uncertainty in the seismic performance of the substructure connections. A few ABC seismic connections were developed and have been demonstrated for potential use in high seismic regions. Among these, grouted-ducts have been one of the more promising details. However, past research utilized proprietary and sole-sourced grout materials such as UHPC, which posed barriers toward wide-spread implementation grouted-ducts. To address this issue, the overall goal of this study was to implement the non-proprietary UHPC in grouted-duct ABC seismic connections of precast bridge columns that can emulate the seismic performance of conventional CIP columns.

This study revisited the previously developed UHPC-filled grouted-duct connection (Tazarv and Saiidi 2014) that has been used to connect precast columns to footings with the aim of utilizing a different grout. Reducing the costs and using non-proprietary materials was the focus of this study to establish a less expensive, less restrictive alternative for UHPC-filled grouted-duct connections and avoid sole-sourcing in construction contracts. In a companion study (Subedi et al. 2019), several nonproprietary UHPC mixes were considered and two were developed, refined, and used in 22 large-scale pullout specimens to determine the bond behavior of UHPC-filled grouted ducts. After observing satisfactory performance of these, one was used in grouted-duct connections in two large-scale (42%-scale) column models to connect precast columns to footings. Both column models were tested at UNR under combined axial and cyclic lateral loading to investigate their seismic performance and evaluate their ability to emulate the behavior of CIP column-footing connections. Moreover, analytical investigation for each column model was conducted to simulate the global response of the column models. The analytical models were conducted using finite element computer program OpenSEES and specific modelling assumptions for these connections that include the bond-slip effects, bar debonding effects and rebar-fatigue effects were validated for future implementation and further use in the design of this connection in actual bridges. The focus this report is on column studies.

### 6.2. Conclusions

The findings from the experimental and analytical studies performed on the non-proprietary UHPC-filled duct column-footing led to the following conclusions:

1- The non-proprietary UHPC-filled duct connections presented in this study were emulative of conventional cast-in-place (CIP) column-to-footing connections as indicated by successfully developing the full columns ultimate strength capacities and achieving high drift capacities without connection damage. Accordingly, the precast columns incorporating the UHPC mix developed in this study can be designed in accordance to current bridge codes with no limitations.

2- From the material variability study conducted in this study, it can be shown that: (a) decreasing the cement content is the most influential parameter that adversely affects the compressive strength; (b) decreasing the fibers content will not affect the compressive strength significantly but it will decrease the tensile strength and tensile ductility of the mix; (c) increasing the HRWRA content could be a better way to increase the mix flowability without affecting the compressive strength in highly reinforced members instead of increasing the water content.

3- The non-proprietary UHPC developed in this study is a low-cost alternative to the available proprietary UHPC mixes to be used in the column-to-footing duct connections without increasing the required embedment length of the bars inside the ducts.

4- The observed mode of failure for both column models with fully bonded and debonded longitudinal bars started with the column concrete cover spalling followed by bars buckling and spirals rupture then finally longitudinal bars rupture. The duct connections exhibited no damage such as bar pullout, duct pullout, or conical failure of the footing even at under 12% drift ratio.

5- Debonding of longitudinal bars above and below the column-footing interface was found to be successful in spreading bar yielding and preventing localized rebars strain concentration of reinforcement in UHPC-filled duct connections. However, debonding of bars induced more bar bond-slip effect resulting in softer load-drift behavior compared to the column with fully bonded bars.

6- A simplified finite element model developed using OpenSEES, an open source and publicly available finite element software, was shown to adequately reproduce the seismic response of both column models when it properly accounts for the bond-slip effects in both bars and ducts as well as bar debonding effects.

7- The S1-Bond and S2-Debond column models were able to undergo large inelastic deformations with drift capacities of 10.4% and 9.8%, respectively, compared to 9.9% and 9% for the CIP (conventional column) and PNC (column with proprietary UHPC filled ducts) column models. The measured displacement ductility capacities of S1-Bond and S2-Debond column models were at least 7.0 and 5.7, respectively, which well exceeds the AASHTO requirements for ductility demand of 5.0 for single column bents.

8- Applying a leveling grout at the interface between the column and the footing to ensure full contact between both members is strongly recommended in grouted-duct connections to maintain comparable initial stiffness and degradation behavior as CIP columns.

9- Overall, non-proprietary UHPC-filled duct connections are recommended as suitable precast column-to-footing or column-to-cap beam connections for moderate and high seismic regions because formation of full plastic moment in columns without any connection damage is assured.

## REFERENCES


1. AASHTO. (2010). "AASHTO LRFD Bridge Design Specification," Washington, DC: American Association of State Highway and Transportation Officials.

2. AASHTO. (2014). "AASHTO Guide Specifications for LRFD Seismic Bridge Design," 2nd edition, Washington, DC: American Association of State Highway and Transportation Officials.

3. Abokifa, M., & Moustafa, M. A. (2021). Experimental behavior of poly methyl methacrylate polymer concrete for bridge deck bulb tee girders longitudinal field joints. Construction and Building Materials, 270, 121840.

4. Aboukifa, M., Moustafa, M. A., Itani, A. M., & Naeimi, N. (2019). Durable UHPC Columns with High-Strength Steel (No. ABC-UTC-2013-C3-UNR02-Final). Accelerated Bridge Construction University Transportation Center (ABC-UTC).

5. Aboukifa, M., Moustafa, M., & Itani, A. (2019, June). Behavior of UHPC Column Subjected to Combined Axial and Lateral Loading. In International Interactive Symposium on Ultra-High Performance Concrete (Vol. 2, No. 1). Iowa State University Digital Press.

6. Aboukifa, M., Moustafa, M. A., & Itani, A. (2020). Comparative structural response of UHPC and normal strength concrete columns under combined axial and lateral cyclic loading. Special Publication, 341, 71-96.

7. Aboukifa, M., & Moustafa, M. A. (2021). Experimental seismic behavior of ultra-high performance concrete columns with high strength steel reinforcement. Engineering Structures, 232, 111885.

8. ACI Committee 239. (2012). "Ultra-High Performance Concrete," ACI Fall Convention, Toronto, Ontario, Canada.

9. ACI318. (2011). "Building Code Requirements for Reinforced Concrete," Detroit, Michigan: American Concrete Institute.

10. ACI408R-03. (2003). "Bond and Development of Straight Reinforcing Bars in Tension," ACI Committee 408, 49 pp.

11. Ameli, M.J., Parks, J.E., Brown, D.N., and Pantelides, C.P. (2014). "Grouted Splice Sleeve Connection Alternatives for Precast Reinforced Concrete Bridge Piers in Moderate-to-High Seismic Regions," *Proceeding of Tenth U.S. National Conference on Earthquake Engineering*, Anchorage, Alaska, 10 pp.

12. ASTM A615/A615M-09b. (2009). "Standard Specification for Deformed and Plain Carbon-Steel Bars for Concrete Reinforcement," West Conshohocken, PA, 6 pp.

13. ASTM A706/A706M-09b. (2009). "Standard Specification for Low-Alloy Steel Deformed and Plain Bars for Concrete Reinforcement," West Conshohocken, PA, 6 pp.

14. ASTM C109/C109M-11b. (2011). "Standard Test Method for Compressive Strength of Hydraulic Cement Mortars (Using 2-in. or [50-mm] Cube Specimens)," West Conshohocken, PA, 10 pp.

15. ASTM C39/C39M-12. (2012). "Standard Test Method for Compressive Strength of Cylindrical Concrete Specimens," West Conshohocken, PA, 7 pp.

16. Belleri, A., & Riva, P. (2012). Seismic performance and retrofit of precast concrete grouted sleeve connections.

17. Brenes, F.J., Wood, S.L. and Kreger, M.E. (2006). "Anchorage Requirements for Grouted Vertical-Duct Connectors in Precast Bent Cap Systems," *FHWA/TX-06/0-4176-1*, Center for Transportation Research, University of Texas at Austin.

18. Caltrans. (2006). "Seismic Design Criteria (SDC)," version 1.4. Sacramento, CA.: California Department of Transportation.

19. Caltrans. (2010). "Seismic Design Criteria (SDC)," version 1.6. Sacramento, CA.:California Department of Transportation,.

20. CEB-FIB. (1993). "CEB-FIB Model Code 1990: Design Code Committee EURO International Du Buton," London, UK: Thomas Telford.

21. Cruz Noguez C.A. and Saiidi, M.S. (2012). "Shake Table Studies of a 4-Span Bridge Model with Advanced Materials," *Journal of Structural Engineering*, *ASCE*, Vol. 138, No. 2, pp. 183-192.

22. Culmo, M. (2009). "Connection Details for Prefabricated Bridge Elements and Systems," Federal Highway Administration *Report No. FHWA-IF-09-010*.

23. Culmo, M. P. (2011). "Accelerated Bridge Construction - Experience in Design, Fabrication and Erection of Prefabricated Bridge Elements and Systems," Federal Highway Administration *Report No. FHWA-HIF-12-013*.

24. Eligehausen, R., Popov, E.P. and Bertero, V.V. (1982). "Local Bond Stress-Slip Relationships of Deformed Bars under Generalized Excitations," *Proceedings of the 7th European Conference on Earthquake Engineering*. Vol. 4. Athens: Techn. Chamber of Greece. pp. 69-80.

25. Galvis, F., Correal, J.F., Betancour, N., and Yamin, L. (2015). "Characterization of the Seismic Behavior of a Column-Foundation Connection for Accelerated Bridge Construction," VII Congreso Nacional de Ingenieria Sismica, Bogota, Colombia, 10pp.

26. Graybeal, B. (2006). "Material Property Characterization of Ultra-High Performance Concrete," McLean, VA: FHWA, U.S. Department of Transportation, *Report No. FHWA-HRT-06-103*.

27. Graybeal, B. (2010). "Behavior of Field-Cast Ultra-High Performance Concrete Bridge Deck Connections under Cyclic and Static Structural Loading," Federal Highway Administration *Report No. FHWA-HRT-11-023*.

28. Graybeal, B. and Davis, M. (2008). "Cylinder or Cube: Strength Testing of 80 to 200 MPa (11.6 to 29 ksi) Ultra-High-Performance Fiber-Reinforced Concrete," *ACI Materials Journal*, Vol. 105, No. 6, pp. 603-609.

29. Haber, Z. (2013). "Precast Column-Footing Connections for Accelerated Bridge Construction in Seismic Zones," PhD Dissertation, University of Nevada Reno, 612 pp.

30. Haber, Z.B., Saiidi, M.S. and Sanders, D.H. (2013). "Precast Column-Footing Connections for Accelerated Bridge Construction in Seismic Zones," Center for Civil Engineering Earthquake Research, Department of Civil and Environmental Engineering, University of Nevada, Reno, Nevada, *Report No. CCEER-13-08*, 502 pp.

31. Haber, Z.B., Saiidi, M.S. and Sanders, D.H. (2014). "Seismic performance of precast columns with mechanically spliced column-footing connections. ACI Struct J 2014;111(3):339–650.

32. Haraldsson, O.S., Janes, T.M., Eberhard, M.O. and and Stanton, J.F. (2012). “Seismic Resistance of Socket Connection between Footing and Precast Column,” *Journal of Bridge Engineering, ASCE*, Vol. 18, No. 9, pp. 910-919.

33. JSCE Concrete Library 127. (2008). “Recommendations for Design and Construction of High Performance Fiber Reinforced Cement Composites with Multiple Fine Cracks (HPFRCC),” Japan Society of Civil Engineers.

34. Khaleghi, B., Schultz, E., Seguirant, S., Marsh, L., Haraldsson, O., Eberhard, M. and Stanton, J. (2012). “Accelerated Bridge Construction in Washington State: From research to Practice,” *PCI Journal*, pp 34-49.

35. Mander, J.B., Priestley, M.J.N., Park, R. (1988). “Theoretical Stress-Strain Model for Confined Concrete,” *Journal of Structural Engineering, ASCE*, Vol. 114, No. 8, pp. 1804-1826.

36. Mantawy, I. M., Thonstad, T., Sanders, D. H., Stanton, J. F., & Eberhard, M. O. (2016). Seismic performance of precast, pretensioned, and cast-in-place bridges: Shake table test comparison. Journal of Bridge Engineering, 21(10), 04016071.

37. Marsh, M.L., Wernli, M., Garrett, B.E., Stanton, J.F., Eberhard, M.O. and Weinert, M.D. (2011). “Application of Accelerated Bridge Construction Connections in Moderate-to-High Seismic Regions,” Washington, D.C.: *National Cooperative Highway Research Program (NCHRP) Report No. 698*.

38. Matsumoto, E.E., Waggoner, M.C., Sumen, G. and Kreger, M.E. (2001). “Development of a Precast Bent Cap System,” Center for Transportation Research, The University of Texas at Austin: *FHWA Report No. FHWA/TX-0-1748-2*.

39. Mehrsoroush, A. and Saiidi, M.S. (2014). “Seismic Performance of Two-Column Bridge Piers with Innovative Precast Members and Pipe Pin Connections,” *Proceeding of 7th International Conference on Bridge Maintenance, Safety and Management (IABMAS)*, Shanghai, China.

40. Mo, Y.L., and Chan, J. (1996). “Bond and Slip of Plain Rebars in Concrete,” *Journal of Materials in Civil Engineering, ASCE*, Vol. 8, No.4, pp. 208-211.

41. Monti, G., and Spacone, E. (2000). “Reinforced Concrete Fiber Beam Element with Bond-Slip,” *Journal of Structural Engineering, ASCE*, Vol. 126, No. 6, pp. 654-661.

42. Motaref, S., Saiidi, M.S., and Sanders, D. (2011). "Seismic Response of Precast Bridge Columns with Energy Dissipating Joints," Center for Civil Engineering Earthquake Research, Department of Civil and Environmental Engineering, University of Nevada, Reno, *Report No. CCEER-11-01*.

43. OpenSees. (2013). "Open System for Earthquake Engineering Simulations," Version 2.4.1, Berkeley, CA, Available online: http://opensees.berkeley.edu.

44. Pang, J. B., Steuck, K. P., Cohagen, L., Eberhard, M. O., & Stanton, J. F. (2008). *Rapidly constructible large-bar precast bridge-bent connection* (No. WA-RD 684.2).

45. Popa, V., Papurcu, A., Cotofana, D., & Pascu, R. (2015). Experimental testing on emulative connections for precast columns using grouted corrugated steel sleeves. *Bulletin of Earthquake Engineering*, *13*(8), 2429-2447.

46. Raynor, D.J., Lehman, D.E. and Stanton, J.F. (2002). "Bond-Slip Response of Reinforcing Bars Grouted in Ducts," ACI Structural Journal, Vol. 99, No. 5, pp. 568-576.

47. Restrepo, J.I., Tobolski, M.J. and Matsumoto, E.E. (2011). "Development of a Precast Bent Cap System for Seismic Regions," *NCHRP Report 681*, Washington, D.C.

48. Russell, H.G. and Graybeal B.A. (2013). "Ultra-High Performance Concrete: A State-of-the-Art Report for the Bridge Community," Federal Highway Administration, *Report No. FHWA-HRT-13-060*, 171 pp.

49. SETRA-AFGC. (2002). "Ultra High Performance Fibre-Reinforced Concretes," Interim Recommendations, SETRA-AFGC, Groupe de travail BFUP, Paris, France, 98 pp.

50. Shrestha, G., Saiidi, M.S., Itani, A.M., and Sanders, D.H. (2018). "Seismic Studies of Superstructure and Substructure Connections for Accelerated Bridge Construction, Dissertation, University of Nevada, Reno

51. Soroushian, P. and Choi, K.B. (1989). "Local Bond of Deformed Bars with Different Diameters in Confined Concrete," *ACI Structural Journal*, Vol. 86, No.2, pp. 217-222.

52. Steuck, K.P., Eberhard, M.O. and Stanton, J.F. (2009). "Anchorage of Large- Diameter Reinforcing Bars in Ducts," *ACI Structural Journal*, Vol. 106, No. 4, pp. 506-513.

53. Steuck, K.P., Pang, J.B.K., Eberhard, M.O. and Stanton, J.F. (2008). "Anchorage of Large-diameter Reinforcing Bars Grouted into Ducts," *WA-RD 684.1*, University of Washington, Seattle, Washington.

54. Subedi, D., Moustafa, M.A., and Saiidi, M.S. (2019). "Non-Proprietary UHPC for Anchorage of Large Diameter Column Bars in Grouted Ducts". Center for Civil Engineering Earthquake Research, Department of Civil and Environmental Engineering, University of Nevada, Reno, Nevada, Report No. CCEER-19-06; 2019.

55. Thonstad, T., Mantawy, I. M., Stanton, J. F., Eberhard, M. O., & Sanders, D. H. (2016). Shaking table performance of a new bridge system with pretensioned rocking columns. Journal of Bridge Engineering, 21(4), 04015079.

56. Tazarv, M., and Saiidi M.S. (2014). "Next generation of bridge columns for accelerated bridge construction in high seismic zones". Center for Civil Engineering Earthquake Research, Department of Civil and Environmental Engineering, University of Nevada, Reno, Nevada, Report No. CCEER-14-06; 2014. 400pp.

57. Tazarv, M., and Saiidi, M. S. (2015). "UHPC-filled duct connections for accelerated bridge construction of RC columns in high seismic zones." Eng. Struct., 99(3), 413–422.

58. Utah Department of Transportation. (2010). "Precast Substructure Elements," http://dot.utah.gov, 24 pp.

59. Wang, J.C., Ou, Y.C., Chang, K.C., and Lee, G.C. (2008). "Large-Scale Seismic Tests of Tall Concrete Bridge Columns with Precast Segmental Construction," *Earthquake Engineering and Structural Dynamics*, Vol. 37, pp. 1449-1465.

# LIST OF CCEER PUBLICATIONS

| Report No. | Publication |
|---|---|
| CCEER-84-1 | Saiidi, M., and R. Lawver, "User's Manual for LZAK-C64, A Computer Program to Implement the Q-Model on Commodore 64," Civil Engineering Department, Report No. CCEER-84-1, University of Nevada, Reno, January 1984. |
| CCEER-84-1 | Douglas, B., Norris, G., Saiidi, M., Dodd, L., Richardson, J. and Reid, W., "Simple Bridge Models for Earthquakes and Test Data," Civil Engineering Department, Report No. CCEER-84-1 Reprint, University of Nevada, Reno, January 1984. |
| CCEER-84-2 | Douglas, B. and T. Iwasaki, "Proceedings of the First USA-Japan Bridge Engineering Workshop," held at the Public Works Research Institute, Tsukuba, Japan, Civil Engineering Department, Report No. CCEER-84-2, University of Nevada, Reno, April 1984. |
| CCEER-84-3 | Saiidi, M., J. Hart, and B. Douglas, "Inelastic Static and Dynamic Analysis of Short R/C Bridges Subjected to Lateral Loads," Civil Engineering Department, Report No. CCEER-84-3, University of Nevada, Reno, July 1984. |
| CCEER-84-4 | Douglas, B., "A Proposed Plan for a National Bridge Engineering Laboratory," Civil Engineering Department, Report No. CCEER-84-4, University of Nevada, Reno, December 1984. |
| CCEER-85-1 | Norris, G. and P. Abdollaholiaee, "Laterally Loaded Pile Response: Studies with the Strain Wedge Model," Civil Engineering Department, Report No. CCEER-85-1, University of Nevada, Reno, April 1985. |
| CCEER-86-1 | Ghusn, G. and M. Saiidi, "A Simple Hysteretic Element for Biaxial Bending of R/C in NEABS-86," Civil Engineering Department, Report No. CCEER-86-1, University of Nevada, Reno, July 1986. |
| CCEER-86-2 | Saiidi, M., R. Lawver, and J. Hart, "User's Manual of ISADAB and SIBA, Computer Programs for Nonlinear Transverse Analysis of Highway Bridges Subjected to Static and Dynamic Lateral Loads," Civil Engineering Department, Report No. CCEER-86-2, University of Nevada, Reno, September 1986. |
| CCEER-87-1 | Siddharthan, R., "Dynamic Effective Stress Response of Surface and Embedded Footings in Sand," Civil Engineering Department, Report No. CCEER-86-2, University of Nevada, Reno, June 1987. |
| CCEER-87-2 | Norris, G. and R. Sack, "Lateral and Rotational Stiffness of Pile Groups for Seismic Analysis of Highway Bridges," Civil Engineering Department, Report No. CCEER-87-2, University of Nevada, Reno, June 1987. |
| CCEER-88-1 | Orie, J. and M. Saiidi, "A Preliminary Study of One-Way Reinforced Concrete Pier Hinges Subjected to Shear and Flexure," Civil Engineering Department, Report No. CCEER-88-1, University of Nevada, Reno, January 1988. |
| CCEER-88-2 | Orie, D., M. Saiidi, and B. Douglas, "A Micro-CAD System for Seismic Design of Regular Highway Bridges," Civil Engineering Department, Report No. CCEER-88-2, University of Nevada, Reno, June 1988. |
| CCEER-88-3 | Orie, D. and M. Saiidi, "User's Manual for Micro-SARB, a Microcomputer Program for Seismic Analysis of Regular Highway Bridges," Civil Engineering Department, Report No. CCEER-88-3, University of Nevada, Reno, October 1988. |

CCEER-89-1 Douglas, B., M. Saiidi, R. Hayes, and G. Holcomb, "A Comprehensive Study of the Loads and Pressures Exerted on Wall Forms by the Placement of Concrete," Civil Engineering Department, Report No. CCEER-89-1, University of Nevada, Reno, February 1989.

CCEER-89-2 Richardson, J. and B. Douglas, "Dynamic Response Analysis of the Dominion Road Bridge Test Data," Civil Engineering Department, Report No. CCEER-89-2, University of Nevada, Reno, March 1989.

CCEER-89-2 Vrontinos, S., M. Saiidi, and B. Douglas, "A Simple Model to Predict the Ultimate Response of R/C Beams with Concrete Overlays," Civil Engineering Department, Report NO. CCEER-89-2, University of Nevada, Reno, June 1989.

CCEER-89-3 Ebrahimpour, A. and P. Jagadish, "Statistical Modeling of Bridge Traffic Loads - A Case Study," Civil Engineering Department, Report No. CCEER-89-3, University of Nevada, Reno, December 1989.

CCEER-89-4 Shields, J. and M. Saiidi, "Direct Field Measurement of Prestress Losses in Box Girder Bridges," Civil Engineering Department, Report No. CCEER-89-4, University of Nevada, Reno, December 1989.

CCEER-90-1 Saiidi, M., E. Maragakis, G. Ghusn, Y. Jiang, and D. Schwartz, "Survey and Evaluation of Nevada's Transportation Infrastructure, Task 7.2 - Highway Bridges, Final Report," Civil Engineering Department, Report No. CCEER 90-1, University of Nevada, Reno, October 1990.

CCEER-90-2 Abdel-Ghaffar, S., E. Maragakis, and M. Saiidi, "Analysis of the Response of Reinforced Concrete Structures During the Whittier Earthquake 1987," Civil Engineering Department, Report No. CCEER 90-2, University of Nevada, Reno, October 1990.

CCEER-91-1 Saiidi, M., E. Hwang, E. Maragakis, and B. Douglas, "Dynamic Testing and the Analysis of the Flamingo Road Interchange," Civil Engineering Department, Report No. CCEER-91-1, University of Nevada, Reno, February 1991.

CCEER-91-2 Norris, G., R. Siddharthan, Z. Zafir, S. Abdel-Ghaffar, and P. Gowda, "Soil-Foundation-Structure Behavior at the Oakland Outer Harbor Wharf," Civil Engineering Department, Report No. CCEER-91-2, University of Nevada, Reno, July 1991.

CCEER-91-3 Norris, G., "Seismic Lateral and Rotational Pile Foundation Stiffnesses at Cypress," Civil Engineering Department, Report No. CCEER-91-3, University of Nevada, Reno, August 1991.

CCEER-91-4 O'Connor, D. and M. Saiidi, "A Study of Protective Overlays for Highway Bridge Decks in Nevada, with Emphasis on Polyester-Styrene Polymer Concrete," Civil Engineering Department, Report No. CCEER-91-4, University of Nevada, Reno, October 1991.

CCEER-91-5 O'Connor, D.N. and M. Saiidi, "Laboratory Studies of Polyester-Styrene Polymer Concrete Engineering Properties," Civil Engineering Department, Report No. CCEER-91-5, University of Nevada, Reno, November 1991.

CCEER-92-1 Straw, D.L. and M. Saiidi, "Scale Model Testing of One-Way Reinforced Concrete Pier Hinges Subject to Combined Axial Force, Shear and Flexure," edited by D.N. O'Connor, Civil Engineering Department, Report No. CCEER-92-1, University of Nevada, Reno, March 1992.

CCEER-92-2 Wehbe, N., M. Saiidi, and F. Gordaninejad, "Basic Behavior of Composite Sections Made of Concrete Slabs and Graphite Epoxy Beams," Civil Engineering Department, Report No. CCEER-92-2, University of Nevada, Reno, August 1992.

CCEER-92-3 Saiidi, M. and E. Hutchens, "A Study of Prestress Changes in A Post-Tensioned Bridge During the First 30 Months," Civil Engineering Department, Report No. CCEER-92-3, University of Nevada, Reno, April 1992.

CCEER-92-4 Saiidi, M., B. Douglas, S. Feng, E. Hwang, and E. Maragakis, "Effects of Axial Force on Frequency of Prestressed Concrete Bridges," Civil Engineering Department, Report No. CCEER-92-4, University of Nevada, Reno, August 1992.

CCEER-92-5 Siddharthan, R., and Z. Zafir, "Response of Layered Deposits to Traveling Surface Pressure Waves," Civil Engineering Department, Report No. CCEER-92-5, University of Nevada, Reno, September 1992.

CCEER-92-6 Norris, G., and Z. Zafir, "Liquefaction and Residual Strength of Loose Sands from Drained Triaxial Tests," Civil Engineering Department, Report No. CCEER-92-6, University of Nevada, Reno, September 1992.

CCEER-92-6-A Norris, G., Siddharthan, R., Zafir, Z. and Madhu, R. "Liquefaction and Residual Strength of Sands from Drained Triaxial Tests," Civil Engineering Department, Report No. CCEER-92-6-A, University of Nevada, Reno, September 1992.

CCEER-92-7 Douglas, B., "Some Thoughts Regarding the Improvement of the University of Nevada, Reno's National Academic Standing," Civil Engineering Department, Report No. CCEER-92-7, University of Nevada, Reno, September 1992.

CCEER-92-8 Saiidi, M., E. Maragakis, and S. Feng, "An Evaluation of the Current Caltrans Seismic Restrainer Design Method," Civil Engineering Department, Report No. CCEER-92-8, University of Nevada, Reno, October 1992.

CCEER-92-9 O'Connor, D., M. Saiidi, and E. Maragakis, "Effect of Hinge Restrainers on the Response of the Madrone Drive Undercrossing During the Loma Prieta Earthquake," Civil Engineering Department, Report No. CCEER-92-9, University of Nevada, Reno, February 1993.

CCEER-92-10 O'Connor, D., and M. Saiidi, "Laboratory Studies of Polyester Concrete: Compressive Strength at Elevated Temperatures and Following Temperature Cycling, Bond Strength to Portland Cement Concrete, and Modulus of Elasticity," Civil Engineering Department, Report No. CCEER-92-10, University of Nevada, Reno, February 1993.

CCEER-92-11 Wehbe, N., M. Saiidi, and D. O'Connor, "Economic Impact of Passage of Spent Fuel Traffic on Two Bridges in Northeast Nevada," Civil Engineering Department, Report No. CCEER-92-11, University of Nevada, Reno, December 1992.

CCEER-93-1 Jiang, Y., and M. Saiidi, "Behavior, Design, and Retrofit of Reinforced Concrete One-way Bridge Column Hinges," edited by D. O'Connor, Civil Engineering Department, Report No. CCEER-93-1, University of Nevada, Reno, March 1993.

CCEER-93-2 Abdel-Ghaffar, S., E. Maragakis, and M. Saiidi, "Evaluation of the Response of the Aptos Creek Bridge During the 1989 Loma Prieta Earthquake," Civil Engineering Department, Report No. CCEER-93-2, University of Nevada, Reno, June 1993.

CCEER-93-3 Sanders, D.H., B.M. Douglas, and T.L. Martin, "Seismic Retrofit Prioritization of Nevada Bridges," Civil Engineering Department, Report No. CCEER-93-3, University of Nevada, Reno, July 1993.

CCEER-93-4 Abdel-Ghaffar, S., E. Maragakis, and M. Saiidi, "Performance of Hinge Restrainers in the Huntington Avenue Overhead During the 1989 Loma Prieta Earthquake," Civil Engineering Department, Report No. CCEER-93-4, University of Nevada, Reno, June 1993.

CCEER-93-5 Maragakis, E., M. Saiidi, S. Feng, and L. Flournoy, "Effects of Hinge Restrainers on the Response of the San Gregorio Bridge during the Loma Prieta Earthquake," (in final preparation) Civil Engineering Department, Report No. CCEER-93-5, University of Nevada, Reno.

CCEER-93-6 Saiidi, M., E. Maragakis, S. Abdel-Ghaffar, S. Feng, and D. O'Connor, "Response of Bridge Hinge Restrainers during Earthquakes -Field Performance, Analysis, and Design," Civil Engineering Department, Report No. CCEER-93-6, University of Nevada, Reno, May 1993.

CCEER-93-7 Wehbe, N., Saiidi, M., Maragakis, E., and Sanders, D., "Adequacy of Three Highway Structures in Southern Nevada for Spent Fuel Transportation," Civil Engineering Department, Report No. CCEER-93-7, University of Nevada, Reno, August 1993.

CCEER-93-8 Roybal, J., Sanders, D.H., and Maragakis, E., "Vulnerability Assessment of Masonry in the Reno-Carson City Urban Corridor," Civil Engineering Department, Report No. CCEER-93-8, University of Nevada, Reno, May 1993.

CCEER-93-9 Zafir, Z. and Siddharthan, R., "MOVLOAD: A Program to Determine the Behavior of Nonlinear Horizontally Layered Medium Under Moving Load," Civil Engineering Department, Report No. CCEER-93-9, University of Nevada, Reno, August 1993.

CCEER-93-10 O'Connor, D.N., Saiidi, M., and Maragakis, E.A., "A Study of Bridge Column Seismic Damage Susceptibility at the Interstate 80/U.S. 395 Interchange in Reno, Nevada," Civil Engineering Department, Report No. CCEER-93-10, University of Nevada, Reno, October 1993.

CCEER-94-1 Maragakis, E., B. Douglas, and E. Abdelwahed, "Preliminary Dynamic Analysis of a Railroad Bridge," Report CCEER-94-1, January 1994.

CCEER-94-2 Douglas, B.M., Maragakis, E.A., and Feng, S., "Stiffness Evaluation of Pile Foundation of Cazenovia Creek Overpass," Civil Engineering Department, Report No. CCEER-94-2, University of Nevada, Reno, March 1994.

CCEER-94-3 Douglas, B.M., Maragakis, E.A., and Feng, S., "Summary of Pretest Analysis of Cazenovia Creek Bridge," Civil Engineering Department, Report No. CCEER-94-3, University of Nevada, Reno, April 1994.

CCEER-94-4 Norris, G.M., Madhu, R., Valceschini, R., and Ashour, M., "Liquefaction and Residual Strength of Loose Sands from Drained Triaxial Tests," Report 2, Vol. 1&2, Civil Engineering Department, Report No. CCEER-94-4, University of Nevada, Reno, August 1994.

CCEER-94-5 Saiidi, M., Hutchens, E., and Gardella, D., "Prestress Losses in a Post-Tensioned R/C Box Girder Bridge in Southern Nevada," Civil Engineering Department, CCEER-94-5, University of Nevada, Reno, August 1994.

CCEER-95-1 Siddharthan, R., El-Gamal, M., and Maragakis, E.A., "Nonlinear Bridge Abutment , Verification, and Design Curves," Civil Engineering Department, CCEER-95-1, University of Nevada, Reno, January 1995.

CCEER-95-2 Ashour, M. and Norris, G., "Liquefaction and Undrained Response Evaluation of Sands from Drained Formulation," Civil Engineering Department, Report No. CCEER-95-2, University of Nevada, Reno, February 1995.

CCEER-95-3 Wehbe, N., Saiidi, M., Sanders, D. and Douglas, B., "Ductility of Rectangular Reinforced Concrete Bridge Columns with Moderate Confinement," Civil Engineering Department, Report No. CCEER-95-3, University of Nevada, Reno, July 1995.

CCEER-95-4 Martin, T.., Saiidi, M. and Sanders, D., "Seismic Retrofit of Column-Pier Cap Connections in Bridges in Northern Nevada," Civil Engineering Department, Report No. CCEER-95-4, University of Nevada, Reno, August 1995.

CCEER-95-5 Darwish, I., Saiidi, M. and Sanders, D., "Experimental Study of Seismic Susceptibility Column-

Footing Connections in Bridges in Northern Nevada," Civil Engineering Department, Report No. CCEER-95-5, University of Nevada, Reno, September 1995.

CCEER-95-6 Griffin, G., Saiidi, M. and Maragakis, E., "Nonlinear Seismic Response of Isolated Bridges and Effects of Pier Ductility Demand," Civil Engineering Department, Report No. CCEER-95-6, University of Nevada, Reno, November 1995.

CCEER-95-7 Acharya, S.., Saiidi, M. and Sanders, D., "Seismic Retrofit of Bridge Footings and Column-Footing Connections," Civil Engineering Department, Report No. CCEER-95-7, University of Nevada, Reno, November 1995.

CCEER-95-8 Maragakis, E., Douglas, B., and Sandirasegaram, U., "Full-Scale Field Resonance Tests of a Railway Bridge," A Report to the Association of American Railroads, Civil Engineering Department, Report No. CCEER-95-8, University of Nevada, Reno, December 1995.

CCEER-95-9 Douglas, B., Maragakis, E. and Feng, S., "System Identification Studies on Cazenovia Creek Overpass," Report for the National Center for Earthquake Engineering Research, Civil Engineering Department, Report No. CCEER-95-9, University of Nevada, Reno, October 1995.

CCEER-96-1 El-Gamal, M.E. and Siddharthan, R.V., "Programs to Computer Translational Stiffness of Seat-Type Bridge Abutment," Civil Engineering Department, Report No. CCEER-96-1, University of Nevada, Reno, March 1996.

CCEER-96-2 Labia, Y., Saiidi, M. and Douglas, B., "Evaluation and Repair of Full-Scale Prestressed Concrete Box Girders," A Report to the National Science Foundation, Research Grant CMS-9201908, Civil Engineering Department, Report No. CCEER-96-2, University of Nevada, Reno, May 1996.

CCEER-96-3 Darwish, I., Saiidi, M. and Sanders, D., "Seismic Retrofit of R/C Oblong Tapered Bridge Columns with Inadequate Bar Anchorage in Columns and Footings," A Report to the Nevada Department of Transportation, Civil Engineering Department, Report No. CCEER-96-3, University of Nevada, Reno, May 1996.

CCEER-96-4 Ashour, M., Pilling, R., Norris, G. and Perez, H., "The Prediction of Lateral Load Behavior of Single Piles and Pile Groups Using the Strain Wedge Model," A Report to the California Department of Transportation, Civil Engineering Department, Report No. CCEER-96-4, University of Nevada, Reno, June 1996.

CCEER-97-1-A Rimal, P. and Itani, A. "Sensitivity Analysis of Fatigue Evaluations of Steel Bridges," Center for Earthquake Research, Department of Civil Engineering, University of Nevada, Reno, Nevada Report No. CCEER-97-1-A, September, 1997.

CCEER-97-1-B Maragakis, E., Douglas, B., and Sandirasegaram, U. "Full-Scale Field Resonance Tests of a Railway Bridge," A Report to the Association of American Railroads, Civil Engineering Department, University of Nevada, Reno, May, 1996.

CCEER-97-2 Wehbe, N., Saiidi, M., and D. Sanders, "Effect of Confinement and Flares on the Seismic Performance of Reinforced Concrete Bridge Columns," Civil Engineering Department, Report No. CCEER-97-2, University of Nevada, Reno, September 1997.

CCEER-97-3 Darwish, I., M. Saiidi, G. Norris, and E. Maragakis, "Determination of In-Situ Footing Stiffness Using Full-Scale Dynamic Field Testing," A Report to the Nevada Department of Transportation, Structural Design Division, Carson City, Nevada, Report No. CCEER-97-3, University of Nevada, Reno, October 1997.

CCEER-97-4-A Itani, A. "Cyclic Behavior of Richmond-San Rafael Tower Links," Center for Civil Engineering

Earthquake Research, Department of Civil Engineering, University of Nevada, Reno, Nevada, Report No. CCEER-97-4, August 1997.

CCEER-97-4-B Wehbe, N., and M. Saiidi, “User’s Manual for RCMC v. 1.2 : A Computer Program for Moment-Curvature Analysis of Confined and Unconfined Reinforced Concrete Sections,” Center for Civil Engineering Earthquake Research, Department of Civil Engineering, University of Nevada, Reno, Nevada, Report No. CCEER-97-4, November, 1997.

CCEER-97-5 Isakovic, T., M. Saiidi, and A. Itani, “Influence of new Bridge Configurations on Seismic Performance,” Department of Civil Engineering, University of Nevada, Reno, Report No. CCEER-97-5, September, 1997.

CCEER-98-1 Itani, A., Vesco, T. and Dietrich, A., “Cyclic Behavior of “as Built” Laced Members With End Gusset Plates on the San Francisco Bay Bridge,” Center for Civil Engineering Earthquake Research, Department of Civil Engineering, University of Nevada, Reno, Nevada Report No. CCEER-98-1, March, 1998.

CCEER-98-2 G. Norris and M. Ashour, “Liquefaction and Undrained Response Evaluation of Sands from Drained Formulation,” Center for Civil Engineering Earthquake Research, Department of Civil Engineering, University of Nevada, Reno, Nevada, Report No. CCEER-98-2, May, 1998.

CCEER-98-3 Qingbin, Chen, B. M. Douglas, E. Maragakis, and I. G. Buckle, “Extraction of Nonlinear Hysteretic Properties of Seismically Isolated Bridges from Quick-Release Field Tests,” Center for Civil Engineering Earthquake Research, Department of Civil Engineering, University of Nevada, Reno, Nevada, Report No. CCEER-98-3, June, 1998.

CCEER-98-4 Maragakis, E., B. M. Douglas, and C. Qingbin, “Full-Scale Field Capacity Tests of a Railway Bridge,” Center for Civil Engineering Earthquake Research, Department of Civil Engineering, University of Nevada, Reno, Nevada, Report No. CCEER-98-4, June, 1998.

CCEER-98-5 Itani, A., Douglas, B., and Woodgate, J., “Cyclic Behavior of Richmond-San Rafael Retrofitted Tower Leg,” Center for Civil Engineering Earthquake Research, Department of Civil Engineering, University of Nevada, Reno. Report No. CCEER-98-5, June 1998

CCEER-98-6 Moore, R., Saiidi, M., and Itani, A., “Seismic Behavior of New Bridges with Skew and Curvature,” Center for Civil Engineering Earthquake Research, Department of Civil Engineering, University of Nevada, Reno. Report No. CCEER-98-6, October, 1998.

CCEER-98-7 Itani, A and Dietrich, A, “Cyclic Behavior of Double Gusset Plate Connections,” Center for Civil Engineering Earthquake Research, Department of Civil Engineering, University of Nevada, Reno, Nevada, Report No. CCEER-98-5, December, 1998.

CCEER-99-1 Caywood, C., M. Saiidi, and D. Sanders, “Seismic Retrofit of Flared Bridge Columns with Steel Jackets,” Civil Engineering Department, University of Nevada, Reno, Report No. CCEER-99-1, February 1999.

CCEER-99-2 Mangoba, N., M. Mayberry, and M. Saiidi, “Prestress Loss in Four Box Girder Bridges in Northern Nevada,” Civil Engineering Department, University of Nevada, Reno, Report No. CCEER-99-2, March 1999.

CCEER-99-3 Abo-Shadi, N., M. Saiidi, and D. Sanders, “Seismic Response of Bridge Pier Walls in the Weak Direction,” Civil Engineering Department, University of Nevada, Reno, Report No. CCEER-99-3, April 1999.

CCEER-99-4 Buzick, A., and M. Saiidi, “Shear Strength and Shear Fatigue Behavior of Full-Scale Prestressed Concrete Box Girders,” Civil Engineering Department, University of Nevada, Reno, Report No. CCEER-99-4, April 1999.

CCEER-99-5 Randall, M., M. Saiidi, E. Maragakis and T. Isakovic, “Restrainer Design Procedures For Multi-Span Simply-Supported Bridges,” Civil Engineering Department, University of Nevada, Reno, Report No. CCEER-99-5, April 1999.

CCEER-99-6 Wehbe, N. and M. Saiidi, “User's Manual for RCMC v. 1.2, A Computer Program for Moment-Curvature Analysis of Confined and Unconfined Reinforced Concrete Sections,” Civil Engineering Department, University of Nevada, Reno, Report No. CCEER-99-6, May 1999.

CCEER-99-7 Burda, J. and A. Itani, “Studies of Seismic Behavior of Steel Base Plates,” Civil Engineering Department, University of Nevada, Reno, Report No. CCEER-99-7, May 1999.

CCEER-99-8 Ashour, M. and G. Norris, “Refinement of the Strain Wedge Model Program,” Civil Engineering Department, University of Nevada, Reno, Report No. CCEER-99-8, March 1999.

CCEER-99-9 Dietrich, A., and A. Itani, “Cyclic Behavior of Laced and Perforated Steel Members on the San Francisco-Oakland Bay Bridge,” Civil Engineering Department, University, Reno, Report No. CCEER-99-9, December 1999.

CCEER 99-10 Itani, A., A. Dietrich, “Cyclic Behavior of Built Up Steel Members and their Connections,” Civil Engineering Department, University of Nevada, Reno, Report No. CCEER-99-10, December 1999.

CCEER 99-10-A Itani, A., E. Maragakis and P. He, “Fatigue Behavior of Riveted Open Deck Railroad Bridge Girders,” Civil Engineering Department, University of Nevada, Reno, Report No. CCEER-99-10-A, August 1999.

CCEER 99-11 Itani, A., J. Woodgate, “Axial and Rotational Ductility of Built Up Structural Steel Members,” Civil Engineering Department, University of Nevada, Reno, Report No. CCEER-99-11, December 1999.

CCEER-99-12 Sgambelluri, M., Sanders, D.H., and Saiidi, M.S., “Behavior of One-Way Reinforced Concrete Bridge Column Hinges in the Weak Direction,” Department of Civil Engineering, University of Nevada, Reno, Report No. CCEER-99-12, December 1999.

CCEER-99-13 Laplace, P., Sanders, D.H., Douglas, B, and Saiidi, M, “Shake Table Testing of Flexure Dominated Reinforced Concrete Bridge Columns”, Department of Civil Engineering, University of Nevada, Reno, Report No. CCEER-99-13, December 1999.

CCEER-99-14 Ahmad M. Itani, Jose A. Zepeda, and Elizabeth A. Ware “Cyclic Behavior of Steel Moment Frame Connections for the Moscone Center Expansion,” Department of Civil Engineering, University of Nevada, Reno, Report No. CCEER-99-14, December 1999.

CCEER 00-1 Ashour, M., and Norris, G. “Undrained Lateral Pile and Pile Group Response in Saturated Sand,” Civil Engineering Department, University of Nevada, Reno, Report No. CCEER-00-1, May 1999. January 2000.

CCEER 00-2 Saiidi, M. and Wehbe, N., “A Comparison of Confinement Requirements in Different Codes for Rectangular, Circular, and Double-Spiral RC Bridge Columns,” Civil Engineering Department, University of Nevada, Reno, Report No. CCEER-00-2, January 2000.

CCEER 00-3 McElhaney, B., M. Saiidi, and D. Sanders, “Shake Table Testing of Flared Bridge Columns With Steel Jacket Retrofit,” Civil Engineering Department, University of Nevada, Reno, Report No. CCEER-00-3, January 2000.

CCEER 00-4 Martinovic, F., M. Saiidi, D. Sanders, and F. Gordaninejad, “Dynamic Testing of Non-Prismatic Reinforced Concrete Bridge Columns Retrofitted with FRP Jackets,” Civil Engineering Department, University of Nevada, Reno, Report No. CCEER-00-4, January 2000.

CCEER 00-5 Itani, A., and M. Saiidi, "Seismic Evaluation of Steel Joints for UCLA Center for Health Science Westwood Replacement Hospital," Civil Engineering Department, University of Nevada, Reno, Report No. CCEER-00-5, February 2000.

CCEER 00-6 Will, J. and D. Sanders, "High Performance Concrete Using Nevada Aggregates," Civil Engineering Department, University of Nevada, Reno, Report No. CCEER-00-6, May 2000.

CCEER 00-7 French, C., and M. Saiidi, "A Comparison of Static and Dynamic Performance of Models of Flared Bridge Columns," Civil Engineering Department, University of Nevada, Reno, Report No. CCEER-00-7, October 2000.

CCEER 00-8 Itani, A., H. Sedarat, "Seismic Analysis of the AISI LRFD Design Example of Steel Highway Bridges," Civil Engineering Department, University of Nevada, Reno, Report No. CCEER 00-08, November 2000.

CCEER 00-9 Moore, J., D. Sanders, and M. Saiidi, "Shake Table Testing of 1960's Two Column Bent with Hinges Bases," Civil Engineering Department, University of Nevada, Reno, Report No. CCEER 00-09, December 2000.

CCEER 00-10 Asthana, M., D. Sanders, and M. Saiidi, "One-Way Reinforced Concrete Bridge Column Hinges in the Weak Direction," Civil Engineering Department, University of Nevada, Reno, Report No. CCEER 00-10, April 2001.

CCEER 01-1 Ah Sha, H., D. Sanders, M. Saiidi, "Early Age Shrinkage and Cracking of Nevada Concrete Bridge Decks," Civil Engineering Department, University of Nevada, Reno, Report No. CCEER 01-01, May 2001.

CCEER 01-2 Ashour, M. and G. Norris, "Pile Group program for Full Material Modeling a Progressive Failure," Civil Engineering Department, University of Nevada, Reno, Report No. CCEER 01-02, July 2001.

CCEER 01-3 Itani, A., C. Lanaud, and P. Dusicka, "Non-Linear Finite Element Analysis of Built-Up Shear Links," Civil Engineering Department, University of Nevada, Reno, Report No. CCEER 01-03, July 2001.

CCEER 01-4 Saiidi, M., J. Mortensen, and F. Martinovic, "Analysis and Retrofit of Fixed Flared Columns with Glass Fiber-Reinforced Plastic Jacketing," Civil Engineering Department, University of Nevada, Reno, Report No. CCEER 01-4, August 2001

CCEER 01-5 Not Published

CCEER 01-6 Laplace, P., D. Sanders, and M. Saiidi, "Experimental Study and Analysis of Retrofitted Flexure and Shear Dominated Circular Reinforced Concrete Bridge Columns Subjected to Shake Table Excitation," Civil Engineering Department, University of Nevada, Reno, Report No. CCEER 01-6, June 2001.

CCEER 01-7 Reppi, F., and D. Sanders, "Removal and Replacement of Cast-in-Place, Post-tensioned, Box Girder Bridge," Civil Engineering Department, University of Nevada, Reno, Report No. CCEER 01-7, December 2001.

CCEER 02-1 Pulido, C., M. Saiidi, D. Sanders, and A. Itani, "Seismic Performance and Retrofitting of Reinforced Concrete Bridge Bents," Civil Engineering Department, University of Nevada, Reno, Report No. CCEER 02-1, January 2002.

CCEER 02-2 Yang, Q., M. Saiidi, H. Wang, and A. Itani, "Influence of Ground Motion Incoherency on Earthquake Response of Multi-Support Structures," Civil Engineering Department, University of Nevada, Reno, Report No. CCEER 02-2, May 2002.

CCEER 02-3 M. Saiidi, B. Gopalakrishnan, E. Reinhardt, and R. Siddharthan, "A Preliminary Study of Shake Table Response of A Two-Column Bridge Bent on Flexible Footings," Civil Engineering Department, University of Nevada, Reno, Report No. CCEER 02-03, June 2002.

CCEER 02-4 Not Published

CCEER 02-5 Banghart, A., Sanders, D., Saiidi, M., "Evaluation of Concrete Mixes for Filling the Steel Arches in the Galena Creek Bridge," Civil Engineering Department, University of Nevada, Reno, Report No. CCEER 02-05, June 2002.

CCEER 02-6 Dusicka, P., Itani, A., Buckle, I. G., "Cyclic Behavior of Shear Links and Tower Shaft Assembly of San Francisco – Oakland Bay Bridge Tower," Civil Engineering Department, University of Nevada, Reno, Report No. CCEER 02-06, July 2002.

CCEER 02-7 Mortensen, J., and M. Saiidi, "A Performance-Based Design Method for Confinement in Circular Columns," Civil Engineering Department, University of Nevada, Reno, Report No. CCEER 02-07, November 2002.

CCEER 03-1 Wehbe, N., and M. Saiidi, "User's manual for SPMC v. 1.0 : A Computer Program for Moment-Curvature Analysis of Reinforced Concrete Sections with Interlocking Spirals," Center for Civil Engineering Earthquake Research, Department of Civil Engineering, University of Nevada, Reno, Nevada, Report No. CCEER-03-1, May, 2003.

CCEER 03-2 Wehbe, N., and M. Saiidi, "User's manual for RCMC v. 2.0 : A Computer Program for Moment-Curvature Analysis of Confined and Unconfined Reinforced Concrete Sections," Center for Civil Engineering Earthquake Research, Department of Civil Engineering, University of Nevada, Reno, Nevada, Report No. CCEER-03-2, June, 2003.

CCEER 03-3 Nada, H., D. Sanders, and M. Saiidi, "Seismic Performance of RC Bridge Frames with Architectural-Flared Columns," Civil Engineering Department, University of Nevada, Reno, Report No. CCEER 03-3, January 2003.

CCEER 03-4 Reinhardt, E., M. Saiidi, and R. Siddharthan, "Seismic Performance of a CFRP/ Concrete Bridge Bent on Flexible Footings," Civil Engineering Department, University of Nevada, Reno, Report No. CCEER 03-4, August 2003.

CCEER 03-5 Johnson, N., M. Saiidi, A. Itani, and S. Ladkany, "Seismic Retrofit of Octagonal Columns with Pedestal and One-Way Hinge at the Base," Center for Civil Engineering Earthquake Research, Department of Civil Engineering, University of Nevada, Reno, Nevada, and Report No. CCEER-03-5, August 2003.

CCEER 03-6 Mortensen, C., M. Saiidi, and S. Ladkany, "Creep and Shrinkage Losses in Highly Variable Climates," Center for Civil Engineering Earthquake Research, Department of Civil Engineering, University of Nevada, Reno, Report No. CCEER-03-6, September 2003.

CCEER 03- 7 Ayoub, C., M. Saiidi, and A. Itani, "A Study of Shape-Memory-Alloy-Reinforced Beams and Cubes," Center for Civil Engineering Earthquake Research, Department of Civil Engineering, University of Nevada, Reno, Nevada, Report No. CCEER-03-7, October 2003.

CCEER 03-8 Chandane, S., D. Sanders, and M. Saiidi, "Static and Dynamic Performance of RC Bridge Bents with Architectural-Flared Columns," Center for Civil Engineering Earthquake Research,

Department of Civil Engineering, University of Nevada, Reno, Nevada, Report No. CCEER-03-8, November 2003.

CCEER 04-1 Olaegbe, C., and Saiidi, M., "Effect of Loading History on Shake Table Performance of A Two-Column Bent with Infill Wall," Center for Civil Engineering Earthquake Research, Department of Civil Engineering, University of Nevada, Reno, Nevada, Report No. CCEER-04-1, January 2004.

CCEER 04-2 Johnson, R., Maragakis, E., Saiidi, M., and DesRoches, R., "Experimental Evaluation of Seismic Performance of SMA Bridge Restrainers," Center for Civil Engineering Earthquake Research, Department of Civil Engineering, University of Nevada, Reno, Nevada, Report No. CCEER-04-2, February 2004.

CCEER 04-3 Moustafa, K., Sanders, D., and Saiidi, M., "Impact of Aspect Ratio on Two-Column Bent Seismic Performance," Center for Civil Engineering Earthquake Research, Department of Civil Engineering, University of Nevada, Reno, Nevada, Report No. CCEER-04-3, February 2004.

CCEER 04-4 Maragakis, E., Saiidi, M., Sanchez-Camargo, F., and Elfass, S., "Seismic Performance of Bridge Restrainers At In-Span Hinges," Center for Civil Engineering Earthquake Research, Department of Civil Engineering, University of Nevada, Reno, Nevada, Report No. CCEER-04-4, March 2004.

CCEER 04-5 Ashour, M., Norris, G. and Elfass, S., "Analysis of Laterally Loaded Long or Intermediate Drilled Shafts of Small or Large Diameter in Layered Soil," Center for Civil Engineering Earthquake Research, Department of Civil Engineering, University of Nevada, Reno, Nevada, Report No. CCEER-04-5, June 2004.

CCEER 04-6 Correal, J., Saiidi, M. and Sanders, D., "Seismic Performance of RC Bridge Columns Reinforced with Two Interlocking Spirals," Center for Civil Engineering Earthquake Research, Department of Civil Engineering, University of Nevada, Reno, Nevada, Report No. CCEER-04-6, August 2004.

CCEER 04-7 Dusicka, P., Itani, A. and Buckle, I., "Cyclic Response and Low Cycle Fatigue Characteristics of Plate Steels," Center for Civil Engineering Earthquake Research, Department of Civil Engineering, University of Nevada, Reno, Nevada, Report No. CCEER-04-7, November 2004.

CCEER 04-8 Dusicka, P., Itani, A. and Buckle, I., "Built-up Shear Links as Energy Dissipaters for Seismic Protection of Bridges," Center for Civil Engineering Earthquake Research, Department of Civil Engineering, University of Nevada, Reno, Nevada, Report No. CCEER-04-8, November 2004.

CCEER 04-9 Sureshkumar, K., Saiidi, S., Itani, A. and Ladkany, S., "Seismic Retrofit of Two-Column Bents with Diamond Shape Columns," Center for Civil Engineering Earthquake Research, Department of Civil Engineering, University of Nevada, Reno, Nevada, Report No. CCEER-04-9, November 2004.

CCEER 05-1 Wang, H. and Saiidi, S., "A Study of RC Columns with Shape Memory Alloy and Engineered Cementitious Composites," Center for Civil Engineering Earthquake Research, Department of Civil Engineering, University of Nevada, Reno, Nevada, Report No. CCEER-05-1, January 2005.

CCEER 05-2 Johnson, R., Saiidi, S. and Maragakis, E., "A Study of Fiber Reinforced Plastics for Seismic Bridge Restrainers," Center for Civil Engineering Earthquake Research, Department of Civil Engineering, University of Nevada, Reno, Nevada, Report No. CCEER-05-2, January 2005.

CCEER 05-3 Carden, L.P., Itani, A.M., Buckle, I.G, "Seismic Load Path in Steel Girder Bridge Superstructures," Center for Civil Engineering Earthquake Research, Department of Civil Engineering, University of Nevada, Reno, Nevada, Report No. CCEER-05-3, January 2005.

CCEER 05-4 Carden, L.P., Itani, A.M., Buckle, I.G, "Seismic Performance of Steel Girder Bridge Superstructures with Ductile End Cross Frames and Seismic Isolation," Center for Civil Engineering Earthquake

Research, Department of Civil Engineering, University of Nevada, Reno, Nevada, Report No. CCEER-05-4, January 2005.

CCEER 05-5 Goodwin, E., Maragakis, M., Itani, A. and Luo, S., "Experimental Evaluation of the Seismic Performance of Hospital Piping Subassemblies," Center for Civil Engineering Earthquake Research, Department of Civil Engineering, University of Nevada, Reno, Nevada, Report No. CCEER-05-5, February 2005.

CCEER 05-6 Zadeh M. S., Saiidi, S, Itani, A. and Ladkany, S., "Seismic Vulnerability Evaluation and Retrofit Design of Las Vegas Downtown Viaduct," Center for Civil Engineering Earthquake Research, Department of Civil Engineering, University of Nevada, Reno, Nevada, Report No. CCEER-05-6, February 2005.

CCEER 05-7 Phan, V., Saiidi, S. and Anderson, J., "Near Fault (Near Field) Ground Motion Effects on Reinforced Concrete Bridge Columns," Center for Civil Engineering Earthquake Research, Department of Civil Engineering, University of Nevada, Reno, Nevada, Report No. CCEER-05-7, August 2005.

CCEER 05-8 Carden, L., Itani, A. and Laplace, P., "Performance of Steel Props at the UNR Fire Science Academy subjected to Repeated Fire," Center for Civil Engineering Earthquake Research, Department of Civil Engineering, University of Nevada, Reno, Nevada, Report No. CCEER-05-8, August 2005.

CCEER 05-9 Yamashita, R. and Sanders, D., "Shake Table Testing and an Analytical Study of Unbonded Prestressed Hollow Concrete Column Constructed with Precast Segments," Center for Civil Engineering Earthquake Research, Department of Civil Engineering, University of Nevada, Reno, Nevada, Report No. CCEER-05-9, August 2005.

CCEER 05-10 Not Published

CCEER 05-11 Carden, L., Itani., A., and Peckan, G., "Recommendations for the Design of Beams and Posts in Bridge Falsework," Center for Civil Engineering Earthquake Research, Department of Civil Engineering, University of Nevada, Reno, Nevada, Report No. CCEER-05-11, October 2005.

CCEER 06-01 Cheng, Z., Saiidi, M., and Sanders, D., "Development of a Seismic Design Method for Reinforced Concrete Two-Way Bridge Column Hinges," Center for Civil Engineering Earthquake Research, Department of Civil Engineering, University of Nevada, Reno, Nevada, Report No. CCEER-06-01, February 2006.

CCEER 06-02 Johnson, N., Saiidi, M., and Sanders, D., "Large-Scale Experimental and Analytical Studies of a Two-Span Reinforced Concrete Bridge System," Center for Civil Engineering Earthquake Research, Department of Civil Engineering, University of Nevada, Reno, Nevada, Report No. CCEER-06-02, March 2006.

CCEER 06-03 Saiidi, M., Ghasemi, H. and Tiras, A., "Seismic Design and Retrofit of Highway Bridges," Proceedings, Second US-Turkey Workshop, Center for Civil Engineering Earthquake Research, Department of Civil Engineering, University of Nevada, Reno, Nevada, Report No. CCEER-06-03, May 2006.

CCEER 07-01 O'Brien, M., Saiidi, M. and Sadrossadat-Zadeh, M., "A Study of Concrete Bridge Columns Using Innovative Materials Subjected to Cyclic Loading," Center for Civil Engineering Earthquake Research, Department of Civil Engineering, University of Nevada, Reno, Nevada, Report No. CCEER-07-01, January 2007.

CCEER 07-02 Sadrossadat-Zadeh, M. and Saiidi, M., "Effect of Strain rate on Stress-Strain Properties and Yield Propagation in Steel Reinforcing Bars," Center for Civil Engineering Earthquake Research, Department of Civil Engineering, University of Nevada, Reno, Nevada, Report No. CCEER-07-02, January 2007.

CCEER 07-03 Sadrossadat-Zadeh, M. and Saiidi, M., "Analytical Study of NEESR-SG 4-Span Bridge Model Using OpenSees," Center for Civil Engineering Earthquake Research, Department of Civil Engineering, University of Nevada, Reno, Nevada, Report No. CCEER-07-03, January 2007.

CCEER 07-04 Nelson, R., Saiidi, M. and Zadeh, S., "Experimental Evaluation of Performance of Conventional Bridge Systems," Center for Civil Engineering Earthquake Research, Department of Civil Engineering, University of Nevada, Reno, Nevada, Report No. CCEER-07-04, October 2007.

CCEER 07-05 Bahen, N. and Sanders, D., "Strut-and-Tie Modeling for Disturbed Regions in Structural Concrete Members with Emphasis on Deep Beams," Center for Civil Engineering Earthquake Research, Department of Civil Engineering, University of Nevada, Reno, Nevada, Report No. CCEER-07-05, December 2007.

CCEER 07-06 Choi, H., Saiidi, M. and Somerville, P., "Effects of Near-Fault Ground Motion and Fault-Rupture on the Seismic Response of Reinforced Concrete Bridges," Center for Civil Engineering Earthquake Research, Department of Civil Engineering, University of Nevada, Reno, Nevada, Report No. CCEER-07-06, December 2007.

CCEER 07-07 Ashour M. and Norris, G., "Report and User Manual on Strain Wedge Model Computer Program for Files and Large Diameter Shafts with LRFD Procedure," Center for Civil Engineering Earthquake Research, Department of Civil Engineering, University of Nevada, Reno, Nevada, Report No. CCEER-07-07, October 2007.

CCEER 08-01 Doyle, K. and Saiidi, M., "Seismic Response of Telescopic Pipe Pin Connections," Center for Civil Engineering Earthquake Research, Department of Civil Engineering, University of Nevada, Reno, Nevada, Report No. CCEER-08-01, February 2008.

CCEER 08-02 Taylor, M. and Sanders, D., "Seismic Time History Analysis and Instrumentation of the Galena Creek Bridge," Center for Civil Engineering Earthquake Research, Department of Civil Engineering, University of Nevada, Reno, Nevada, Report No. CCEER-08-02, April 2008.

CCEER 08-03 Abdel-Mohti, A. and Pekcan, G., "Seismic Response Assessment and Recommendations for the Design of Skewed Post-Tensioned Concrete Box-Girder Highway Bridges," Center for Civil Engineering Earthquake Research, Department of Civil and Environmental Engineering, University of Nevada, Reno, Nevada, Report No. CCEER-08-03, September 2008.

CCEER 08-04 Saiidi, M., Ghasemi, H. and Hook, J., "Long Term Bridge Performance Monitoring, Assessment & Management," Proceedings, FHWA/NSF Workshop on Future Directions," Center for Civil Engineering Earthquake Research, Department of Civil and Environmental Engineering, University of Nevada, Reno, Nevada, Report No. CCEER 08-04, September 2008.

CCEER 09-01 Brown, A., and Saiidi, M., "Investigation of Near-Fault Ground Motion Effects on Substandard Bridge Columns and Bents," Center for Civil Engineering Earthquake Research, Department of Civil and Environmental Engineering, University of Nevada, Reno, Nevada, Report No. CCEER-09-01, July 2009.

CCEER 09-02 Linke, C., Pekcan, G., and Itani, A., "Detailing of Seismically Resilient Special Truss Moment Frames," Center for Civil Engineering Earthquake Research, Department of Civil and Environmental Engineering, University of Nevada, Reno, Nevada, Report No. CCEER-09-02, August 2009.

CCEER 09-03 Hillis, D., and Saiidi, M., "Design, Construction, and Nonlinear Dynamic Analysis of Three Bridge Bents Used in a Bridge System Test," Center for Civil Engineering Earthquake Research, Department of Civil and Environmental Engineering, University of Nevada, Reno, Nevada, Report No. CCEER-09-03, August 2009.

CCEER 09-04 Bahrami, H., Itani, A., and Buckle, I., "Guidelines for the Seismic Design of Ductile End Cross Frames in Steel Girder Bridge Superstructures," Center for Civil Engineering Earthquake Research, Department of Civil and Environmental Engineering, University of Nevada, Reno, Nevada, Report No. CCEER-09-04, September 2so009.

CCEER 10-01 Zaghi, A. E., and Saiidi, M., "Seismic Design of Pipe-Pin Connections in Concrete Bridges," Center for Civil Engineering Earthquake Research, Department of Civil and Environmental Engineering, University of Nevada, Reno, Nevada, Report No. CCEER-10-01, January 2010.

CCEER 10-02 Pooranampillai, S., Elfass, S., and Norris, G., "Laboratory Study to Assess Load Capacity Increase of Drilled Shafts through Post Grouting," Center for Civil Engineering Earthquake Research, Department of Civil and Environmental Engineering, University of Nevada, Reno, Nevada, Report No. CCEER-10-02, January 2010.

CCEER 10-03 Itani, A., Grubb, M., and Monzon, E, "Proposed Seismic Provisions and Commentary for Steel Plate Girder Superstructures," Center for Civil Engineering Earthquake Research, Department of Civil and Environmental Engineering, University of Nevada, Reno, Nevada, Report No. CCEER-10-03, June 2010.

CCEER 10-04 Cruz-Noguez, C., Saiidi, M., "Experimental and Analytical Seismic Studies of a Four-Span Bridge System with Innovative Materials," Center for Civil Engineering Earthquake Research, Department of Civil and Environmental Engineering, University of Nevada, Reno, Nevada, Report No. CCEER-10-04, September 2010.

CCEER 10-05 Vosooghi, A., Saiidi, M., "Post-Earthquake Evaluation and Emergency Repair of Damaged RC Bridge Columns Using CFRP Materials," Center for Civil Engineering Earthquake Research, Department of Civil and Environmental Engineering, University of Nevada, Reno, Nevada, Report No. CCEER-10-05, September 2010.

CCEER 10-06 Ayoub, M., Sanders, D., "Testing of Pile Extension Connections to Slab Bridges," Center for Civil Engineering Earthquake Research, Department of Civil and Environmental Engineering, University of Nevada, Reno, Nevada, Report No. CCEER-10-06, October 2010.

CCEER 10-07 Builes-Mejia, J. C. and Itani, A., "Stability of Bridge Column Rebar Cages during Construction," Center for Civil Engineering Earthquake Research, Department of Civil and Environmental Engineering, University of Nevada, Reno, Nevada, Report No. CCEER-10-07, November 2010.

CCEER 10-08 Monzon, E.V., "Seismic Performance of Steel Plate Girder Bridges with Integral Abutments," Center for Civil Engineering Earthquake Research, Department of Civil and Environmental Engineering, University of Nevada, Reno, Nevada, Report No. CCEER-10-08, November 2010.

CCEER 11-01 Motaref, S., Saiidi, M., and Sanders, D., "Seismic Response of Precast Bridge Columns with Energy Dissipating Joints," Center for Civil Engineering Earthquake Research, Department of Civil and Environmental Engineering, University of Nevada, Reno, Nevada, Report No. CCEER-11-01, May 2011.

CCEER 11-02 Harrison, N. and Sanders, D., "Preliminary Seismic Analysis and Design of Reinforced Concrete Bridge Columns for Curved Bridge Experiments," Center for Civil Engineering Earthquake Research, Department of Civil and Environmental Engineering, University of Nevada, Reno, Nevada, Report No. CCEER-11-02, May 2011.

CCEER 11-03 Vallejera, J. and Sanders, D., "Instrumentation and Monitoring the Galena Creek Bridge," Center for Civil Engineering Earthquake Research, Department of Civil and Environmental Engineering, University of Nevada, Reno, Nevada, Report No. CCEER-11-03, September 2011.

CCEER 11-04 Levi, M., Sanders, D., and Buckle, I., “Seismic Response of Columns in Horizontally Curved Bridges,” Center for Civil Engineering Earthquake Research, Department of Civil and Environmental Engineering, University of Nevada, Reno, Nevada, Report No. CCEER-11-04, December 2011.

CCEER 12-01 Saiidi, M., “NSF International Workshop on Bridges of the Future – Wide Spread Implementation of Innovation,” Center for Civil Engineering Earthquake Research, Department of Civil and Environmental Engineering, University of Nevada, Reno, Nevada, Report No. CCEER-12-01, January 2012.

CCEER 12-02 Larkin, A.S., Sanders, D., and Saiidi, M., “Unbonded Prestressed Columns for Earthquake Resistance,” Center for Civil Engineering Earthquake Research, Department of Civil and Environmental Engineering, University of Nevada, Reno, Nevada, Report No. CCEER-12-02, January 2012.

CCEER 12-03 Arias-Acosta, J. G., Sanders, D., “Seismic Performance of Circular and Interlocking Spirals RC Bridge Columns under Bidirectional Shake Table Loading Part 1,” Center for Civil Engineering Earthquake Research, Department of Civil and Environmental Engineering, University of Nevada, Reno, Nevada, Report No. CCEER-12-03, September 2012.

CCEER 12-04 Cukrov, M.E., Sanders, D., “Seismic Performance of Prestressed Pile-To-Bent Cap Connections,” Center for Civil Engineering Earthquake Research, Department of Civil and Environmental Engineering, University of Nevada, Reno, Nevada, Report No. CCEER-12-04, September 2012.

CCEER 13-01 Carr, T. and Sanders, D., “Instrumentation and Dynamic Characterization of the Galena Creek Bridge,” Center for Civil Engineering Earthquake Research, Department of Civil and Environmental Engineering, University of Nevada, Reno, Nevada, Report No. CCEER-13-01, January 2013.

CCEER 13-02 Vosooghi, A. and Buckle, I., “Evaluation of the Performance of a Conventional Four-Span Bridge During Shake Table Tests,” Center for Civil Engineering Earthquake Research, Department of Civil and Environmental Engineering, University of Nevada, Reno, Nevada, Report No. CCEER-13-02, January 2013.

CCEER 13-03 Amirihormozaki, E. and Pekcan, G., “Analytical Fragility Curves for Horizontally Curved Steel Girder Highway Bridges,” Center for Civil Engineering Earthquake Research, Department of Civil and Environmental Engineering, University of Nevada, Reno, Nevada, Report No. CCEER-13-03, February 2013.

CCEER 13-04 Almer, K. and Sanders, D., “Longitudinal Seismic Performance of Precast Bridge Girders Integrally Connected to a Cast-in-Place Bentcap,” Center for Civil Engineering Earthquake Research, Department of Civil and Environmental Engineering, University of Nevada, Reno, Nevada, Report No. CCEER-13-04, April 2013.

CCEER 13-05 Monzon, E.V., Itani, A.I., and Buckle, I.G., “Seismic Modeling and Analysis of Curved Steel Plate Girder Bridges,” Center for Civil Engineering Earthquake Research, Department of Civil and Environmental Engineering, University of Nevada, Reno, Nevada, Report No. CCEER-13-05, April 2013.

CCEER 13-06 Monzon, E.V., Buckle, I.G., and Itani, A.I., “Seismic Performance of Curved Steel Plate Girder Bridges with Seismic Isolation,” Center for Civil Engineering Earthquake Research, Department of Civil and Environmental Engineering, University of Nevada, Reno, Nevada, Report No. CCEER-13-06, April 2013.

CCEER 13-07 Monzon, E.V., Buckle, I.G., and Itani, A.I., “Seismic Response of Isolated Bridge Superstructure to Incoherent Ground Motions,” Center for Civil Engineering Earthquake Research, Department of Civil and Environmental Engineering, University of Nevada, Reno, Nevada, Report No. CCEER-13-07, April 2013.

CCEER 13-08 Haber, Z.B., Saiidi, M.S., and Sanders, D.H., "Precast Column-Footing Connections for Accelerated Bridge Construction in Seismic Zones," Center for Civil Engineering Earthquake Research, Department of Civil and Environmental Engineering, University of Nevada, Reno, Nevada, Report No. CCEER-13-08, April 2013.

CCEER 13-09 Ryan, K.L., Coria, C.B., and Dao, N.D., "Large Scale Earthquake Simulation of a Hybrid Lead Rubber Isolation System Designed under Nuclear Seismicity Considerations," Center for Civil Engineering Earthquake Research, Department of Civil and Environmental Engineering, University of Nevada, Reno, Nevada, Report No. CCEER-13-09, April 2013.

CCEER 13-10 Wibowo, H., Sanford, D.M., Buckle, I.G., and Sanders, D.H., "The Effect of Live Load on the Seismic Response of Bridges," Center for Civil Engineering Earthquake Research, Department of Civil and Environmental Engineering, University of Nevada, Reno, Nevada, Report No. CCEER-13-10, May 2013.

CCEER 13-11 Sanford, D.M., Wibowo, H., Buckle, I.G., and Sanders, D.H., "Preliminary Experimental Study on the Effect of Live Load on the Seismic Response of Highway Bridges," Center for Civil Engineering Earthquake Research, Department of Civil and Environmental Engineering, University of Nevada, Reno, Nevada, Report No. CCEER-13-11, May 2013.

CCEER 13-12 Saad, A.S., Sanders, D.H., and Buckle, I.G., "Assessment of Foundation Rocking Behavior in Reducing the Seismic Demand on Horizontally Curved Bridges," Center for Civil Engineering Earthquake Research, Department of Civil and Environmental Engineering, University of Nevada, Reno, Nevada, Report No. CCEER-13-12, June 2013.

CCEER 13-13 Ardakani, S.M.S. and Saiidi, M.S., "Design of Reinforced Concrete Bridge Columns for Near-Fault Earthquakes," Center for Civil Engineering Earthquake Research, Department of Civil and Environmental Engineering, University of Nevada, Reno, Nevada, Report No. CCEER-13-13, July 2013.

CCEER 13-14 Wei, C. and Buckle, I., "Seismic Analysis and Response of Highway Bridges with Hybrid Isolation," Center for Civil Engineering Earthquake Research, Department of Civil and Environmental Engineering, University of Nevada, Reno, Nevada, Report No. CCEER-13-14, August 2013.

CCEER 13-15 Wibowo, H., Buckle, I.G., and Sanders, D.H., "Experimental and Analytical Investigations on the Effects of Live Load on the Seismic Performance of a Highway Bridge," Center for Civil Engineering Earthquake Research, Department of Civil and Environmental Engineering, University of Nevada, Reno, Nevada, Report No. CCEER-13-15, August 2013.

CCEER 13-16 Itani, A.M., Monzon, E.V., Grubb, M., and Amirihormozaki, E. "Seismic Design and Nonlinear Evaluation of Steel I-Girder Bridges with Ductile End Cross-Frames," Center for Civil Engineering Earthquake Research, Department of Civil and Environmental Engineering, University of Nevada, Reno, Nevada, Report No. CCEER-13-16, September 2013.

CCEER 13-17 Kavianipour, F. and Saiidi, M.S., "Experimental and Analytical Seismic Studies of a Four-span Bridge System with Composite Piers," Center for Civil Engineering Earthquake Research, Department of Civil and Environmental Engineering, University of Nevada, Reno, Nevada, Report No. CCEER-13-17, September 2013.

CCEER 13-18 Mohebbi, A., Ryan, K., and Sanders, D., "Seismic Response of a Highway Bridge with Structural Fuses for Seismic Protection of Piers," Center for Civil Engineering Earthquake Research,

Department of Civil and Environmental Engineering, University of Nevada, Reno, Nevada, Report No. CCEER-13-18, December 2013.

CCEER 13-19 Guzman Pujols, Jean C., Ryan, K.L., "Development of Generalized Fragility Functions for Seismic Induced Content Disruption," Center for Civil Engineering Earthquake Research, Department of Civil and Environmental Engineering, University of Nevada, Reno, Nevada, Report No. CCEER-13-19, December 2013.

CCEER 14-01 Salem, M. M. A., Pekcan, G., and Itani, A., "Seismic Response Control Of Structures Using Semi-Active and Passive Variable Stiffness Devices," Center for Civil Engineering Earthquake Research, Department of Civil and Environmental Engineering, University of Nevada, Reno, Nevada, Report No. CCEER-14-01, May 2014.

CCEER 14-02 Saini, A. and Saiidi, M., "Performance-Based Probabilistic Damage Control Approach for Seismic Design of Bridge Columns," Center For Civil Engineering Earthquake Research, Department Of Civil and Environmental Engineering, University of Nevada, Reno, Nevada, Report No. CCEER-14-02, May 2014.

CCEER 14-03 Saini, A. and Saiidi, M., "Post Earthquake Damage Repair of Various Reinforced Concrete Bridge Components," Center For Civil Engineering Earthquake Research, Department Of Civil and Environmental Engineering, University of Nevada, Reno, Nevada, Report No. CCEER-14-03, May 2014.

CCEER 14-04 Monzon, E.V., Itani, A.M., and Grubb, M.A., "Nonlinear Evaluation of the Proposed Seismic Design Procedure for Steel Bridges with Ductile End Cross Frames," Center For Civil Engineering Earthquake Research, Department Of Civil and Environmental Engineering, University of Nevada, Reno, Nevada, Report No. CCEER-14-04, July 2014.

CCEER 14-05 Nakashoji, B. and Saiidi, M.S., "Seismic Performance of Square Nickel-Titanium Reinforced ECC Columns with Headed Couplers," Center For Civil Engineering Earthquake Research, Department Of Civil and Environmental Engineering, University of Nevada, Reno, Nevada, Report No. CCEER-14-05, July 2014.

CCEER 14-06 Tazarv, M. and Saiidi, M.S., "Next Generation of Bridge Columns for Accelerated Bridge Construction in High Seismic Zones," Center For Civil Engineering Earthquake Research, Department Of Civil and Environmental Engineering, University of Nevada, Reno, Nevada, Report No. CCEER-14-06, August 2014.

CCEER 14-07 Mehrsoroush, A. and Saiidi, M.S., "Experimental and Analytical Seismic Studies of Bridge Piers with Innovative Pipe Pin Column-Footing Connections and Precast Cap Beams," Center For Civil Engineering Earthquake Research, Department Of Civil and Environmental Engineering, University of Nevada, Reno, Nevada, Report No. CCEER-14-07, December 2014.

CCEER 15-01 Dao, N.D. and Ryan, K.L., "Seismic Response of a Full-scale 5-story Steel Frame Building Isolated by Triple Pendulum Bearings under 3D Excitations," Center For Civil Engineering Earthquake Research, Department Of Civil and Environmental Engineering, University of Nevada, Reno, Nevada, Report No. CCEER-15-01, January 2015.

CCEER 15-02 Allen, B.M. and Sanders, D.H., "Post-Tensioning Duct Air Pressure Testing Effects on Web Cracking," Center For Civil Engineering Earthquake Research, Department Of Civil and Environmental Engineering, University of Nevada, Reno, Nevada, Report No. CCEER-15-02, January 2015.

CCEER 15-03 Akl, A. and Saiidi, M.S., "Time-Dependent Deflection of In-Span Hinges in Prestressed Concrete Box Girder Bridges," Center For Civil Engineering Earthquake Research, Department Of Civil

and Environmental Engineering, University of Nevada, Reno, Nevada, Report No. CCEER-15-03, May 2015.

CCEER 15-04 Zargar Shotorbani, H. and Ryan, K., "Analytical and Experimental Study of Gap Damper System to Limit Seismic Isolator Displacements in Extreme Earthquakes," Center For Civil Engineering Earthquake Research, Department Of Civil and Environmental Engineering, University of Nevada, Reno, Nevada, Report No. CCEER-15-04, June 2015.

CCEER 15-05 Wieser, J., Maragakis, E.M., and Buckle, I., "Experimental and Analytical Investigation of Seismic Bridge-Abutment Interaction in a Curved Highway Bridge," Center For Civil Engineering Earthquake Research, Department Of Civil and Environmental Engineering, University of Nevada, Reno, Nevada, Report No. CCEER-15-05, July 2015.

CCEER 15-06 Tazarv, M. and Saiidi, M.S., "Design and Construction of Precast Bent Caps with Pocket Connections for High Seismic Regions," Center For Civil Engineering Earthquake Research, Department Of Civil and Environmental Engineering, University of Nevada, Reno, Nevada, Report No. CCEER-15-06, August 2015.

CCEER 15-07 Tazarv, M. and Saiidi, M.S., "Design and Construction of Bridge Columns Incorporating Mechanical Bar Splices in Plastic Hinge Zones," Center For Civil Engineering Earthquake Research, Department Of Civil and Environmental Engineering, University of Nevada, Reno, Nevada, Report No. CCEER-15-07, August 2015.

CCEER 15-08 Sarraf Shirazi, R., Pekcan, G., and Itani, A.M., "Seismic Response and Analytical Fragility Functions for Curved Concrete Box-Girder Bridges," Center For Civil Engineering Earthquake Research, Department Of Civil and Environmental Engineering, University of Nevada, Reno, Nevada, Report No. CCEER-15-08, December 2015.

CCEER 15-09 Coria, C.B., Ryan, K.L., and Dao, N.D., "Response of Lead Rubber Bearings in a Hybrid Isolation System During a Large Scale Shaking Experiment of an Isolated Building," Center For Civil Engineering Earthquake Research, Department Of Civil and Environmental Engineering, University of Nevada, Reno, Nevada, Report No. CCEER-15-09, December 2015.

CCEER 16-01 Mehraein, M and Saiidi, M.S., "Seismic Performance of Bridge Column-Pile-Shaft Pin Connections for Application in Accelerated Bridge Construction," Center For Civil Engineering Earthquake Research, Department Of Civil and Environmental Engineering, University of Nevada, Reno, Nevada, Report No. CCEER-16-01, May 2016.

CCEER 16-02 Varela Fontecha, S. and Saiidi, M.S., "Resilient Earthquake-Resistant Bridges Designed For Disassembly," Center For Civil Engineering Earthquake Research, Department Of Civil and Environmental Engineering, University of Nevada, Reno, Nevada, Report No. CCEER-16-02, May 2016.

CCEER 16-03 Mantawy, I. M, and Sanders, D. H., "Assessment of an Earthquake Resilient Bridge with Pretensioned, Rocking Columns," Center For Civil Engineering Earthquake Research, Department Of Civil and Environmental Engineering, University of Nevada, Reno, Nevada, Report No. CCEER-16-03, May 2016.

CCEER 16-04 Mohammed, M, Biasi, G., and Sanders, D., "Post-earthquake Assessment of Nevada Bridges using ShakeMap/ShakeCast," Center For Civil Engineering Earthquake Research, Department Of Civil and Environmental Engineering, University of Nevada, Reno, Nevada, Report No. CCEER-16-04, May 2016.

CCEER 16-05 Jones, J, Ryan, K., and Saiidi, M, "Toward Successful Implementation of Prefabricated Deck Panels to Accelerate the Bridge Construction Process," Center For Civil Engineering Earthquake

Research, Department Of Civil and Environmental Engineering, University of Nevada, Reno, Nevada, Report No. CCEER-16-05, August 2016.

CCEER 16-06 Mehrsoroush, A. and Saiidi, M., "Probabilistic Seismic Damage Assessment for Sub-standard Bridge Columns," Center For Civil Engineering Earthquake Research, Department Of Civil and Environmental Engineering, University of Nevada, Reno, Nevada, Report No. CCEER-16-06, November 2016.

CCEER 16-07 Nielsen, T., Maree, A., and Sanders, D., "Experimental Investigation into the Long-Term Seismic Performance of Dry Storage Casks," Center For Civil Engineering Earthquake Research, Department Of Civil and Environmental Engineering, University of Nevada, Reno, Nevada, Report No. CCEER-16-07, December 2016.

CCEER 16-08 Wu, S., Buckle, I., and Itani, A., "Effect of Skew on Seismic Performance of Bridges with Seat-Type Abutments," Center For Civil Engineering Earthquake Research, Department Of Civil and Environmental Engineering, University of Nevada, Reno, Nevada, Report No. CCEER-16-08, December 2016.

CCEER 16-09 Mohammed, M., and Sanders, D., "Effect of Earthquake Duration on Reinforced Concrete Bridge Columns," Center For Civil Engineering Earthquake Research, Department Of Civil and Environmental Engineering, University of Nevada, Reno, Nevada, Report No. CCEER-16-09, December 2016.

CCEER 16-10 Guzman Pujols, J., and Ryan, K., "Slab Vibration and Horizontal-Vertical Coupling in the Seismic Response of Irregular Base-Isolated and Conventional Buildings," Center For Civil Engineering Earthquake Research, Department Of Civil and Environmental Engineering, University of Nevada, Reno, Nevada, Report No. CCEER-16-10, December 2016.

CCEER 17-01 White, L., Ryan, K., and Buckle, I., "Thermal Gradients in Southwestern United States and the Effect on Bridge Bearing Loads," Center For Civil Engineering Earthquake Research, Department Of Civil and Environmental Engineering, University of Nevada, Reno, Nevada, Report No. CCEER-17-01, May 2017.

CCEER 17-02 Mohebbi, A., Saiidi, M., and Itani, A., "Development and Seismic Evaluation of Pier Systems w/Pocket Connections, CFRP Tendons, and ECC/UHPC Columns," Center For Civil Engineering Earthquake Research, Department Of Civil and Environmental Engineering, University of Nevada, Reno, Nevada, Report No. CCEER-17-02, May 2017.

CCEER 17-03 Mehrsoroush, A., Saiidi, M., and Ryan, K., "Development of Earthquake-resistant Precast Pier Systems for Accelerated Bridge Construction in Nevada," Center For Civil Engineering Earthquake Research, Department Of Civil and Environmental Engineering, University of Nevada, Reno, Nevada, Report No. CCEER-17-03, June 2017.

CCEER 17-04 Abdollahi, B., Saiidi, M., Siddharthan, R., and Elfass, S., "Shake Table Studies on Soil-Abutment-Structure Interaction in Skewed Bridges," Center For Civil Engineering Earthquake Research, Department Of Civil and Environmental Engineering, University of Nevada, Reno, Nevada, Report No. CCEER-17-04, July 2017.

CCEER 17-05 Shrestha, G., Itani, A., and Saiidi, M., "Seismic Performance of Precast Full-Depth Decks in Accelerated Bridge Construction," Center for Civil Engineering Earthquake Research, Department of Civil and Environmental Engineering, University of Nevada, Reno, Nevada, Report No. CCEER-17-05, September 2017.

CCEER 17-06 Wu, S., Buckle, I., and Ryan, K., "Large-Scale Experimental Verification of an Optically-Based Sensor System for Monitoring Structural Response," Center for Civil Engineering Earthquake

Research, Department of Civil and Environmental Engineering, University of Nevada, Reno, Nevada, Report No. CCEER-17-06, October 2017.

CCEER 17-07 Nada, H., and Sanders, D., "Analytical Investigation into Bridge Column Innovations for Mitigating Earthquake Damage," Center For Civil Engineering Earthquake Research, Department Of Civil and Environmental Engineering, University of Nevada, Reno, Nevada, Report No. CCEER-17-07, October 2017.

CCEER 18-01 Maree, A. F., and Sanders, D., "Performance and Design of Anchorage Zones for Post-Tensioned Box Girder Bridges," Center for Civil Engineering Earthquake Research, Department of Civil and Environmental Engineering, University of Nevada, Reno, Nevada, Report No. CCEER-18-01, January 2018.

CCEER 18-02 Mostafa, K., and Sanders, D., "Improving the Long-Term Performance of Bridge Decks using Deck and Crack Sealers," Center for Civil Engineering Earthquake Research, Department of Civil and Environmental Engineering, University of Nevada, Reno, Nevada, Report No. CCEER-18-02, March 2018.

CCEER 18-03 Blount, S., Ryan, K., Henry, R., Lu, Y., and Elwood, K., "Evaluation of lower damage concepts for enhanced repairability of reinforced concrete walls," Center for Civil Engineering Earthquake Research, Department of Civil and Environmental Engineering, University of Nevada, Reno, Nevada, Report No. CCEER-18-03, June 2018.

CCEER 18-04 Mohebbi, A., Jordan, E., and Saiidi, M., "Exploratory Experimental Studies of Spliced Cam Shape Memory Alloy Bars for Seismic Application," Center for Civil Engineering Earthquake Research, Department Of Civil and Environmental Engineering, University of Nevada, Reno, Nevada, Report No. CCEER-18-04, September 2018.

CCEER 19-01 Saint Pierre, E., Elfass, S., Watters, R., Norris, G., and Ashour, M. "Improving Strain Wedge Model Capabilities in Analyzing Laterally Loaded Drilled Shafts in Cemented Soils," Center for Civil Engineering Earthquake Research, Department of Civil and Environmental Engineering, University of Nevada, Reno, Nevada, Report No. CCEER-19-01, March 2019.

CCEER 19-02 Benjumea, J., Saiidi, M., and Itani, A., "Experimental and Analytical Seismic Studies of a Two-Span Bridge System with Precast Concrete Elements and ABC Connections," Center for Civil Engineering Earthquake Research, Department of Civil and Environmental Engineering, University of Nevada, Reno, Nevada, Report No. CCEER-19-02, May 2019.

CCEER 19-03 Subedi, D., Moustafa, M., and Saiidi, M., "Non-Proprietary UHPC for Anchorage of Large Diameter Column Bars in Grouted Ducts," Center for Civil Engineering Earthquake Research, Department of Civil and Environmental Engineering, University of Nevada, Reno, Nevada, Report No. CCEER-19-03, May 2019.

CCEER 19-04 Shoushtari, E, D., Saiidi, M., Itani, A., and Moustafa, M., "Shake Table Studies of a Steel Girder Bridge System with ABC Connections," Center for Civil Engineering Earthquake Research, Department of Civil and Environmental Engineering, University of Nevada, Reno, Nevada, Report No. CCEER-19-04, June 2019.

CCEER 19-05 Wu, S., Miah, M., and McCallen, D., "Four Canonical Steel Moment Frame Buildings and Inter-Code Comparisons of Nonlinear Building Response," Center for Civil Engineering Earthquake Research, Department of Civil and Environmental Engineering, University of Nevada, Reno, Nevada, Report No. CCEER-19-05, September 2019.

CCEER 20-01 Schwartz, T., Saiidi, M., and Moustafa, M., “Simplifying Cast-in-Place Joint Design Using ABC Pocket Connection Details in High Seismic Regions,” Center for Civil Engineering Earthquake Research, Department of Civil and Environmental Engineering, University of Nevada, Reno, Nevada, Report No. CCEER-20-01, January 2020.

CCEER 20-02 Shrestha, G., Saiidi, M., and Sanders, D., “Seismic Studies of Spliced Columns and Anchorage of Large Diameter Bars in Grouted Duct,” Center for Civil Engineering Earthquake Research, Department of Civil and Environmental Engineering, University of Nevada, Reno, Nevada, Report No. CCEER-20-02, February 2020.

CCEER 20-03 Ozsahin, E. and Pekcan, G., “Torsional Ground Motion Effects on the Seismic Response of Continuous Box-girder Highway Bridges,” Center for Civil Engineering Earthquake Research, Department of Civil and Environmental Engineering, University of Nevada, Reno, Nevada, Report No. CCEER-20-03, April 2020.

CCEER 20-04 Wu, S., Eckert, E., Huang, J., and McCallen, D., “Evaluation of the Domain Reduction Method Applied to Broad-Band, Near-Fault Earthquake Ground Motions with Inter-Code Comparisons,” Center for Civil Engineering Earthquake Research, Department of Civil and Environmental Engineering, University of Nevada, Reno, Nevada, Report No. CCEER-20-04, June 2020.

CCEER 20-05 Jones, J., Saiidi, M., and Itani, A., “Experimental and Analytical Studies of a Two-Span Bridge System with Precast Elements Incorporating Rebar Hinge and Socket Connections,” Center for Civil Engineering Earthquake Research, Department of Civil and Environmental Engineering, University of Nevada, Reno, Nevada, Report No. CCEER-20-05, August 2020.

CCEER 20-06 Camarena, C., Saiidi, M., and Moustafa, M., “Development and Seismic Evaluation of Cast-in-Place Emulating ABC Pocket Connections and SMA Reinforced Two-Way Column Hinges,” Center for Civil Engineering Earthquake Research, Department of Civil and Environmental Engineering, University of Nevada, Reno, Nevada, Report No. CCEER-20-06, August 2020.

CCEER 20-07 Kenawy, M. and McCallen, D., “Regional-Scale Seismic Risk to Reinforced Concrete Buildings Based on Physics-Based Earthquake Ground Motion Simulations,” Center for Civil Engineering Earthquake Research, Department of Civil and Environmental Engineering, University of Nevada, Reno, Nevada, Report No. CCEER-20-07, September 2020.

CCEER 20-08 Aboukifa, M., Moustafa, M., and Saiidi, M., “Seismic Response of Precast Columns with Non-Proprietary UHPC-Filled Ducts ABC Connections,” Center for Civil Engineering Earthquake Research, Department of Civil and Environmental Engineering, University of Nevada, Reno, Nevada, Report No. CCEER-20-08, October 2020.